NASA-TM-87703 19860016804

NASA Technical Memorandum 87703

Langley Aerospace Test Highlights 1985

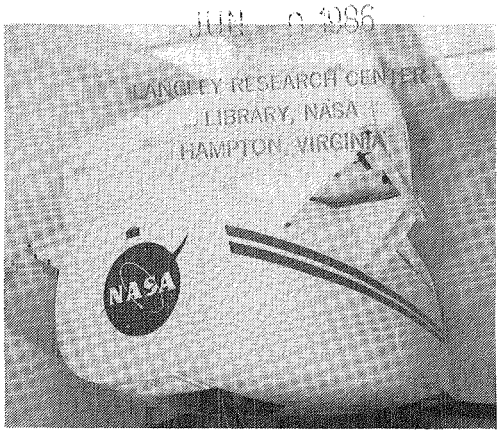

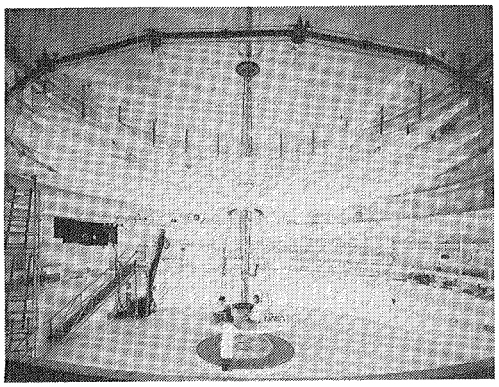

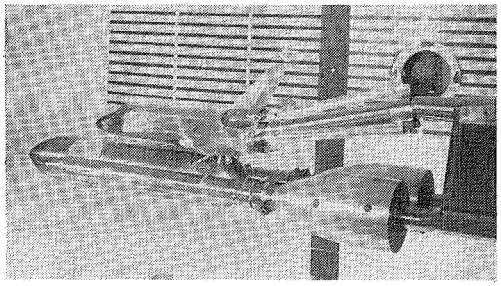

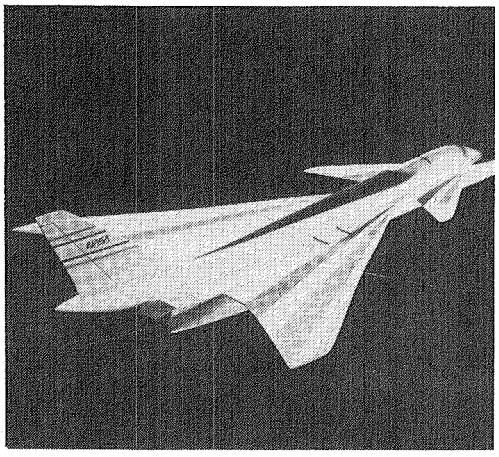

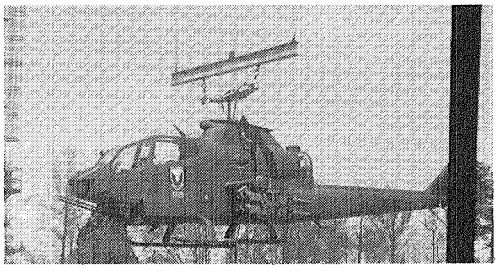

NASA
National Aeronautics
and Space Administration

NASA Technical Memorandum 87703

Langley Aerospace Test Highlights 1985

NASA
National Aeronautics and
Space Administration

Langley Research Center
Hampton, Virginia 23665-5225

1986

Foreword

The role of the Langley Research Center is to perform basic and applied research necessary for the advancement of aeronautics and space flight, to generate new and advanced concepts for the accomplishment of related national goals, and to provide research advice, technological support, and assistance to other NASA installations, other government agencies, and industry. This report highlights some of the significant tests which were performed during calendar year 1985 in Langley test facilities, a number of which are unique in the world. The report illustrates both the broad range of the research and technology activities at the Langley Research Center and the contributions of this work toward maintaining United States leadership in aeronautics and space research. Other highlights of Langley research and technology for 1985 are described in *Research and Technology—1985 Annual Report of the Langley Research Center.* Further information about both reports is available from the Office of the Chief Scientist, Mail Stop 103, Langley Research Center, Hampton, Virginia 23665 (804-865-3316).

Richard H. Petersen
Director

Availability Information

For additional information on any highlight, contact the individual identified with the highlight. This individual is generally either a member or a leader of the research group. Commercial telephone users may dial the listed extension preceded by (804) 865. Telephone users with access to the Federal Telecommunications System (FTS) may dial the extension preceded by 928.

Contents

30- by 60-Foot Tunnel

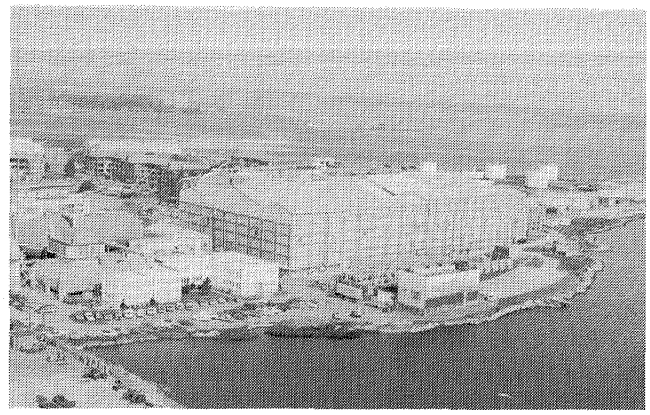

The Langley 30- by 60-Foot Tunnel is a continuous-flow open-throat double-return tunnel powered by two 4000-horsepower electric motors, each driving a four-blade 35.5-ft-diameter fan. The tunnel test section is 30 ft high and 60 ft wide and is capable of speeds up to 100 mph. The tunnel was first put into operation in 1931 and has been used continuously since then to study the low-speed aerodynamics of commercial and military aircraft. The large open-throat test section lends itself readily to tests of large-scale models and to unique test methods with small-scale models.

Large-scale and full-scale aircraft tests are conducted with the strut mounting system. This test method can handle airplanes up to the size of present-day light twin-engine airplanes. Such tests provide static aerodynamic performance and stability and control data, including the measurement of power effects, wing pressure distributions, and flow visualization.

Small-scale models can be tested to determine both static and dynamic aerodynamics. For all captive tests, the models are sting mounted with internal strain gauge balances. The captive test methods include conventional static tests for performance and stability and control, forced-oscillation tests for aerodynamic damping, and rotary tests for spin aerodynamics. Dynamically scaled subscale models, properly instrumented, are also freely flown in the large test section with a simple tether to study their dynamic stability characteristics at low speed and at high angles of attack. A small computer is used in this free-flight test technique to represent the important characteristics of the airplane flight control system.

The Langley 12-Foot Low-Speed Tunnel, which is used extensively for static tests prior to entry in the 30- by 60-ft tunnel, is an atmospheric wind tunnel with a 12-ft octagonal cross section for model testing. The tunnel serves as a diagnostic facility for exploratory research primarily in the area of high-angle-of-attack stability and control studies of various airplane and spacecraft configurations. Preliminary tests are conducted in the 12-ft low-speed tunnel on simple models prior to testing in higher speed facilities on more sophisticated models, to obtain more efficient test planning and effective use of occupancy time in higher speed facilities.

Advanced Fighter Free-Flight Tests

As part of a NASA/Grumman cooperative program to investigate the high-angle-of-attack flight dynamics of advanced fighter aircraft, free-flight tests of a 0.14-scale model of a research fighter configuration (RFC) were conducted in the 30- by 60-ft tunnel. The primary goal of the RFC design is to achieve efficient supersonic cruise as well as a high level of transonic and low-speed maneuverability. The main features of the design are a highly swept variable-twist/camber wing, a conventional vertical tail, and an all-movable canard for pitch control. The objectives of the free-flight program were to investigate high-angle-of-attack stability and control of the configuration and to study the impact of incorporating multi-axis thrust vectoring controls on these characteristics.

During the tests the model was flown unconstrained in the test section of the tunnel and was remotely controlled by pilots located at positions around the test section. Inputs from the pilots and motion sensor signals from the model were fed into a

digital computer, which generated commands to drive the control surfaces on the model. The tunnel speed was varied to fly the model at different angles of attack.

The test results showed that the basic configuration has good flying characteristics up to an angle of attack of about 28°. Above this, the stability degraded rapidly, so that controlled flight above 32° angle of attack was not possible. With the thrust vectoring system activated, controllability of the model was enhanced significantly, which allowed flight to much higher angles of attack.
(Sue B. Grafton, 2184)

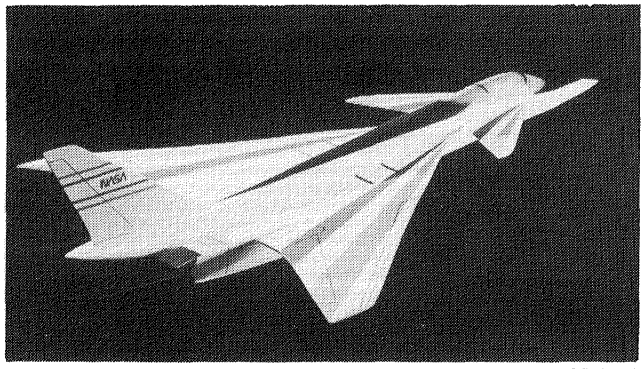

L-85-4476

0.14-scale model of research fighter configuration.

General Aviation Application of Stall/Spin-Resistant Natural Laminar Flow Wing

As part of a cooperative research program with the Cessna Aircraft Company, low-speed wind tunnel tests were conducted in the 30- by 60-ft tunnel on a full-scale modified Cessna 210 aircraft. The test aircraft was modified to include a new natural laminar flow (NLF) airfoil and a high-aspect-ratio wing that could be fitted with various wing leading-edge modifications. The NLF airfoil was designed to improve cruise performance by maintaining NLF to 70 percent wing chord on both upper and lower surfaces. The primary leading-edge modification, an outboard leading-edge droop, was designed to improve the stall/spin resistance of the aircraft by maintaining attached flow at the wing tips at and beyond the angle of attack for normal wing stall. The droop airfoil section was derived from another NLF airfoil to minimize the drag penalty of the modification.

Results of chemical sublimation tests and hot film boundary layer measurements verified the extent of NLF to 70 percent wing chord on both upper and lower surfaces. Drag measurements indicated that the large extent of NLF would be responsible for either a 10-percent increase in cruise speed and range for the same power, or a 23-percent increase in range for the same speed. Flow visualization tests conducted with the full-scale aircraft and roll damping tests conducted with a subscale model showed that the outboard droop was effective in maintaining attached flow at the wingtips and reducing unstable roll damping at the stall. Because the outboard droop was designed for NLF, it was found to be responsible for only a minor performance penalty.
(Daniel G. Murri, 2184)

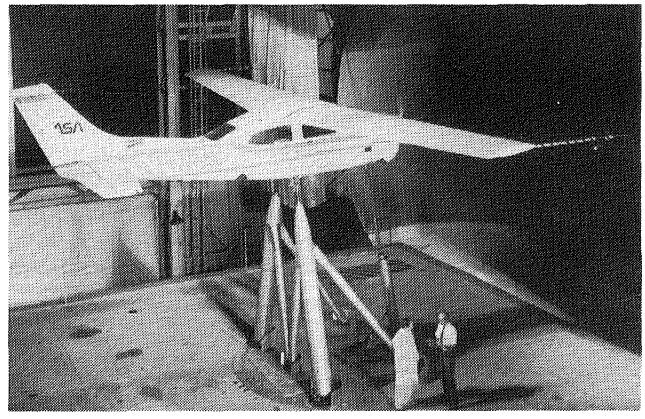

L-85-10,439

Full-scale modified Cessna 210 airplane in 30- by 60-ft tunnel.

Powered-Lift STOVL Fighter Free-Flight Tests

Free-flight tests were conducted on a 15-percent scale model of the General Dynamics E-7 configuration in the Langley 30- by 60-ft tunnel. The E-7 is an advanced supersonic fighter airplane concept that incorporates a wing ejector and a vectorable main

nozzle to provide the powered lift required for short takeoff and vertical landing (STOVL) capability. During hover and transition, attitude control is provided by small reaction jet thrusters located in the nose, wing, and tail sections. For conventional flight, control is derived from elevon and rudder surfaces. The purpose of the free-flight investigation was to study the dynamic stability and control characteristics of the configuration in hover, transition, and low-speed conventional flight. The tests covered an equivalent full-scale speed range from 0 to 150 knots. During the flights, augmentation of the basic airframe stability was provided by three-axis angular rate feedback with the gains scheduled as a function of airspeed.

Results of the investigation indicated that with an increase of reaction jet control power above the baseline design, satisfactory flying characteristics could be attained in the hover and transition flight modes. Successful flights were made from hover through transition to forward flight and in reverse sequence. Stability and control characteristics of the configuration during conventional flight were also found to be satisfactory for angles of attack up to about 30°. At higher angles of attack, however, rapid degradation in stability was observed which ultimately caused loss of control near $\alpha = 40°$.
(Donald R. Riley, 2184)

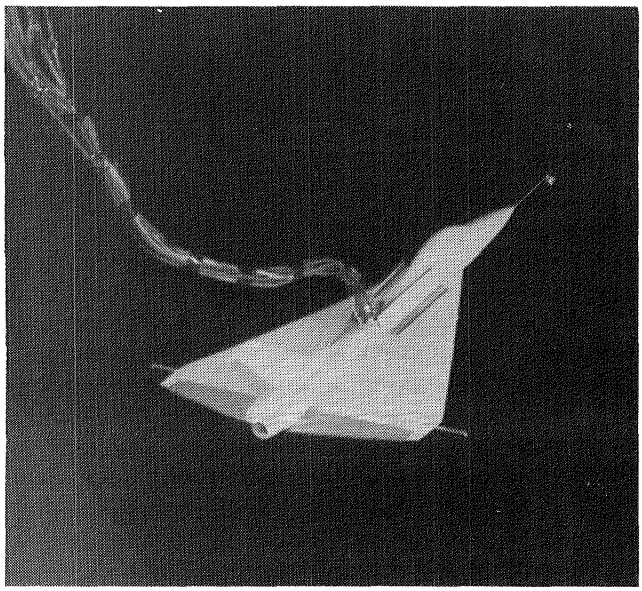

L-85-8480

15-percent scale model of E-7 configuration in 30- by 60-ft tunnel.

Crosswind Tests of Army Scout Helicopter Model

A 21-percent scale model of the Army OH-58D AHIP scout helicopter was tested in the 30- by 60-ft tunnel to investigate the potential for loss of tail rotor effectiveness in sideward flight. The primary objective of the test was to determine the wind azimuth angle at which the tip vortex from the main rotor disk would enter the tail rotor. This is a common phenomenon on single-rotor helicopters, and previous experience with the OH-58A and OH-58C helicopters indicated that the critical condition for left sideward flight azimuth would be with a yaw angle of about 57° nose right. This earlier experience was, however, based on data obtained with helicopters having two-blade main rotors, and there was some question as to the suitability of using the data for application to the OH-58D with its four-blade main rotor.

The model used in the investigation had a powered tail rotor and a four-blade general research main rotor, and included a mast-mounted sight. The model was moved through a yaw range from 10° to 100° nose right for a range of advance ratios from 0 (hover) to 0.08 (34 knots) at a simulated gross weight of 4500 lb. Smoke was injected into the tunnel windstream ahead of the model, and the smoke entrained in the rotor vortices was illuminated by high-intensity strobe lights. Analysis of flow visualization videotapes revealed that the rotor disk tip vortex ingestion

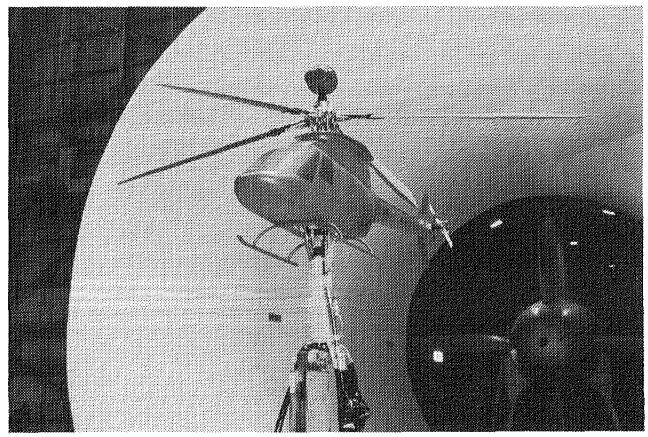

L-85-5036

21-percent scale model of Army OH-58D AHIP scout helicopter installed in 30- by 60-foot tunnel.

was somewhat less severe than for the OH-58C. The data are of particular use to flight test personnel in planning and conducting flight tests to evaluate OH-58D directional aerodynamic characteristics in cross winds.
(Susan L. Althoff, 3611)

Wind Tunnel Free-Flight Test of EA-6B Configuration

As part of a broad program to improve the cruise maneuverability of the Navy EA-6B electronic countermeasures aircraft, a high-angle-of-attack stability and control investigation was conducted in the 30- by 60-ft tunnel. The EA-6B is an electronic-warfare version of the A-6 series aircraft. Although the A-6 and the EA-6B have identical NACA 64-series airfoils, in fleet use the EA-6B routinely operates at gross weights 10,000 to 15,000 lb higher than the A-6. This higher gross weight has severely constrained the maneuvering capability of the configuration. The investigation consisted of static force tests on a 1/8.5-scale model, which was subsequently flown with the free-flight test technique in the 30- by 60-ft tunnel. The objective of the test program was to increase the maximum usable lift with an improvement in lateral-directional stability and lateral control near stall.

The investigation revealed that the maneuverability capability of the aircraft was limited because of instability that resulted from an adverse vortex flow at the vertical tail. Several modifications were developed in the test program which can be implemented easily on the fleet aircraft. The modifications consisted of airfoil contour improvements, a glove leading-edge extension, a droop extension on the inboard flap, a fin extension, and use of the speed brakes for lateral-control augmentation. The free-flight tests demonstrated that this enhanced maneuver configuration was directionally and laterally stable beyond stall with a 25-percent increase in maximum usable lift over that of the basic design.
(Frank L. Jordan, Jr., 2184)

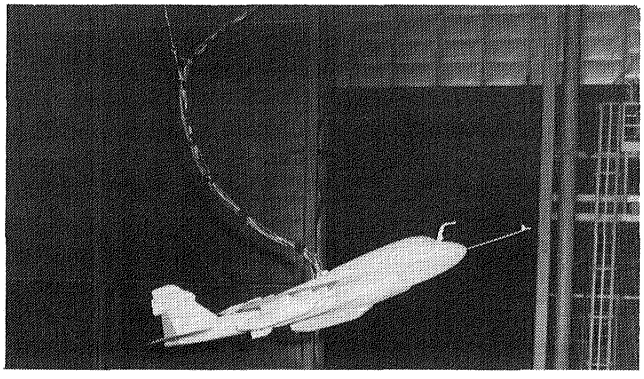

L-85-8914

Free-flight test of EA-6B configuration in 30- by 60-ft tunnel.

Aerodynamic Stability and Control Investigation of Canard-Configured General Aviation Airplane

As part of a broad research program to improve the stall/spin resistance of general aviation aircraft, wind tunnel tests were conducted on a 0.175-scale model of the OMAC laser 300 configuration in the 12-ft low-speed tunnel to determine its low-speed high-angle-of-attack aerodynamic characteristics. The model was instrumented with two internal strain gauge balances to measure the aerodynamic forces and moments as well as over 200 pressure orifices to measure pressure distributions. An air motor was installed to provide power effects. Stability and control characteristics were obtained over an angle-of-attack range from −6° to 50° and an angle-of-sideslip range from −20° to 20°. Flow field characteristics were documented with flow visualization techniques that included surface tufts to study flow separation characteristics, smoke flow to study flow field interactions, and liquid crystal oils to study boundary layer transition characteristics.

Initial exploratory testing of the basic configuration resulted in some slight planform modifications for improved static longitudinal stability. Power effects were not found to be significant on the aerodynamic characteristics, and lateral-directional stability characteristics were found to be satisfactory. Flow visualization studies indicated that the outboard region of the main wings stalled prematurely due to the upwash flow field of the canard tip vortex. As a result, an outboard wing leading-edge droop was installed and was found to be effective in keeping the

flow attached in the outboard wing area up to 35° angle of attack. Attached flow on the wing outboard panel is very desirable near stall conditions because it provides increased roll damping characteristics (i.e., reduced wing rock tendency), increased roll control authority, and increased longitudinal stability.
(Long P. Yip, 2184)

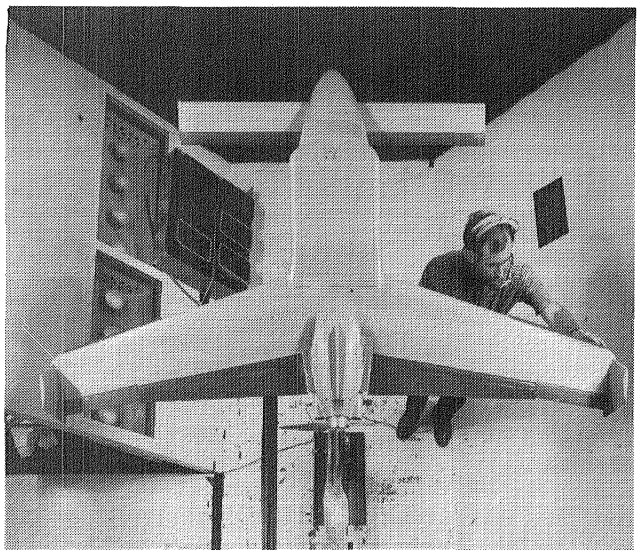

L-85-12,680

0.175-scale model of OMAC configuration installed in 12-ft tunnel.

Low-Turbulence Pressure Tunnel

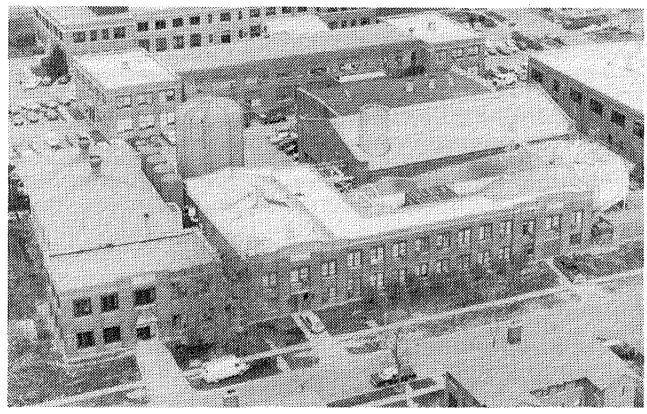

The Langley Low-Turbulence Pressure Tunnel (LTPT) is a single-return closed-circuit tunnel that can be operated at pressures from near vacuum to 10 atm. The test section is rectangular in shape (3 ft wide and 7.5 ft in height and length) and the contraction ratio is 17.6:1. The LTPT is capable of testing at Mach numbers from 0.05 to 0.50 and unit Reynolds numbers from 0.1×10^6 to 15×10^6 per foot. The tunnel has provisions for removal of the sidewall boundary layer by means of a closed-loop suction system mounted inside the pressure chamber. This system utilizes slotted vertical sidewalls just ahead of the model test section, and the removed air is reinjected through an annular slot downstream of the test section. A flow control system allows the flow and pressure requirements to be varied as dictated by tunnel operation. This system can be used to provide boundary layer control (BLC) for low-drag airfoil research.

A BLC system for high-lift airfoil testing is also available. This system utilizes compressed dry air and involves tangential blowing from slots located on the sidewall mounting endplates. Flowmeters can be used to monitor the amount of air blown into the tunnel. An automatically controlled vent valve is utilized to remove the air injected into the tunnel by this system. A high-lift model support and force balance system is provided to handle both single-element and multiple-element airfoils.

The measured turbulence level of the LTPT is very low due to the large contraction ratio and the many fine-mesh antiturbulence screens. The excellent flow quality of this facility makes it particularly suitable for testing low-drag airfoils. Recent flow quality measurements in the LTPT indicate that the velocity fluctuations in the test section range from 0.025 percent at Mach 0.05 to 0.30 percent at Mach 0.20 at the highest unit Reynolds number.

The drive system is a 2000-horsepower direct-current motor with power supplied from a motor-generator set. The tunnel stagnation temperature is controlled by a heat exchanger, which provides both heating and cooling via steam injectors and modulated valves that control the flow volume of water through a set of coils.

High-Lift Airfoil Research

Two-dimensional airfoil tests have been conducted on two different high-lift airfoils equipped with leading- and trailing-edge flaps in the Langley Low-Turbulence Pressure Tunnel. The principal objective of this cooperative research program with Douglas Aircraft Co. and the Boeing Co. was to obtain systematic data on a modern transport multielement high-lift wing section simulating full-scale Reynolds number and Mach number.

Each airfoil model was fabricated with removable leading- and trailing-edge sections. The models tested were configured both as a baseline airfoil and as a high-lift airfoil with the slat extended and a single- and a double-slotted trailing-edge flap deflected. Tests were conducted with and without sidewall blowing, and the results showed that blowing greatly improved the maximum lift and stall behavior of the high-lift airfoil. Two-dimensionality of the flow was verified with several rows of spanwise surface pressure taps on the model and fluorescent minituffs on the model and sidewall end plates.

Results showed excellent agreement between the measured model loads both with the balance and by

integration of the chordwise surface pressure distribution. All systems worked well, and demonstrated that Langley has a unique high-lift, high Reynolds number test capability. Future tests are planned for an in-house energy-efficient transport high-lift airfoil equipped with leading- and trailing-edge tangential blowing slots to delay separation and thereby increase maximum lift.
(Harry L. Morgan, 2631)

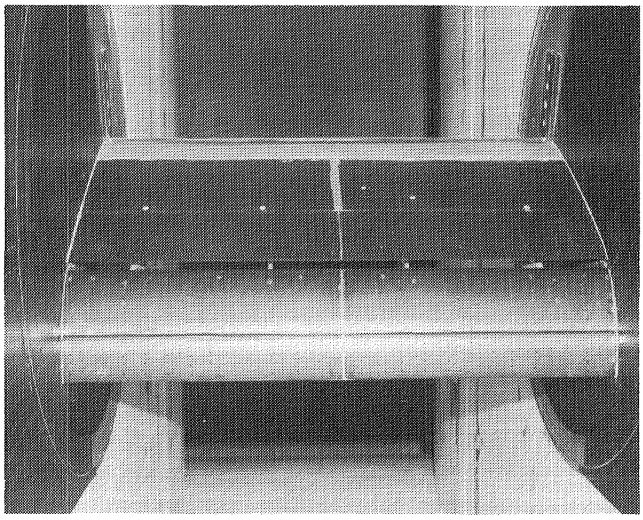

L-85-4424

Douglas high-lift model in LTPT.

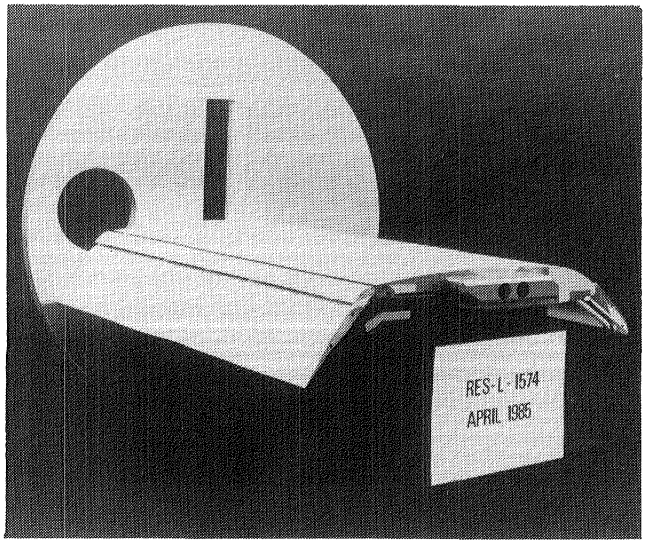

Boeing high-lift model in LTPT.

EA-6B Wing Improvement Program

The Airfoil Aerodynamics Complex recently provided substantial support to a wing improvement program for the EA-6B Navy aircraft. An objective of the joint NASA/Navy/Grumman program is to increase the aircraft maneuvering and low-speed performance through increases in the maximum lift capability of the wing. Wing modifications were addressed and were made at Langley with state-of-the-art low-speed and transonic two- and three-dimensional analysis computational techniques. The high- and low-speed performance of several modified airfoils was tested in the Langley 6- by 28-Inch Transonic Tunnel and the Low-Turbulence Pressure Tunnel, respectively.

Results of the variation of both the maximum lift coefficient ($C_{l\,max}$) with low-speed Mach number and the drag coefficient (C_d) with high-speed Mach number are shown. The high-speed drag data corresponded to a cruise lift coefficient of 0.4. The first modification indicated a definite gain in maximum lift and a significant drag penalty at high speeds. This drag penalty was unpredictable by theory, but was assumed to be associated with the trailing-edge modification. A second modification to the trailing-edge (Mod 2 T.E.) was tested, and the drag penalty was almost eliminated without any loss in maximum lift.
(William G. Sewall, 4516)

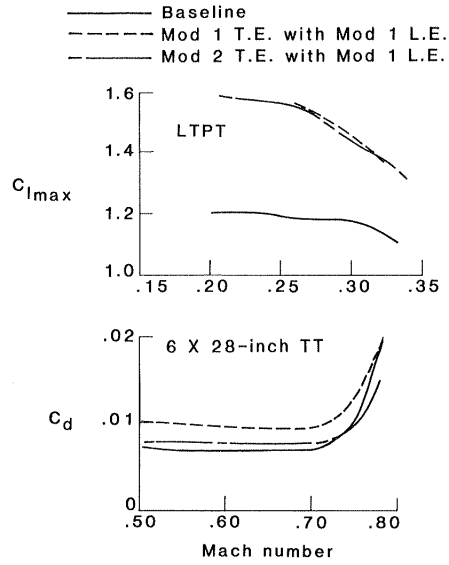

EA-6B airfoil modifications.

20-Foot Vertical Spin Tunnel

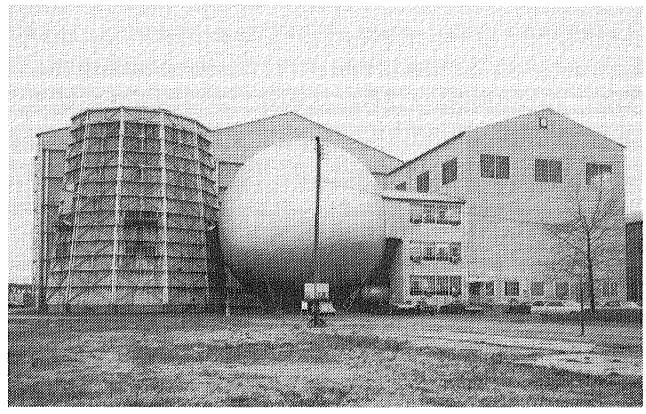

The Langley 20-Foot Vertical Spin Tunnel is the only operational spin tunnel in the United States and one of only two in the free world. The tunnel, which is used to investigate spin characteristics of dynamically scaled aircraft models, is vertical with a closed-circuit annular return passage. The vertical test section has 12 sides and is 20 ft wide and 25 ft high. The test medium is air. Tunnel speed can be varied from 0 to 90 ft/sec with accelerations to 15 ft/sec^2. This facility is powered by a 1300-horsepower main drive.

Spin recovery characteristics are studied via remote actuation of the aerodynamic controls of models to predetermined positions. Force and moment testing is performed with a gooseneck rotary-arm model support, which permits angles of attack from 0° to ±90° and sideslip angles from 0° to ±20°. Motion picture and video records are used to record the spinning and recovery characteristics in the spin tunnel tests. Force and moment data from the rotary balance tests are recorded in coefficient form and stored on magnetic tapes.

Rotary Balance Tests of Military Aircraft

Some current military aircraft that have been in the fleet for a number of years are being updated to improve performance and other characteristics to better meet today's mission requirements. The Grumman A-6 aircraft is one such aircraft. Rotary balance tests in the Langley 20-Foot Vertical Spin Tunnel have been made on the A-6 to determine if configuration changes alter the spin characteristics.

Results of the rotary balance tests showed that the modified design has some of the same characteristics as the basic A-6. That is, the horizontal tail has an adverse influence on the vertical tail, decreases damping in yaw at spinning attitudes, and decreases the rudder effectiveness for spin recovery. When the horizontal tail trailing edge is deflected up by a large angle (24°), the yaw damping is increased and the rudder becomes more effective for spin recovery.

The spin modes calculated from the rotary balance data indicated that the spin angle of attack is 55° to 60°. The results are in good agreement with the spin data obtained on the A-6 airplane and in the spin tunnel tests.

(James S. Bowman, Jr., 2521)

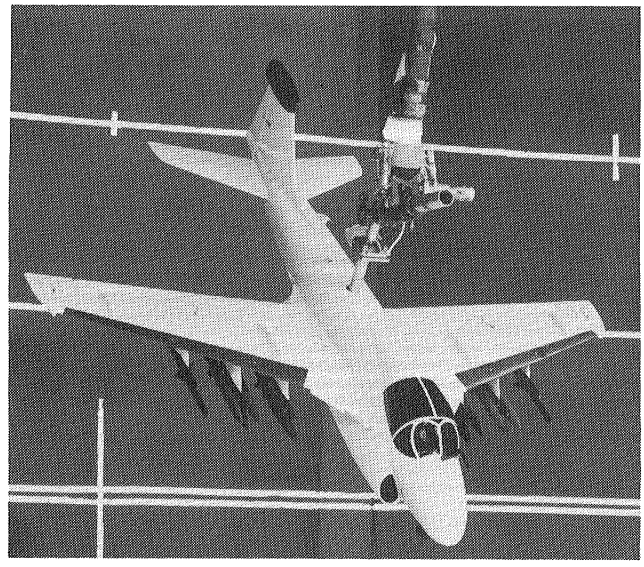

L-85-9877

Test of 1/11 scale model of A-6E airplane configuration.

7- by 10-Foot High-Speed Tunnel

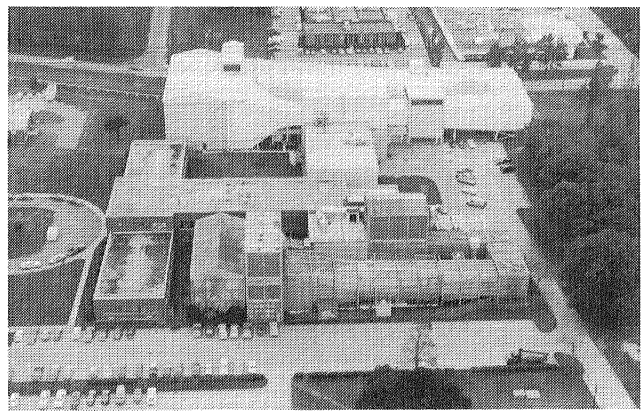

The Langley 7- by 10-Foot High-Speed Tunnel is a closed-circuit single-return continuous-flow atmospheric tunnel with a test section 6.6 ft high, 9.6 ft wide, and 10 ft long. The tunnel is fan driven and is powered by a 14,000-horsepower electric motor. It operates over a Mach number range from 0.2 to 0.9 to produce a maximum Reynolds number of 4×10^6 per foot. In addition to static testing of complete and semispan models, the facility is equipped for both steady-state roll and oscillatory stability testing.

The facility has an important role in a wide range of basic and applied aerodynamics research, including advanced vortex lift concepts, fuel-conservative aircraft design technology, highly maneuverable aircraft concepts, and the development of improved aerodynamic theories such as the difficult separated-flow and jet interaction effects needed for computer-aided design and analysis.

Pivotable Strakes for High-Angle-of Attack Control

Until recent years, strakes were viewed as fixed, highly swept inboard appendages to wings of moderate sweep. Their ability to improve the high-angle-of-attack performance of these wings is well established. The present investigation was intended to show that strakes can also be effective when articulated (pivoted) as a control device and can still retain their basic advantage.

A series of pivotable strakes was tested in combination with a 44° swept wing to determine their ability to provide pitch control at high angles of attack. The tests were carried out in the 7- by 10-foot high-speed tunnel at nominal Mach numbers of 0.3 to 0.4. A total of five strakes with various aspect ratios and shapes were tested (at negative deflection angles of 5°, 10°, 15°, and 20°) through an angle-of-attack range up to approximately 50°. In addition, a cranked delta wing with 70° sweep was tested with two different pivotable apex flaps.

The test results clearly indicated good control potential for both the pivotable strakes and the apex flaps. Lift and drag both decreased with negative strake/flap deflection, so the lift-drag ratio was little affected beyond angles of attack of 10°. Moment increments were provided primarily by the strakes themselves and not by induced effects on the wing, despite the fact that changes in the induced effects on wing lift were significant.

(Jerome T. Foughner, 2961)

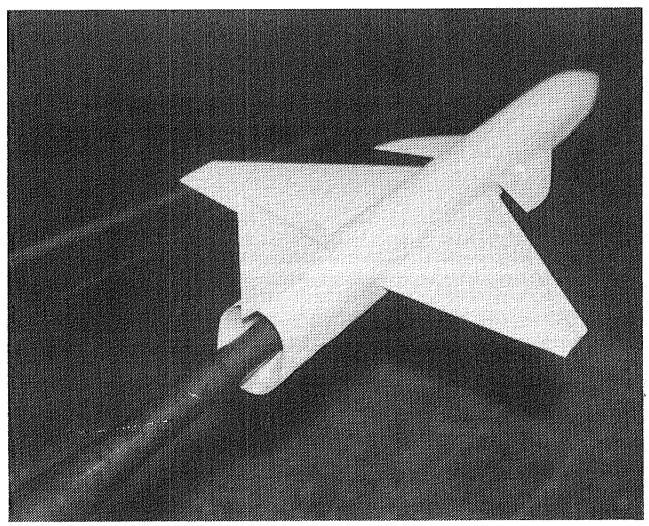

L-84-4626

44° swept-wing model with strakes deflected.

EA-6B Maneuver Improvements Modification

A cooperative test with Grumman Aerospace Corp. was conducted in the Langley 7- by 10-ft high-speed tunnel. One of the objectives of the test was to verify a Langley computationally designed wing modification for the EA-6B aircraft. An objective of the joint Navy/Grumman ADCAP (advanced capability) program for the EA-6B is to increase maneuver performance, particularly at low speeds, while maintaining high-speed cruise performance. This problem was addressed at Langley with state-of-the-art low-speed and transonic two- and three-dimensional analysis computational techniques. A modification to the leading-edge slat and trailing-edge flap was defined which yielded a predicted 14-percent increase in low-speed maximum lift coefficient with only a minimal increase in computed wave drag at high-speed cruise conditions. The modification was characterized by a blunter, slightly drooped (relative to the baseline) leading-edge slat and a cusped trailing-edge flap with a relatively thick trailing edge.

Experimental testing of the modifications was necessary to verify the computational predictions and to assess interactions and aerodynamics effects for which accurate and reliable predictions are not available (such as the effect of installed stores on high-lift performance and base drag resulting from the thick trailing edge). Data from the wind tunnel test indicated an increase of 15 percent in maximum lift for the EA-6B with seven stores at $M = 0.4$. Drag data at $M = 0.8$ showed decreased drag at lift coefficients (C_L) above 0.30 with a maximum drag increment of 0.0018 at 0.1 lift coefficient. These data provided needed verification of the computational design as well as guidance in further refinement of the design.

(Edgar G. Waggoner, 2601)

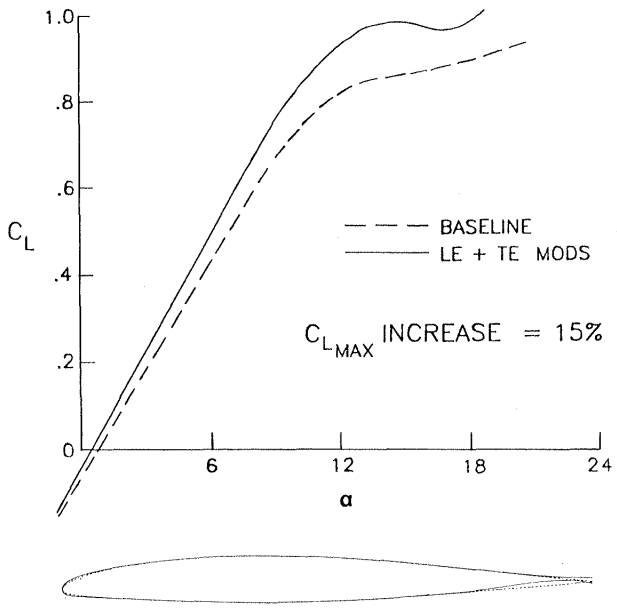

Lift characteristics of baseline and modified EA-6B aircraft with seven stores at M = *0.4.*

4- by 7-Meter Tunnel

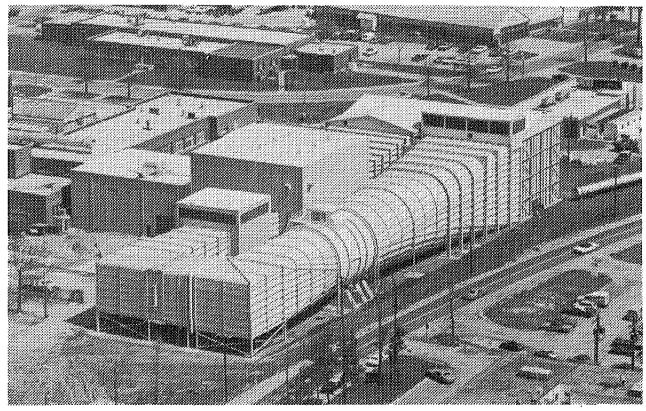

The Langley 4- by 7-Meter Tunnel (formerly V/STOL Tunnel, or Vertical/Short Takeoff and Landing Tunnel) is used for low-speed testing of powered and unpowered models of various fixed- and rotary-wing civil and military aircraft. The tunnel is powered by an 8000-horsepower electrical drive system, which can provide precise tunnel speed control from 0 to 200 knots with the Reynolds number per meter ranging from 0 to 0.64×10^7. The test section is 4.4 m high, 6.6 m wide, and approximately 15.2 m long. The tunnel can be operated as a closed tunnel with slotted walls or as one or more open configurations when the side walls and ceiling are removed to allow extra testing capability, such as flow visualization and acoustic tests. The tunnel is equipped with a two-component laser velocimeter system. Futhermore, boundary layer suction on the floor at the entrance to the test section and a moving-belt ground board for operation at test section flow velocities up to 70 knots can be installed for ground effect tests.

Modifications for improved aerodynamic and acoustic testing

Langley has recently completed significant modifications to the 4- by 7-meter tunnel to improve and expand its aerodynamic and acoustic test capability. One of the more significant aerodynamic improvements was achieved through the use of flow deflectors installed downstream of the first corner of the tunnel circuit to improve the performance of the tunnel fan. The deflectors resulted in a more uniform velocity distribution into the tunnel drive system and eliminated regions of large-scale flow separation in the return leg of the tunnel circuit.

A new turbulence reduction system consisting of a grid, a honeycomb, and four fine-mesh screens dramatically reduced the level of longitudinal turbulence intensity in the tunnel test section. This system provided a reduction in turbulence of 50 percent or more for the closed test section configuration. Periodic flow pulsations that occurred at several speeds in the unmodified configuration of the open test section were eliminated by installation of a new flow collector.

Acoustic reverberations in the open test section were reduced through the use of sound-absorbing panels on the test chamber walls. A major operational improvement was achieved through the construction of a specially designed laser velocimeter laboratory for setup and maintenance of the two-component laser velocimetry system. Finally, an addition to the model preparation area which includes a support system and rotor test cell provides the capability to assemble and test rotor models in hovering conditions prior to actual entry into the tunnel.

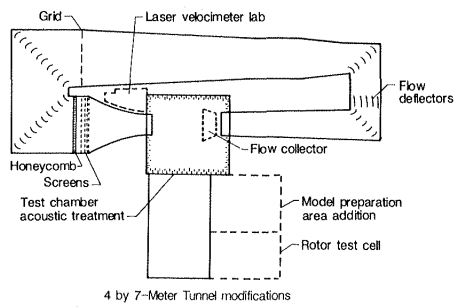

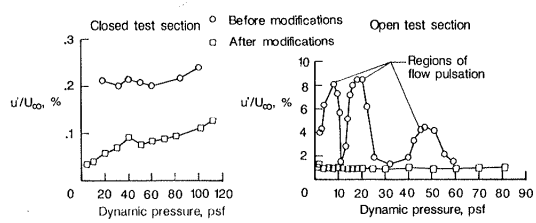

Effect of flow improvement modifications on longitudinal turbulence intensity (u'/U_∞).

Effect of Heavy Rain on Airplane Aerodynamics

Tests have continued in the 4- by 7-m tunnel to investigate the effect of rain on airplane aerodynamics. A wing section model representative of a transport airplane in a landing configuration with leading edge-slat and a double slotted flap was mounted between two large end plates and located in the back portion of the tunnel. A water spray manifold was located 25 ft upstream of the model in the forward part of the test section. The manifold produced a simulated rain environment of a very heavy rainfall. The tests were run at tunnel speeds of 112 to 159 ft/sec.

The data showed that for the extreme rain rates, the maximum lift capability of the model was reduced by 20 percent. However, because of a lack of established scaling parameters, extrapolation of these results to full scale is not possible. Tests are planned on a larger scale wing with an outdoor moving carriage facility and an overhead spray system for rain simulation. These tests will provide definitive answers on the effect of rain on aerodynamics.

(R. Earl Dunham, Jr., 3274)

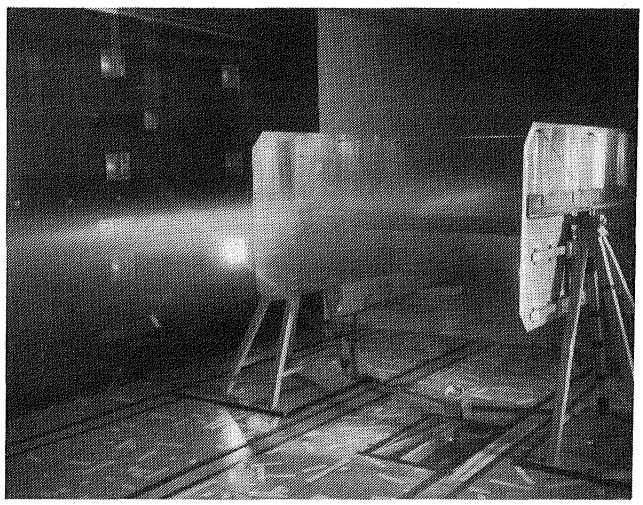

L-85-13,352

Wing section model mounted in 4- by7-m tunnel.

8-Foot Transonic Pressure Tunnel

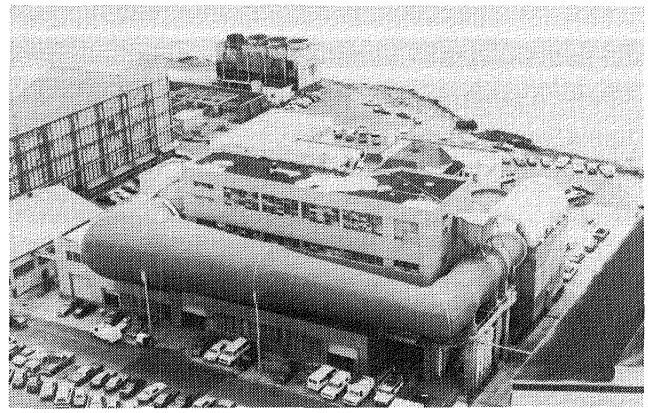

The Langley 8-Foot Transonic Pressure Tunnel is a closed-circuit single-return variable-density continuous-flow wind tunnel. The test section walls are slotted (5 percent porosity) top and bottom, with solid sidewalls fitted with windows for schlieren flow visualization. In 1982, the facility was modified for flow quality improvements and reconfigured for low-drag testing of a large-chord swept laminar flow control airfoil at transonic speeds. A honeycomb and screens were permanently installed in the settling chamber to suppress the turbulence level in the test section. A contoured liner was installed on all four walls of the test section to simulate interference-free flow about an infinite yawed wing. This contoured liner produces a contraction ratio of 25:1 and covers existing floor and ceiling slots. An adjustable sonic throat is also located at the end of the test section to block upstream propagation of diffuser noise.

The combination of honeycomb, screens, and choke provides a very low disurbance level in the test region at transonic speeds. Except for the honeycomb and screens, the changes are reversible. In the current configuration, the stagnation pressure can be varied from about 0.25 to 1.25 atm up to a Mach number of less than 0.85 with the transonic slots closed by the liner. The stagnation temperature is controlled by water-cooled fins upstream of the settling chamber. Tunnel air can be dried by a dryer that uses silica gel desiccant to prevent fogging due to expansion in the high-speed nozzle.

Laminar Flow Control Tests

Langley researchers have defined an experiment designed to investigate the physical phenomena associated with laminar flow and low-profile drag on advanced swept supercritical airfoils. Tests will allow the evaluation and documentation of the combination of suction control laminarization and supercritical airfoil technology at conditions typical of high-performance transports.

Performance testing with the laminar flow control (LFC) experiment, installed in the 8-ft TPT, has been ongoing since September 1982. Two suction concepts will be evaluated for their ability to maintain laminar flow over the same airfoil geometry for separate tunnel tests. One concept involves removal of the slow-moving air near the surface through discretely spaced fine slots along the airfoil span. The other accomplishes this by suction through porous spanwise strips.

Results to date on the swept airfoil with discrete slots indicate that full-chord suction laminarization can be achieved with very low drag up to high speeds and high Reynolds numbers. Suction laminarization over an extensive supercritical zone was also obtained for high chord Reynolds numbers before transition moved forward. The measured suction drag represents about two-thirds and the wake drag about one-third of the total drag. This drag is considerably below that for an equivalent turbulent airfoil. A comparison of measured transition results with boundary layer stability analysis indicated agreement with linear stability theory for this test. Overall slotted surface results demonstrated that LFC and supercritical airfoil technology is compatible with low drag, depending on the extent of the suction laminarization zone applied. The porous surface configuration is being installed, and testing will begin in the spring of 1986.

(William D. Harvey, 2631)

Experimental Investigation of Maneuvering Reentry Research Vehicle at Subsonic Mach Numbers

A maneuvering reentry research vehicle (MRRV) has been proposed by the Air Force as a test bed for experiments in the hypersonic flight regime. The MRRV was conceived as a vehicle that could provide flight in the hypersonic regime along trajectories that the Space Shuttle could not fly because of aerodynamic and safety concerns. The MRRV would serve as a convenient means of testing thermal protection systems, structural concepts, guidance and control systems, and other future technologies, as well as alternative flight paths for advanced reentry spacecraft.

As part of the development of the MRRV, force and moment tests were conducted on a 3.5-percent scale model of the vehicle in the Langley Diffuser Flow Apparatus, which is part of the 8-ft TPT complex. The tests were conducted at nominal Mach numbers of 0.4, 0.6, 0.8, and 0.9 in air for an angle-of-attack range from –2° to 15°. Lateral-directional data were obtained at sideslip angles of 0° and –3.3°.

The test schedule included investigations of the effects of body flap, elevon, and speedbrake deflection on pitch, as well as the effects of elevon deflections on roll, rudder effectiveness, and sideslip derivatives. In addition, three noses of different radii were tested to determine bluntness effects. Preliminary analysis of the data showed that although the basic configuration is longitudinally unstable, trim points exist for several combinations of control surface deflections for the range of Mach numbers tested.

(Gregory J. Brauckmann, 2483)

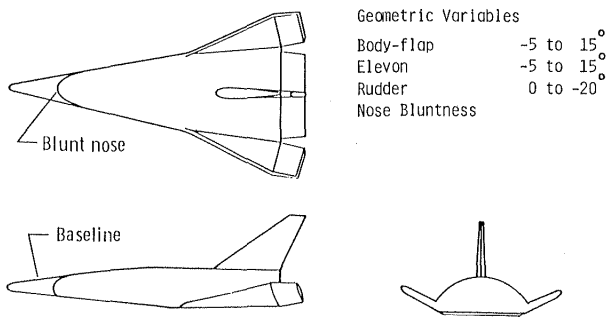

Sketch of test model.

Transonic Dynamics Tunnel

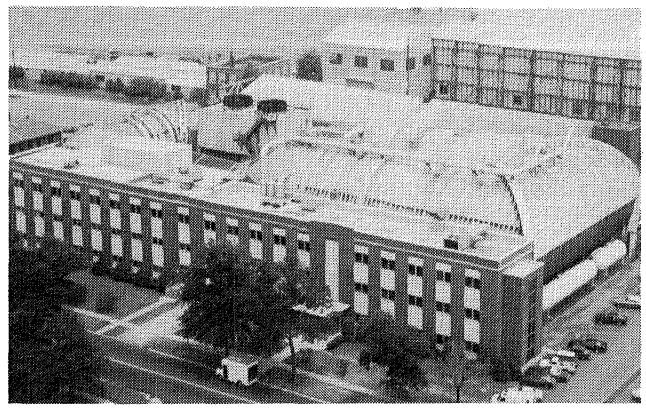

Conversion of the original Langley 19-Foot Pressure Tunnel into the Transonic Dynamics Tunnel (TDT) was begun in the late 1950s to satisfy the need for a large transonic wind tunnel dedicated specifically to work on the dynamics and aeroelastic problems associated with the development of high-speed aircraft. Since the facility became operational in 1960, it has been used almost exclusively to clear new designs for safety from flutter and buffet, to evaluate solutions to aeroelastic problems, and to research aeroelastic phenomena at transonic speeds.

The tunnel is a slotted-throat single-return closed-circuit wind tunnel with a 16-ft^2 test section. The stagnation pressure can be varied from slightly above atmospheric to near vacuum, and the Mach number can be varied from 0 to 1.2. Both test section Mach number and density are continuously controllable. The facility can use either air or Freon 12 as the test medium. Freon is usually used because it has several advantages over air as a test medium for dynamically scaled aeroelastic model testing. The tunnel has a Freon reclamation system so that the gas can be purified and reused.

The facility is equipped with many features uniquely suited to dynamic and aeroelasticity testing. These include a computerized data acquisition system especially designed to rapidly process large quantities of dynamic data, a means of rapidly reducing test section Mach number and dynamic pressure to protect models from damage when aeroelastic instabilities occur, a system of oscillating vanes to generate sinusoidal variations in tunnel flow angle for use in gust response studies, and special mount systems which enable simulation of airplane free-flight dynamic motions.

During much of 1985, the tunnel complex was being modified to provide 50-percent higher test dynamic pressures in the transonic speed range. The test medium density capability was increased by 50 percent in that speed range, which allows models to be built 50 percent heavier and still meet the mass density scaling ratios required for proper modeling of full-size aircraft. For strength considerations, this becomes very significant as full-size aircraft become more structually efficient. To provide this increased density capability, the existing fan motor was rewound to increase the power rating from 20,000 to 30,000 hp. Additional tunnel cooling capacity was provided to accommodate the increased tunnel power limit. Other major modifications included changes to the electrical power distribution system and installation of a new speed control system.

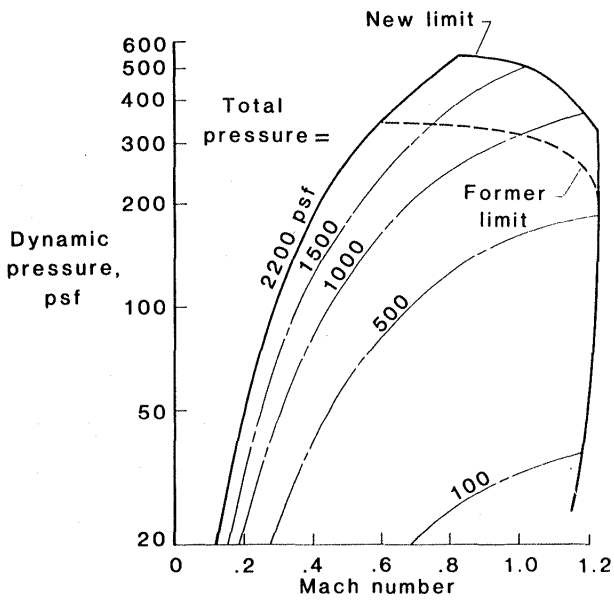

Former and present operational boundaries of TDT.

NASA Propfan Testbed Aircraft Shown Safe From Flutter in TDT Test

The NASA Propfan Test Assessment (PTA) program is under way to evaluate by flight tests the operational performance of a new propeller design (propfan). A propfan offers the advantage of high-speed flight at a 15- to 30-percent fuel savings over conventional jet engines. NASA Lewis Research Center has contracted with the Lockheed-Georgia Company to modify and fly a Gulfstream G-II airplane as a testbed with a propfan and powerplant on the left wing, as shown in the figure. The flight test article consists of an eight-blade propfan powered by a turbine engine through a gearbox. Airplane modifications included strengthening of the left inboard wing and the addition of a balance boom (approximately 2500 lbm) on the right wing and a flutter boom (approximately 300 lbm) on the left wing. To help ensure the flutter safety of this unusual asymmetric airplane, a 1/9-size flutter model was tested in the Langley Transonic Dynamics Tunnel. The test objectives were to demonstrate flutter safety margins for representative airplane configurations and to obtain flutter data for correlation with analysis.

The flutter model was furnished by Lockheed-Georgia. The tests were conducted in Freon-12 at Mach numbers up to 0.9 and at up to 1.44 times scaled flight dynamic pressures. The model was supported on a two-cable mount system and tested in a trimmed level attitude by remote control of the all-movable horizontal tail, right-wing flaperon, and rudder. The model components were elastically and dynamically scaled except that the empennage and propfan blades were overstiff and the fuselage mass properties were altered to eliminate a mount instability. In propeller-on tests, the propfans were windmilling.

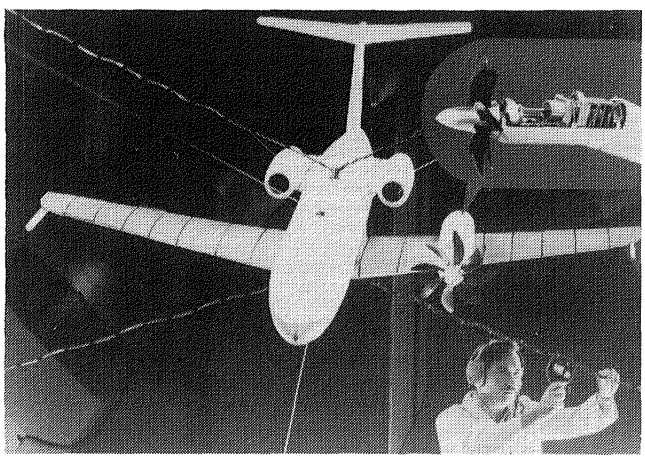

L-85-13,350

Cable-mounted flutter model in TDT. Inset shows propfan engine and nacelle simulation.

For the airplane represented by the scaled flutter model, the tests demonstrated that the propfan testbed airplane has the required flutter safety margin. Flutter test analysis correlations were good.
(Charles L. Ruhlin, 2661)

Active Control of DAST ARW-2 Wing Semispan in TDT

In 1983 tests were made in the Langley Transonic Dynamics Tunnel (TDT) with the DAST (drones for aerodynamic and structural testing) ARW-2 (aeroelastic research wing number 2) right semispan cantilevered to the tunnel wall. These tests were done primarily to obtain experimental steady and unsteady aerodynamic pressure data for use in the evaluation and refinement of new analytical codes to predict unsteady aerodynamic forces on supercritical airfoils in the transonic region. However, large-amplitude lowly damped motion that occurred in the transonic region led, by extrapolation of a measure of the damping estimates, to the prediction of an instability near a Mach number of 0.9 for a range of dynamic pressures.

A second series of tests of the right semispan was begun recently in the TDT. One of the objectives of these tests was to use an active control law to add damping in the critical mode and thereby suppress the apparent instability. Constrained optimization techniques were employed to design a control law that uses compensated acceleration feedback to drive an outboard trailing-edge control surface. The model of the plant used in the control law design was based solely upon a limited amount of forced response data available from the previous tests.

Results obtained to date in the second series of tests have shown that, although the damping in the critical mode becomes quite small and reaches a minimum near Mach 0.93, there is no instability with the control law off. The control law was turned on and was shown to increase damping significantly at test

conditions at Mach 0.92 and below. Closed-loop testing was discontinued above Mach 0.92 because visualization tests with tufts showed conditions to be well within the Mach number region in which flow was completely separated in the region of the control surface. This made the control law less effective for small deflections.

Experimental results are shown in the figure for Mach 0.85 and a dynamic pressure of 135 lb/ft^2. The figure shows the frequency response of an accelerometer output due to contol surface input for the control system off and on. It is evident that the control law has added significant damping in the critical mode.

(William M. Adams, Jr., 3744)

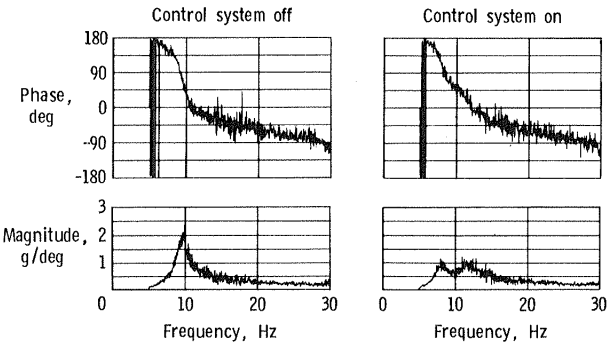

Frequency response of accelerometer output due to command control surface input.

Langley Blackhawk Rotor Design Shows Performance Improvements Over Existing Rotor

A planned Army program to upgrade the UH-60 (Blackhawk) helicopter includes the design and qualification of new rotor blades to improve performance in hover and forward flight. As part of this effort, a model of an advanced rotor blade designed at the Army Aerostructures Directorate using technology that optimized blade planform, airfoil section, twist, and solidity was tested in the TDT. The TDT was chosen because of its unique ability to use Freon-12 as a test medium. Tests in Freon-12 allow closer simulation of a full-scale aerodynamic environment than is possible in air. This better simulation was critical to an evaluation of the advanced rotor blade design.

The tests involved 1/6-size aeroelastically scaled models of both the existing baseline Blackhawk rotor and the advanced growth Blackhawk (GBH) rotor. Each of the model rotors was tested at various rotor tasks defined by aircraft gross weight and propulsive force requirements at forward speeds up to approximately 170 knots. At each test condition, measurements of main-rotor torque were made to evaluate differences in performance between the two rotors.

Some illustrative performance results in terms of the variation of horsepower required with velocity (V) are shown in the figure for a nominal design condition used by the Army, namely, 4000 ft altitude and 95° F ambient temperature. The data are also shown in nondimensional form, with rotor torque coefficient (C_Q) versus advance ratio μ. Similar results were obtained for other temperature and altitude conditions. The data indicated substantial improvements in performance for the advanced GBH blade at all forward speeds for the two gross weight conditions presented. Although the data are not shown here, the GBH rotor also showed significant performance improvements in hover (about a 5-percent increase in hover efficiency). Both the experimental hover and the forward-flight performance results are also in agreement with analytical predictions (not shown in the figure) made prior to the test with the analyses used in the GBH design process.

(William T. Yeager, Jr., 2661)

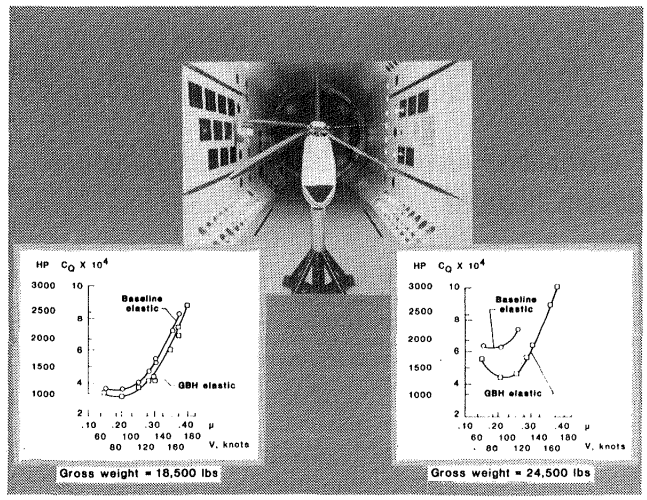

L-83-1395

Growth Blackhawk rotor blade requires less power.

16-Foot Transonic Tunnel

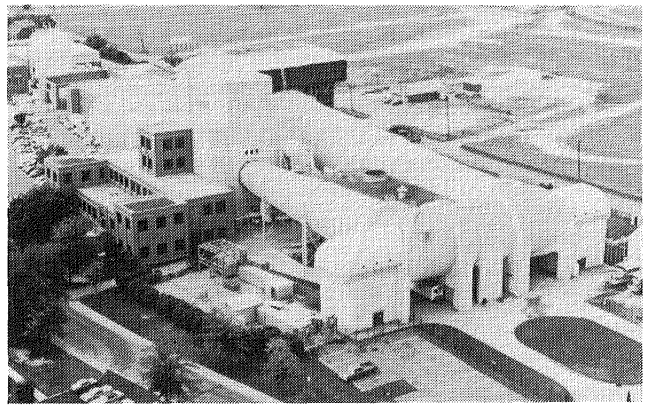

The Langley 16-Foot Transonic Tunnel is a closed-circuit single-return continuous-flow atmospheric tunnel. Speeds up to Mach 1.05 are obtained with the tunnel main-drive fans, and speeds from Mach 1.05 up to Mach 1.30 are obtained with a combination of main-drive and test section plenum suction. The slotted octagonal test section measures 15.5 ft across the flats. The tunnel is equipped with an air exchanger with adjustable intake and exit vanes to provide some temperature control. This facility has a main drive of 60,000 horsepower and a 36,000-horsepower compressor provides test section plenum suction.

This tunnel is used for force, moment, pressure, flow visualization, and propulsion-airframe integration studies. Model mounting consists of sting, sting-strut, and fixed-strut arrangements. Propulsion simulation studies are made with dry, cold, high-pressure air.

Parametric Study of Single-Expansion Ramp Nozzles

An investigation was conducted in the 16-Foot Transonic Tunnel to determine the performance characteristics of single-expansion ramp nozzles (SERN), for which the exhaust flow expansion process occurs both internally and externally. Internal expansion occurs from the nozzle throat up to the end of the nozzle lower flap, and external expansion occurs from the end of the lower flap to the end of the upper external expansion ramp. The objective of this investigation was to develop guidelines to design SERN installations with high installed performance through variation of the six external and internal geometric parameters for both convergent and convergent-divergent SERN. These results form the only data base available at forward speeds for this range of geometric nozzle parameters. This test was conducted at Mach numbers from 0.6 to 1.2 and angles of attack from −6° to 6°. The nozzle pressure ratio varied from 1 (jet off) to 10.

The results indicated that at static conditions, the convergent SERN demonstrated higher performance than the convergent-divergent nozzles. The convergent nozzles also had flat thrust performance, whereas the convergent-divergent type tended to have two performance peaks. However, the convergent-divergent nozzles had substantially higher performance at forward speeds.

(Francis J. Capone, 2673)

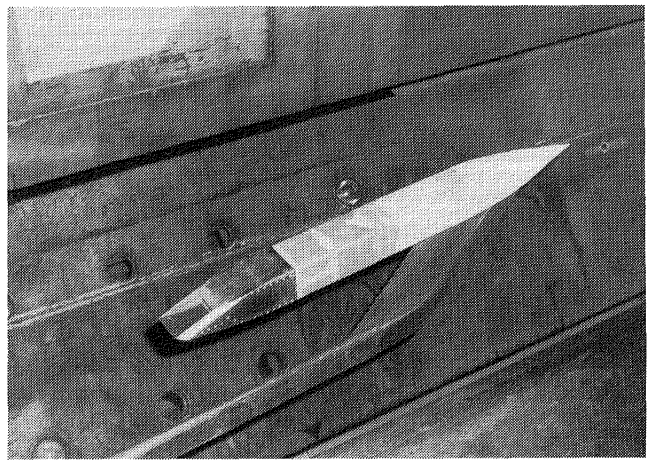

L-85-3393

Model of single-expansion ramp nozzle in 16-Foot Transonic Tunnel.

Effect of Empennage on Nozzle/ Afterbody Surface Pressures

An investigation was conducted in the 16-Foot Transonic Tunnel to study the effects of horizontal and vertical tails on the nozzle/afterbody surface pressure distributions. Past experimental investigations have shown that horizontal and vertical tails are a major contributor to the high unfavorable interference drag known to be present on high-performance fighter aircrafts. The purpose of this study, therefore, is to develop an understanding of the flow interactions associated with the integration of the empennage and to develop a set of highly accurate, detailed surface pressure data on the nozzle, afterbody, and tail surfaces. These pressure data are needed in order to verify new computational methods under development.

The investigation was conducted with a single-engine pressure model over an angle-of-attack range from –3° to 6° at Mach numbers from 0.60 to 1.20. Over 300 static pressures were measured on the surface of the model in the vicinity of the tails while nozzle pressure ratio and angle of attack were varied at each Mach number. Three empennage arrangements (aft, staggered, and forward) were investigated with a typical dry power convergent-divergent nozzle installed. The results of this study indicated that at Mach numbers between 0.90 and 1.20, the flow disturbances caused by the horizontal and vertical tails extended completely around the configuration afterbody. The data also showed that as the horizontal and vertical tails are moved closer to the nozzle, the extent of flow separation on the nozzle is increased.
(James R. Burley, 2673)

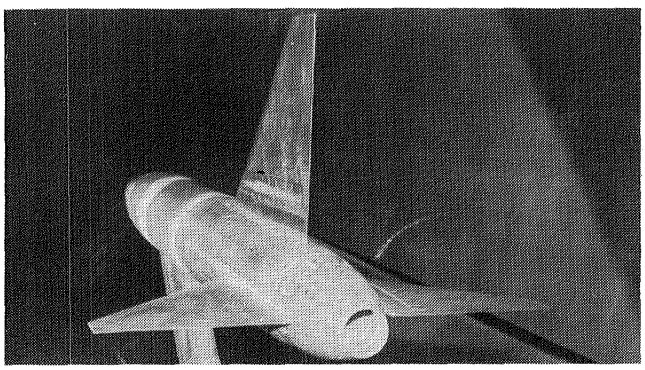

L-85-2295

Single-engine pressure model in 16-Foot Transonic Tunnel.

F-14 Yaw Vane Investigation

Most of today's high-performance fighter aircraft are limited in maneuvering capability by the fact that the lateral stability of the configurations deteriorates at the higher angles of attack. It would be desirable to enable the aircraft to maneuver even though this condition exists. One of the methods proposed to give configurations high-angle-of-attack maneuvering capability is to utilize the propulsion system and vector the exhaust for powered controls. For future configurations, the use of vectoring nonaxisymmetric nozzles will provide the desired maneuvering capability. However, for existing configurations this solution will not be possible, and other methods will have to be developed. One of the proposed solutions for an existing aircraft, the Navy F-14, is to mount vanes on the aircraft afterbody which can be rotated into the exhaust flow to vector the exhaust and produce the desired yawing moment and side force. This concept has previously been investigated at low speeds and has shown promise. The present investigation was initiated to determine the effectiveness of the concept at high subsonic and transonic speeds as installed on the F-14.

The yaw vane concept was investigated on a 1/12-scale propulsion model of the F-14 in the 16-Foot Transonic Tunnel at Mach numbers from 0.7 to 1.25. The figure shows the F-14 with the cruise nozzle configuration and the yaw vanes installed. Yaw vane

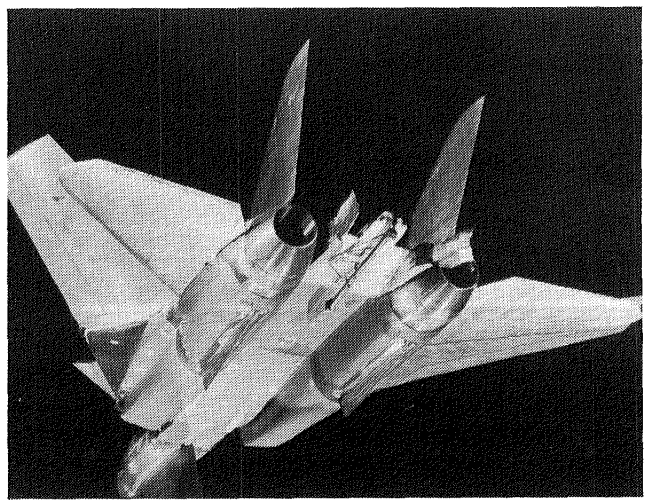

L-85-4242

F-14 propulsion model with yaw vanes installed in 16-Foot Transonic Tunnel.

deflections of 0°, 10°, and 20° were tested. Preliminary results from this investigation showed that the yaw vanes produced yawing moments equivalent to values produced by moderate deflections of the vertical tails.
(David E. Reubush, 2673)

Flow Field Measurements for a Jet Exhausting From Nonaxisymmetric Nozzle Configuration

A test was conducted in the Langley 16-Foot Transonic Tunnel to determine the characteristics of the jet exhausting from a nonaxisymmetric nozzle configuration. The purpose of the tests was to provide detailed pressure data that can be used to verify emerging computational fluid dynamic codes to predict three-dimensional exhaust nozzle flows at transonic speeds. A translating, rotating survey mechanism was used to measure the pitot pressures in the nozzle exhaust at five axial locations downstream of the nozzle exit. The model had a rectangular exhaust nozzle, with the exit area 1.25 times the throat area and a ratio of exit width to height of 1.90. The internal sidewalls of the nozzle were parallel and the upper and lower flaps had an internal divergence angle of 2.56°. The external sidewalls had a boattail angle of 6.93° and the upper and lower flaps had a boattail angle of 17.56°. The tests were conducted at free-stream Mach numbers of 0, 0.6, and 1.2 with the jet operating at a nozzle pressure ratio of 4.0. The ratio of jet stagnation temperature to free-stream stagnation temperature was about 1.0. The Reynolds number of the free stream was about 4×10^6 per foot.

In addition to providing data for code verification, at free-stream Mach numbers of 0.6 and 1.2 the flow field measurements showed evidence of a vortex-like flow near the external corners of the nozzle. This vortex flow was probably caused by the difference in pressures on the sidewall and the upper and lower flaps. At Mach 0.6 the vortex flow dissipated downstream of the nozzle exit. At Mach 1.2, however, the vortex interacted with the shear layer and enhanced the mixing between the jet and the external stream.
(L.E. Putnam, 2673)

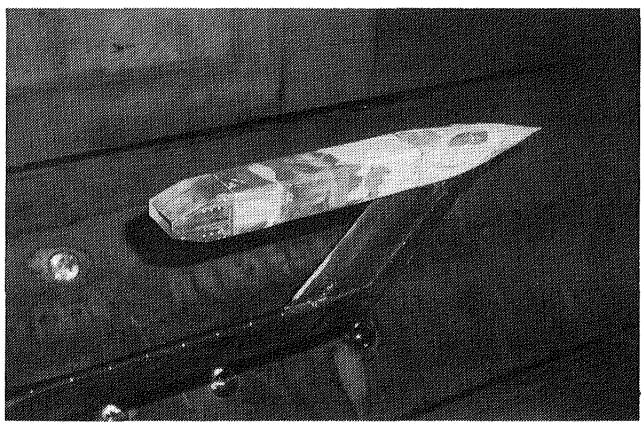

L-80-6676

Nonaxisymmetric nozzle in 16-Foot Transonic Tunnel.

National Transonic Facility

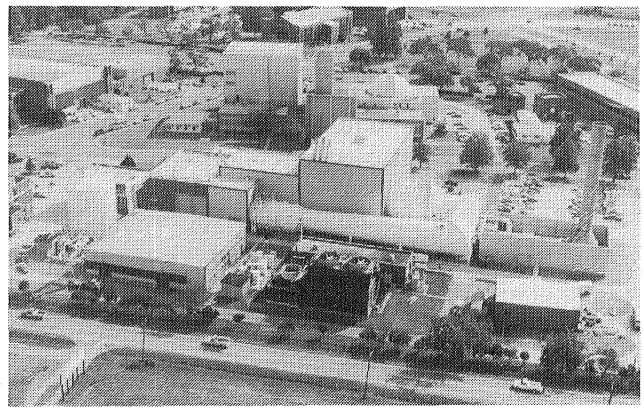

The most difficult aerodynamic regime for aircraft designers to understand is the transonic region, where speeds near Mach 1 (760 mph at sea level) are attained. At these speeds, the flow around an aircraft is distorted by shock waves, and the resulting turbulence decreases lift and increases drag in such complex patterns that designers cannot accurately predict the results. To develop a test facility that would allow full-scale testing of aircraft at such speeds would be very costly and would require an enormous power supply.

NASA Langley's approach to this problem was to use nitrogen gas at high pressures and ultralow temperatures to simulate the transonic flow about a model aircraft that is representative of the full-sized aircraft. The principle that allows this simulation is that even if the sizes, speeds, and altitudes of two aircraft are very different, the aerodynamic properties of the flow about them will be identical if the Reynolds number (a parameter describing the flow which is a function of aircraft size and speed as well as of the density and viscosity of the flow) and the Mach number are the same for the two aircraft. The use of ultralow temperatures in the National Transonic Facility provides Reynolds numbers for small models which are identical to those of full-sized aircraft.

The NTF is a cryogenic fan-drive transonic wind tunnel designed to provide full-scale Reynolds number simulation in the critical flight regions of most current and planned aircraft. It can operate at Mach numbers from 0.2 to 1.2, stagnation pressures from 1 to 9 atm, and stagnation temperatures from 340 to 80 K. The maximum Reynolds number capability is 120×10^6 at a Mach number of 1.0, based on a reference length of 0.25 m.

Construction of the National Transonic Facility was completed in September 1982, and checkout operations started the following month. The maximum Reynolds number was obtained in May 1983. Efforts were then directed toward installation of the model access housings and adjustment or alteration of various tunnel hardware systems. In August 1984 the tunnel was declared operational and was turned over to the user organization for aerodynamic calibration and research and development testing. In December 1984 the first aerodynamic vehicle, Pathfinder I, was installed for checkout of instrumentation systems.

Pathfinder I

The Pathfinder I model is an advanced transport configuration with a high-aspect-ratio supercritical wing. The initial test entry in the NTF served to check out the model instrumentation and associated data acquisition and reduction programs. The on-board

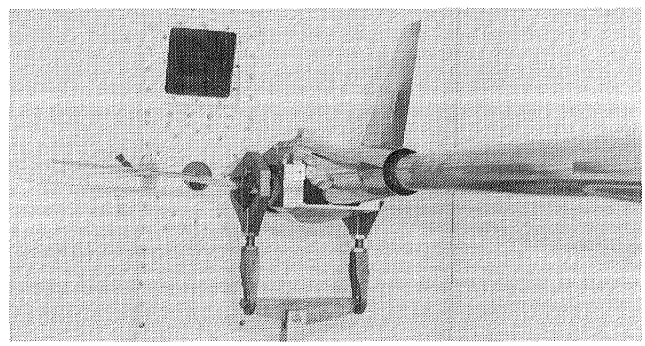

L-84-13,025

Check loading of Pathfinder I model in cryogenic chamber.

instrumentation includes a six-component strain gauge force balance, six electronically scanned pressure modules, an accelerometer type angle-of-attack unit, an electrolytic bubble, and type T thermocouples. Before the Pathfinder was installed in the test section, the model was assembled and statically loaded in a model assembly bay at room temperature primarily to check the balance and software programs. The Pathfinder was then statically loaded at cryogenic temperatures in a cryogenic chamber to check for temperature effects.

Tunnel tests were performed in December 1984 in air at temperatures of approximately 320 K, and in January 1985 tests were performed in nitrogen at temperatures down to 116 K. This initial checkout was considered to be highly successful, with all instrumentation systems operating.
(P.F. Jacobs, 2601)

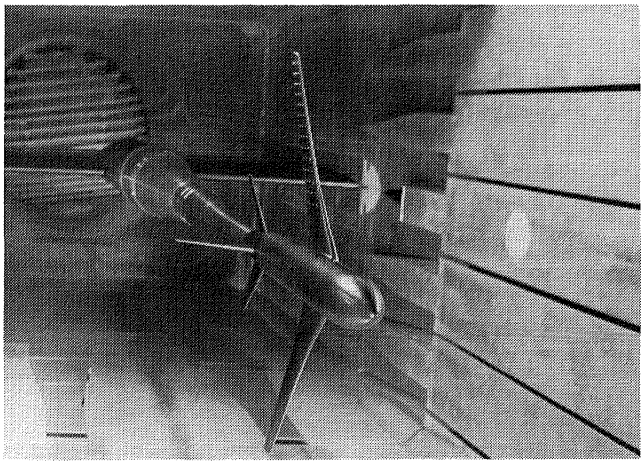

L-84-13,652

Pathfinder I model installed in NTF.

Shuttle Ascent Wing Loads

Shuttle orbiter wing loads measured during ascent differ from wing loads predicted by wind tunnel data. These differences have caused the launch configuration and trajectory parameters to be altered from those desired for optimum performance.

A research program was undertaken in the NTF to better define wing loads through tests at high Reynolds number and to assess the effectiveness of spoilers to reduce wing loads. In addition, the effect of the tank asymmetries on wing loading was investigated. A 0.01-scale model was instrumented with wing, tank, and various base pressures, wing and tank thermocouples, and a wing balance. Solid-body exhaust plume simulators were installed. The model was tested over the Reynolds number range from 5×10^6 to 120×10^6 at Mach numbers from 0.80 to 1.20. Results indicated that the spoilers were effective in reducing wing loads over the Reynolds number and Mach number ranges tested.
(Jerry B. Adcock, 2601)

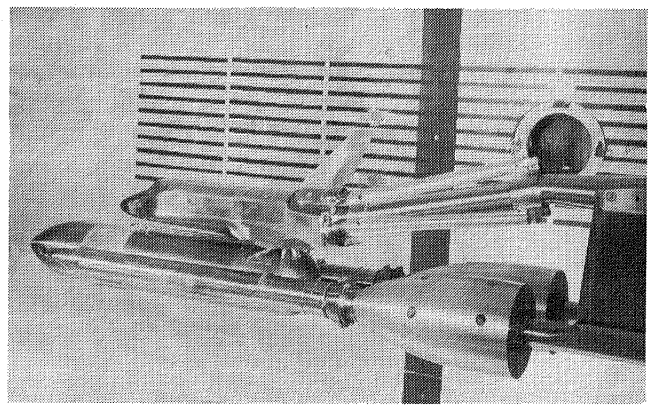

L-85-1774

Scale model of shuttle ascent configuration mounted in NTF.

F-14A Laminar-Flow Wing Design

An F-14A model with modified outer wing panels was tested in the NTF in support of the variable sweep transition flight experiment (VSTFE). The objective of this flight research is to obtain in-flight wing pressure and boundary layer data that will be used to develop a reliable laminar-flow transition prediction method. Two different modifications have been computationally designed for the upper surface of the outer wing panel to yield favorable pressure gradients over a range of Reynolds numbers, lift coefficients, and wing sweep angles. Langley designed a contour modification corresponding to an $M = 0.7$ design condition, and the Boeing Company designed

a modification for an $M = 0.8$ design condition. The designs had been analyzed with various three-dimensional transonic analysis codes that include integrated viscous effects.

It was necessary to experimentally verify the designs and to obtain performance data on the modified configuration before modification of the actual aircraft commenced. The wind tunnel data verified the computational predictions over the entire outer panel except in a region very near the intersection of the outer wing panel and over wing fairing leading edges. In this complex flow region, the experimental data indicated an adverse pressure gradient that was not evident in the computations. These data are being relied on to help define minor contour modifications in this region.

(E.G. Waggoner, 2601)

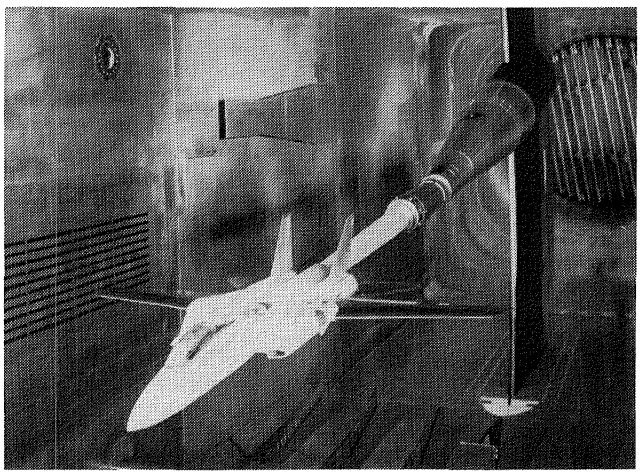

L-85-14,119

Scale model of F-14A mounted in NTF.

EA-6B Maneuver Improvement Modifications

A cooperative test with Grumman Aerospace Corp. was conducted in the NTF. Objectives of the test were to verify computationally designed wing modifications of the EA-6B aircraft to increase low-speed maximum lift, to assess Reynolds number sensitivities of the wing modifications, and to verify experimentally defined configuration modifications to improve lateral-directional stability. The various modifications had previously been tested individually, but not in combination. Hence, interference effects and interactions needed to be assessed.

NTF data verified the computational predictions, the two-dimensional experimental data on the wing section modifications, and the lateral-directional modifications experimentally defined during low-speed tests of the EA-6B configuration. Data from the NTF test also indicated a significant Reynolds number effect on maximum lift coefficient. At a Mach number (M) of 0.3 and a Reynolds number (Re) of 1.4×10^6, the maximum lift coefficient was increased by the addition of a trailing-edge flap modification. However, no additional improvement in maximum lift was observed when the modified leading-edge slat was added. When the Reynolds number was increased by approximately a factor of 4 at the same Mach number, the maximum lift coefficient increased not only with the modifications to the trailing edge but also with the modifications to the leading edge.

(E.G. Waggoner, 2601)

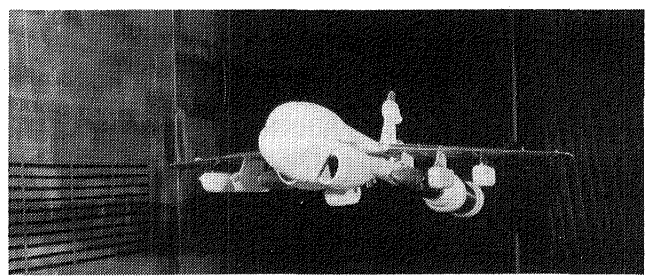

L-85-11,553

Scale model of EA-6B mounted in NTF.

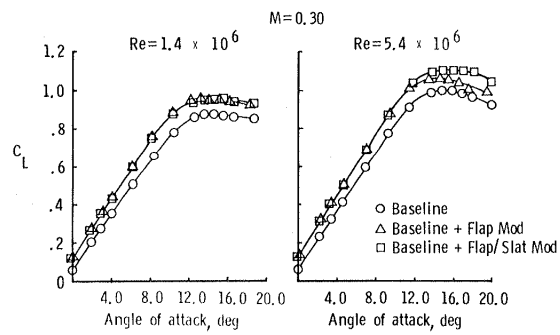

Effect of flap and slat modifications on low-speed lift characteristics for EA-6B.

0.3-Meter Transonic Cryogenic Tunnel

The Langley 0.3-Meter Transonic Cryogenic Tunnel (TCT) is a continuous-flow fan-driven transonic tunnel that uses nitrogen gas as a test medium. It is capable of Mach numbers up to about 1.0, stagnation pressures up to 6 atm, and stagnation temperatures from 340 to about 80 K. The tunnel has been designed to permit different test sections to be installed in the circuit.

The facility was placed in operation in 1973 as a three-dimensional pilot tunnel to demonstrate the cryogenic wind tunnel concept at transonic speeds. The original test section was octagonal and was designed with a manually driven sting type model support system. The successful demonstration of the cryogenic concept in the 0.3-m TCT played a major role in the decision to build the National Transonic Facility. In 1975, the three-dimensional test section was replaced with an 8- by 24-in. two-dimensional test section with slotted top and bottom walls. The two-dimensional test section has motorized model support turntables and a traversing wake survey probe, both of which are computer controlled. At the maximum test condition with a 6-in. model, a chord Reynolds number of 50×10^6 is possible. In 1985, the 8- by 24-in. test section was replaced with a 13- by 13-in. adaptive wall test section designed for two-dimensional testing.

Adaptive wall test section

Shakedown tests on the new adaptive wall test section for the 0.3-m TCT will begin in early 1986. This new test section, which was installed during 1985, is configured for two-dimensional testing. The test section is 55.8 in. long and 13 by 13 in. in cross section at the entrance. All four walls are solid, and the top and bottom walls are flexible and movable. The flexible walls are made of 304 stainless steel and are 71.7 in. long. A 4.1° bend was manufactured into the flexible wall so that the rear 15.9 in. of the flexible walls provide a smooth transition between the end of the test section and the beginning of the fixed diffuser.

The flexible walls are fixed at the upstream end of the test section, whereas the downstream ends are fixed vertically but are free to translate longitudinally

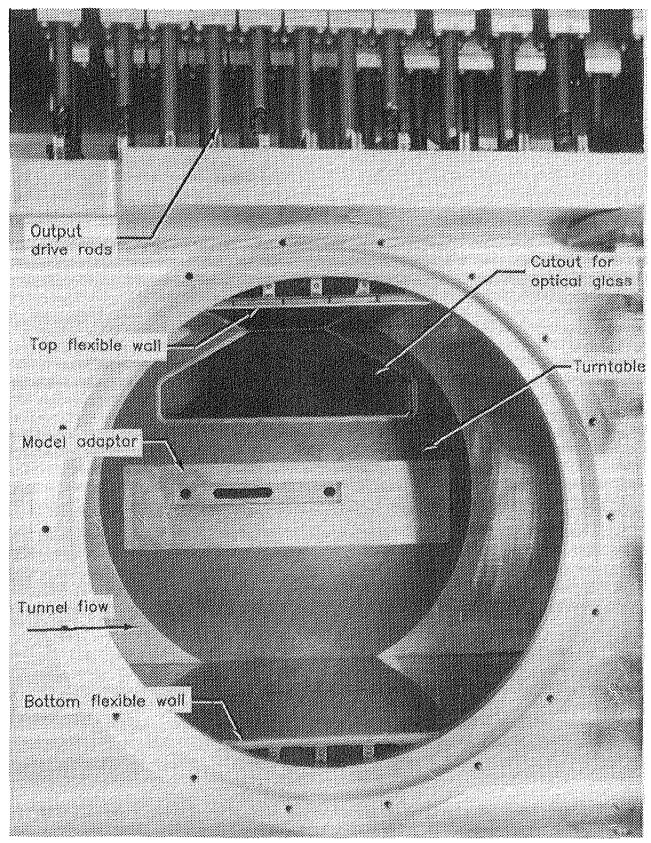

View of test section with pressure wall and nearside turntable removed.

as the wall shape changes. This translation of the flexible wall produces a misalignment between the output drive rods and the attachment fitting on the flexible wall. The attachment fitting is an integral part of the flexible wall. The fitting has a cutout to allow the attachment to bend relative to the flexible wall. A beryllium-copper plate is used to connect the attachment fitting to the output drive rods.

The model mounting system, shown in the figure, is designed for two-dimensional models. The model is supported between two turntables centered 30.7 in. downstream from the entrance of the test section. Models with chords up to 13 in. can be tested over an angle-of-attack range of $\pm 20°$. The turntables are driven by a stepper motor and gearbox mounted externally to the tunnel. Two cutouts are provided in the turntable. The center cutout accepts an adapter to retain the model at the desired position. The use of different adapters enables the model location to be varied relative to the center of the test section. The upper cutout provides a mounting for an optical-quality window for viewing the model during flow visualization experiments. It should be noted that semispan models can be tested with only one of the mounting turntables.

Unitary Plan Wind Tunnel

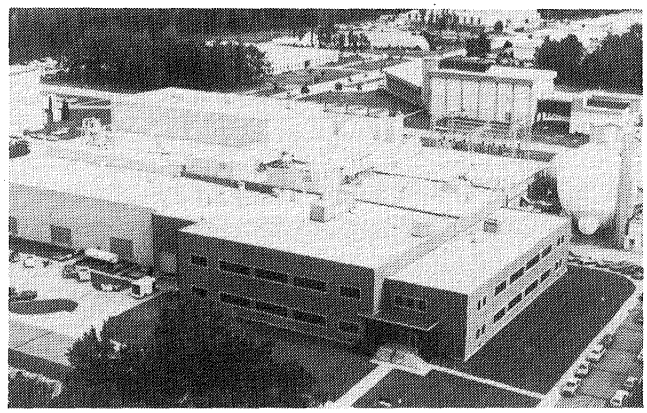

Immediately following World War II, the need for wind tunnel equipment to develop advanced airplanes and missiles was recognized. The military and the National Advisory Committee for Aeronautics (NACA) developed a plan for a series of facilities which was approved by the U.S. Congress in the Unitary Wind Tunnel Plan Act of 1949. This plan included five wind tunnel facilities, three at NACA laboratories and two at the Arnold Engineering Development Center. The Langley Unitary Plan Wind Tunnel was among the three built by NACA. The Unitary Plan Wind Tunnel is a closed-circuit continuous-flow variable-density tunnel with two 4- by 4- by 7-ft test sections. The low-range test section has a design Mach number range of 1.5 to 2.9 and the high-range section Mach number varies from 2.3 to 4.6. The tunnel has sliding-block type nozzles which allow continuous variation in Mach number while on-line. The maximum Reynolds number per foot varies from 6×10^6 to 11×10^6 depending on Mach number. The tunnel is used for force and moment, pressure distribution, jet effects, dynamic stability, and heat transfer studies. Flow visualization data, which are available in both test sections, include schlieren, oil flow, and vapor screen.

Investigation of Planform Effects on Multibody Configurations

An experimental and theoretical program has been established to investigate the supersonic aerodynamics of multibody concepts and to define multibody aerodynamic design logic and goals. Initially, a wind tunnel test of two axisymmetric bodies set on a rectangular planform was conducted to generate a data base and evaluate existing theoretical methods. Based upon these results, a second multibody wind tunnel model was designed, constructed, and tested.

This second multibody model consisted of a center wing/balance housing system to which various sidebodies and outboard wing panels could be attached. The first wind tunnel test on this model determined the impact of sidebody shaping on both longitudinal and lateral-directional characteristics.

A second wind tunnel test was conducted on the model with three different outboard wing panel planforms. Forces and moments were measured at Mach numbers of 1.6, 1.8, 2.0, and 2.16 over a range of angles of attack and angles of yaw. Test results from this study showed the variation in lift and drag-due-to-lift characteristics with planform shape to be similar to that of single-body configurations. However,

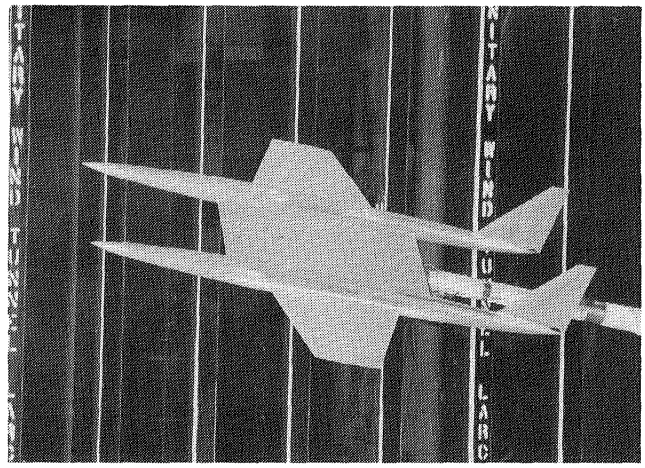

L-85-10,460

Multibody model with trapezoidal wing panels.

the zero-lift wave drag, which varies considerably with planform shape on single-body configurations, did not vary appreciably on the multibody configuration.
(S. Naomi McMillin, 4008)

Store-on-Store Interference Drag Study

The requirement for the next-generation fighter aircraft to have supersonic cruise capability has resulted in the need for supersonic store carriage design guidelines to minimize the zero-lift drag increment due to the stores. In order to develop these guidelines, an experimental study was undertaken to determine the store-on-store interference drag of a series of generic stores mounted in various arrays on a flat plate. The generic stores were cylinders whose nose and afterbody shapes were hemispheres, ogives, and flat surfaces. The various arrays consisted of either two or three stores tangent and semisubmerged mounted in a lateral, tandem, or staggered configuration. A portion of the flat plate was segmented from the plate and is identified as a pallet. The pallet was mounted on one of three dedicated one-component drag balances so that the top surface of the pallet was flush with the plate surface. One of the generic stores was mounted on the metric pallet and the remaining stores were mounted on the nonmetric flat plate. This arrangement allowed the drag of only one store to be measured as the position of the other nonmetric stores was varied. This method permits very accurate store-drag measurements because the one-component drag balance can be sized to measure the drag of only one store. These tests were conducted at Mach numbers of 1.6, 1.9, 2.16, and 2.86 and a Reynolds number of 2.00×10^6 per foot.

Initial test results indicated that for a two-store lateral array, the hemispherical nose and afterbody store showed a favorable store-on-store interference effect at small separation distances and a decrease in favorable interference as the stores were separated. In contrast, an ogive nose and afterbody store in the same type of array showed an unfavorable interference effect at small separation distances and a decrease in unfavorable interference as the stores were separated. The test results indicated that the drag of the stores depends on the type of array (lateral, tandem, staggered), the position of the store in the array, the relative distances between the stores in the array, and the store shape.
(Floyd J. Wilcox, Jr., 4010)

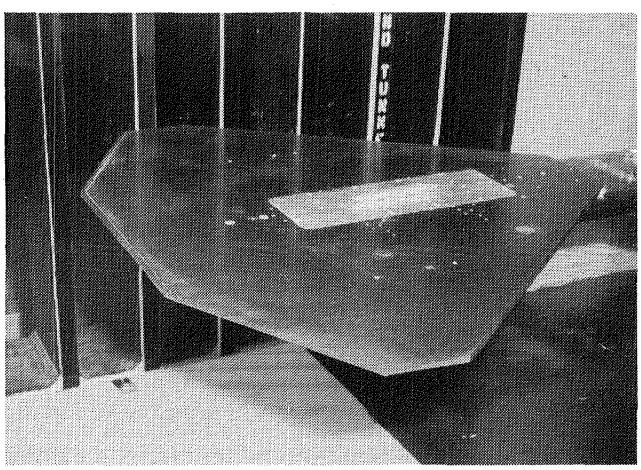

L-85-6678

Single store mounted on flat plate in UPWT.

Separated Flow Flap Study

Over the past 40 years, the understanding of wing leading-edge separated flows at supersonic speeds has not been pursued, theoretically or experimentally, with the same vigor as for attached flows. The reasons for this lack of parallel growth in the two wing design concepts are many, but the two major contributors are the theoretical complexity involved in modeling separated flows and the belief that separated flows at supersonic speeds will always produce large drag penalties. An examination of the existing data base for sharp-leading-edge delta wings raises some doubts about the validity of this second assumption for high-lift conditions. The data suggest that significant improvement in aerodynamic performance can be obtained through the management of wing leading-edge vortices. This present wind tunnel test was conducted to obtain supersonic data on a series of four cambered delta wings of the same planform. Each wing in the series varied in leading-edge deflection only. The supersonic data will be used for method validation and the development of a separated flow wing design logic.

The wind tunnel models were a series of four cambered delta wings of 75° leading-edge sweep. Wing camber consisted of a deflection of the outboard 30 percent of the local wing semispan. Leading-edge deflections were 0°, 5°, 10°, and 15°, measured streamwise. Force, pressure, and flow visualization data were obtained at Mach numbers from 1.5 to 2.8, angles of attack from –4° to 20°, and angles of sideslip from 0° to 8°.

Preliminary results indicated that a vortex system can be positioned on a deflected leading edge at supersonic speeds, and that a 15-percent increase in maximum lift-to-drag ratio results. The data also showed that overdeflection of the leading edge results in massive hinge line separation, which dominates the leading-edge vortex system.

(Richard M. Wood, 4926)

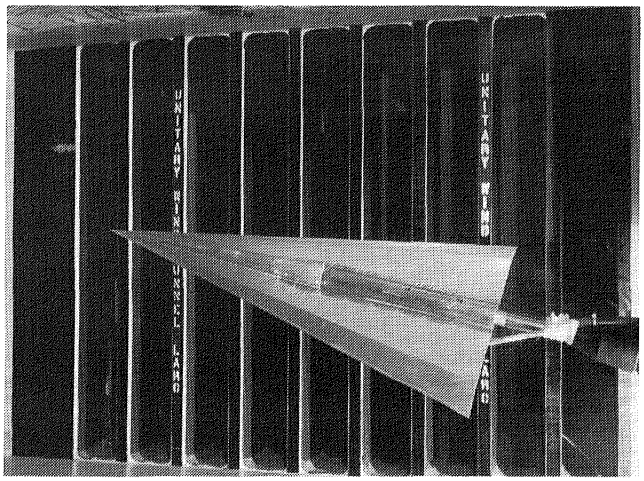

Cambered delta wing with deflected leading-edge flap.

Hypersonic Facilities Complex

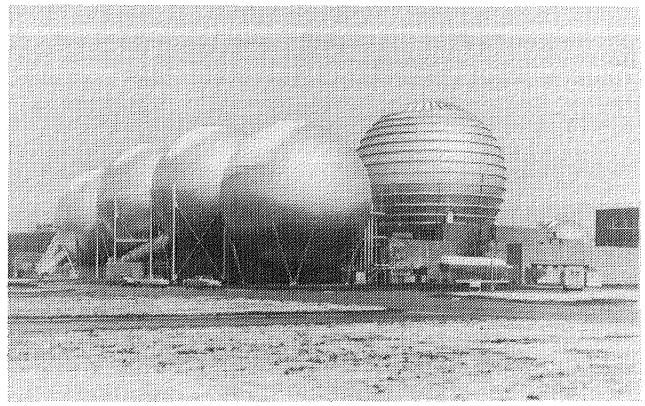

The Hypersonic Facilities Complex consists of several hypersonic wind tunnels located at four Langley sites. They are considered as a complex because these facilities represent a major unique national resource for wind tunnel testing. The complex currently includes the Hypersonic CF_4 (tetrafluoromethane) Tunnel (M = 6), the Mach 6 High Reynolds Number Tunnel, the 20-Inch Mach 6 Tunnel, the Mach 8 Variable-Density Tunnel, the 31-Inch Mach 10 Tunnel, the Hypersonic Nitrogen Tunnel (M = 17), and the Hypersonic Helium Tunnel and its open jet leg (M = 20). These facilities are used to study the aerodynamic and aerothermodynamic phenomena associated with the development of advanced space transportation systems, including future orbital-transfer and launch vehicles; to support the development of advanced military spacecraft capability; to support the development of future planetary entry probes; to support the development of hypersonic missiles and transports; to perform basic fluid mechanics studies, to establish data bases for verification of computer codes, and to develop measurement and testing techniques.

This complex of facilities provides an unparalleled capability at a single installation to study the effects of Mach number, Reynolds number, test gas, and viscous interactions on the hypersonic characteristics of aerospace vehicles. Approximately half the current testing in these facilities is classified, thus restricting the amount and content of test results that can be reported in the open literature.

20-INCH M-6 TUNNEL
M_∞ = 6 AIR R_∞ 0.7-9.0x10^6

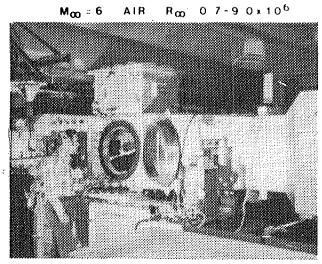

M-8 VAR.-DENS. TUNNEL
M_∞ = 8 AIR R_∞ = 0.1-10.7x10^6

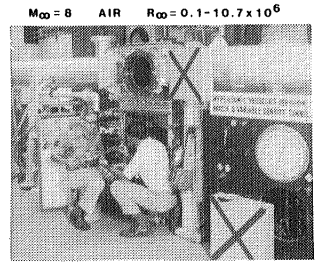

31-INCH M-10 TUNNEL
M_∞ = 10 AIR R_∞ = 0.4-2.4x10^6

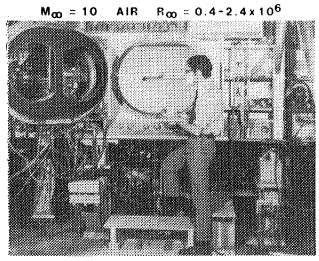

NITROGEN TUNNEL
M_∞ = 17 N_2 R_∞ = 0.35x10^6

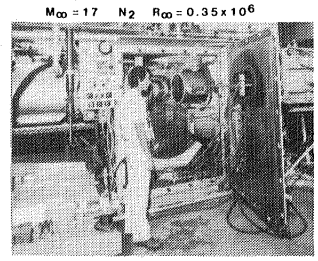

CF_4 TUNNEL
M_∞ = 6 CF_4 R_∞ = 0.25-0.55x10^6

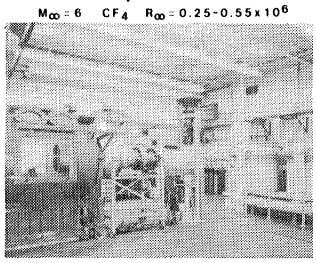

HIGH R_∞ M-6 TUNNEL
M_∞ = 6 AIR R_∞ = 0.8-42.0x10^6

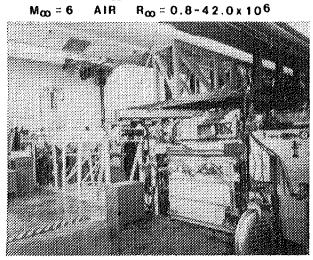

HELIUM TUNNEL
M_∞ = 19-21.6 He R_∞ = 3.5-12.5x10^6

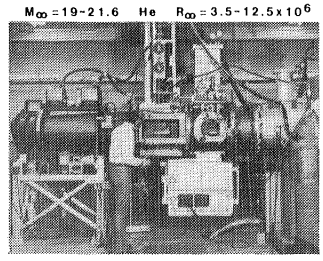

OPEN JET LEG-HE TUNNEL
M_∞ = 20 He R_∞ 6.0x10^6

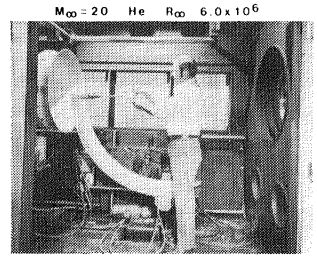

Pressure Distributions on SEADS at Mach 21.5

In support of the Shuttle Entry Air Data Systems (SEADS), pressure distributions were measured on a 0.02-scale model of the forward fuselage of the Space Shuttle orbiter in the Hypersonic Helium Tunnel at Mach 21.5. Data at 36 locations, 20 SEADS locations, and 16 development flight instrumentation locations were measured on the model at angles of attack from 0° to 50° and angles of sideslip from −5° to +5°. Flow blockage problems of the relatively large model were solved by the fabrication of special stings with model mounting blocks at 15°, 30°, and 45°, which kept the model in the uniform flow region of the tunnel as the angle of attack of the model was increased to 50°. The present data compared favorably with results previously obtained at Mach 6 and Mach 10.3 in air and completed both the algorithm development and the calibration of SEADS in ground-based facilities over the Mach number range from entry down to subsonic approach and landing.
(George C. Ashby, Jr., 2483)

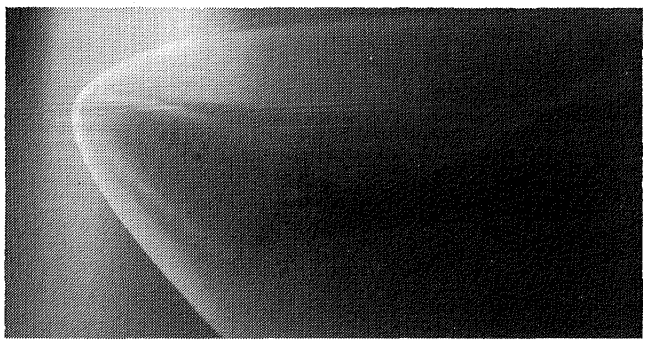

L-84-10,975

Pressure distributions measured on SEADS model.

Aerodynamic Characteristics of Proposed AOTV With Payload

Aerodynamic coefficients were measured on an Aeroassisted Orbital Transfer Vehicle (AOTV) proposed by NASA Ames Research Center. This vehicle consists of a drag brake, which is similar to a 70° half-angle spherically blunted cone with a small skirt, and a cylindrical payload attached perpendicularly to the base of the brake. These tests were performed in the Hypersonic CF_4 Tunnel for angles of attack from 4° to 20° to simulate the high normal-shock density ratio (or low ratio of specific heats within the shock layer) aspect of a real gas. (As the gas within the shock layer dissociates in hypersonic flight, the density ratio across the shock increases to values 2 to 4 times larger than those obtained in hypersonic wind tunnels that use air as the test gas.) The CF_4 tunnel provided a density ratio of 12 at Mach 6.

The Ames brake with and without the payload was longitudinally stable over the present range of angle of attack, and the ratio of lift to drag over this range was 0.06 to −0.30. The payload was shielded with a shroud attached to the sting to examine the effect of the payload. Use of this shroud revealed that the free shear layer, which originates at the brake shoulder and impinges on the payload, has an appreciable influence on the normal force and pitching moment, particularly at the higher angles of attack.
(John R. Micol, 3984)

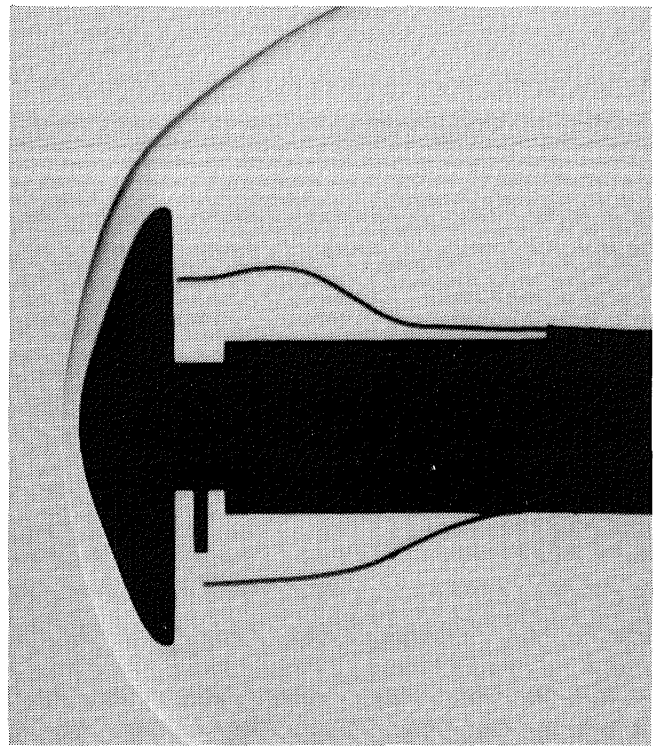

Schlieren photograph of Ames AOTV drag brake force model in Hypersonic CF_4 Tunnel.

Simulation of Real-Gas Effects on Heating to a Control Surface

Heating distributions were measured on the surface of a spherically blunted, bent-nose biconic and on the trailing-edge flap. Flaps with deflection angles from 0° to 30° were instrumented with thin-film resistance heat transfer gauges. This type of gauge was also used to measure heating distributions along various rays of the biconic surface, including the region just upstream of the flap. Tests were performed in the 20-Inch Mach 6 Tunnel and the Hypersonic CF_4 Tunnel to determine the effect of lowered gamma (ratio of specific heats) within the shock layer on flap heating. These tests simulated the low-gamma aspect of a real (dissociated) gas, such as occurs in flights. The angle of attack was varied from 0° to 20°.

The lower gamma in tetrafluoromethane (CF_4) significantly reduced the bow shock detachment distance, and as a result the interaction between bow shock and flap occurred at a lower angle of attack than for ideal air. This interaction was quite complex, particularly for high flap deflection angles, which corresponded to separated flow upstream of the flap. For several combinations of angle of attack and flap deflection angle, flap heating rates were comparable to the heating on the spherical nose.

(Charles G. Miller, 3984)

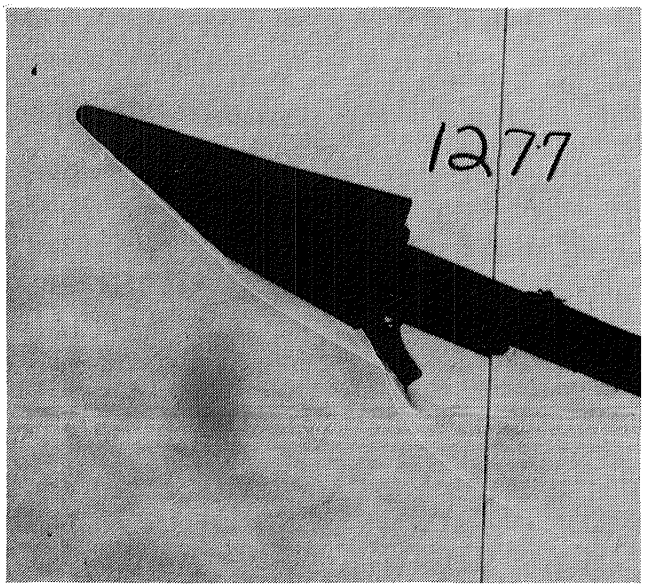

Schlieren photograph of bent-nose biconic heat transfer model in Hypersonic CF_4 Tunnel.

Comparison of Measured and Computed Heating Distributions on Large-Angle Sphere Cone

Heating distributions were measured on a 70° half-angle spherically blunted cone with a sharp corner and a bluntness ratio of 0.5. This configuration is representative of candidate Aeroassisted Orbital Transfer Vehicles (AOTV) with low lift-to-drag ratios. Tests were performed in the 31-Inch Mach 10 Tunnel, the 20-Inch Mach 6 Tunnel, and the Hypersonic CF_4 Tunnel for angles of attack from 0° to 20°. Heating distributions for this range of angle of attack were predicted with the High Alpha Inviscid Solution (HALIS) code developed at Langley to generate the inviscid flow field and with a three-dimensional axisymmetric analogue (3DAA) code to predict boundary layer flow properties.

Measured heating distributions at the lower angles of attack were characterized by a monotonic decrease in heating as the flow expanded over the spherical nose onto the conical section. This was followed by a rapid increase in heating as the flow approached the corner. The heating level just upstream of the corner was nearly the same as that on the spherical nose. At the higher angles of attack, where the stagnation point moved off the spherical nose onto the cone, heating levels at the corner actually exceeded the level elsewhere on the front surface. Heating distributions predicted with the HALIS-3DAA codes were in good agreement with measurements (within 10 percent).

(Raymond E. Midden, 3984)

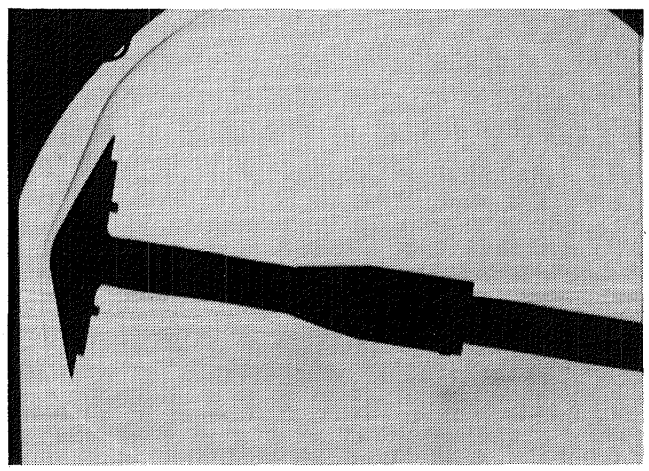

Schlieren photograph of 70° sphere cone heat transfer model in Hypersonic CF_4 Tunnel.

Hypersonic Parametric Study of Proposed AFE

A family of proposed Aeroassisted Flight Experiment (AFE) models was tested in four Langley hypersonic facilities—the 31-Inch Mach 10 Tunnel, the Hypersonic CF_4 Tunnel, the Hypersonic Helium Tunnel, and the 20-Inch Mach 6 Tunnel. These model configurations, proposed by NASA Johnson Space Center, were raked-off 60° half-angle elliptic cones with different combinations of bluntness, skirt radius (i.e., corner radius), and skirt "wrap-around" subtended angle. Forces and moments, thermal distributions, surface streamline patterns, and shock shapes were measured in the various wind tunnels, which provided a range of Mach number, Reynolds number, and normal-shock density ratio. The angle of attack was varied from −10° to 10°.

All configurations tested were statically stable. Measured stability was predicted accurately (to within 5 percent) with a High Alpha Inviscid Solution Code (HALIS), but was poorly predicted by Newtonian theory. In general, the effects of bluntness, skirt radius, and skirt angle on aerodynamic characteristics were small. An increase in density ratio resulted in a lower trim angle of attack and a slight increase in stability. Force and moment measurements implied that the free shear layer originating at the shoulder impinged close to the base, particularly at low angles of attack. Oil flow patterns and schlieren photographs confirmed this. Oil flow patterns on the blunt front face showed that the movement of the stagnation point followed the geometric stagnation point and thus was well behaved. Thermal mappings that used the phase change paint technique revealed that the heating level was nearly constant over a large portion of the face and increased as the flow approached the skirt.

(William F. Hinson, 3984)

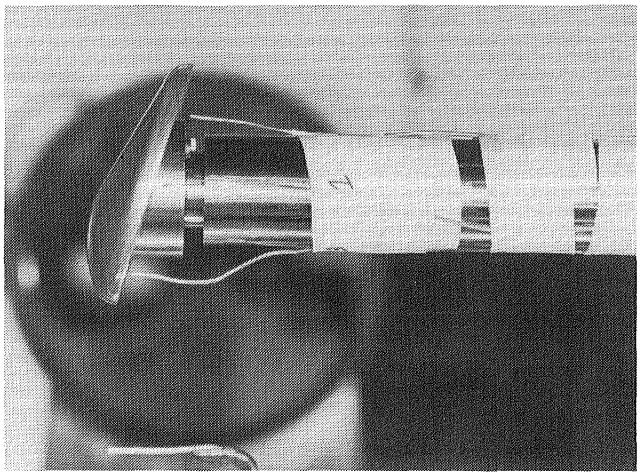

L-85-10,928

Proposed AFE force model in Hypersonic CF_4 Tunnel.

Multiple Inward Turning Scoop Inlet Test

One inlet concept being considered for hypersonic missile application is the Johns Hopkins University/Applied Physics Laboratory (JHU/APL) Multiple Inward Turning Scoop (MITS) inlet system. This system features four inlets mounted around the periphery of a conical forebody. The flow from all four is ducted into one internal chamber. As a first step in an experimental investigation of the performance characteristics of this concept, a 1/3-scale model of the forebody with only one inlet was built by JHU/APL. The model exit flow could be surveyed with a rotating rake or measured with a plenum having a precision American Society of Mechanical Engineers (ASME) exit nozzle. Initial testing was done over the supersonic speed range at other facilities. The extension of research into the hypersonic speed range resulted in a cooperative research program between JHU/APL and Langley. The model was tested in the 20-Inch Mach 6 Tunnel.

Model pressures were measured with a 48-port electronically scanned pressure (ESP) module located immediately below the test section floor. Twenty-five model pressure orifices were located on the cowl and centerbody (ramp) surfaces. The rotating rake consisted of 12 pitot and 4 static probes. The plenum assembly was instrumented with four nozzle static orifices, four internal static orifices, and a stagnation temperature probe. Tests were made over a ±8° angle-of-attack range for three model roll orientation angles (0°, 45°, and 90°) and at unit Reynolds numbers ranging from 2×10^6 to 4×10^6 per foot.

The results indicated that at 0° angle of attack, the capture ratio was several percent higher than inviscid prediction up to the maximum test sideslip angles of ±8°. At 8° angle of attack the measured capture ratio was 6 percent higher than predicted with the inlet on the windward surface of the model

and 19 percent lower with the inlet on the leeward side. Schlieren photographs indicated a rapid thickening of the boundary layer on the leeward side of the forebody as angle of attack was increased.
(William J. Monta, 4014)

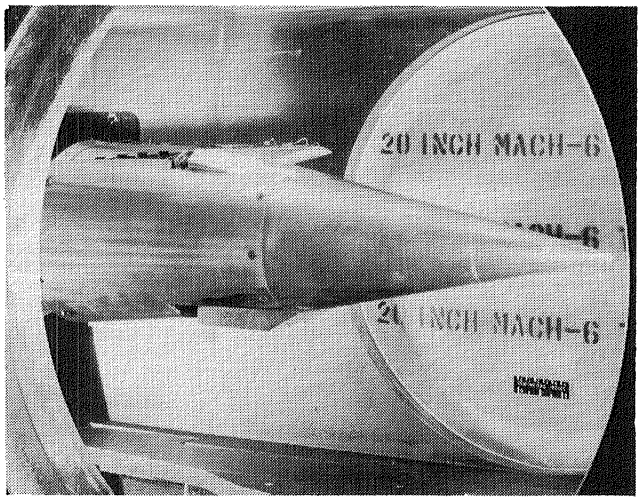

L-85-10,373

1/3-scale model of JHU/APL forebody with single inlet.

Scramjet Test Complex

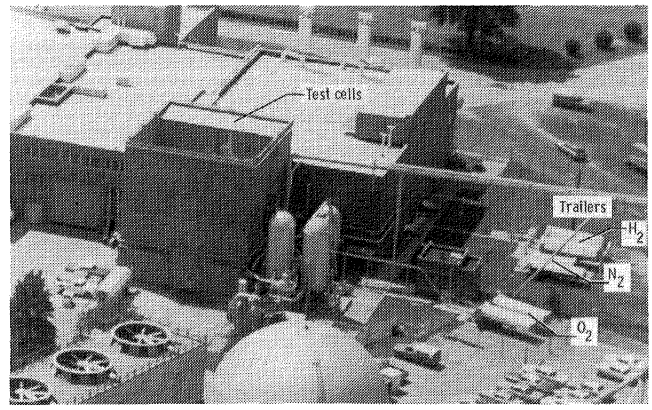

After an almost 15-year lull in interest for hypersonic flight, there is again a strong emphasis on the potential for a number of applications. These include a real "aerospace plane", or transatmospheric vehicle, which would be able to take off from a conventional runway and fly to orbit, as well as a variety of hypersonic airplane concepts for military reconnaissance, strike, or semiglobal transport. Langley has maintained a research team that has been working on basic hypersonics continuously throughout the last several decades. Facilities that played a key role at Langley in developing the present Shuttle configuration have been applied to a wide variety of other aerospace vehicles. Langley, the lead Center in defining Shuttle II, has been the only research organization in the nation to continuously maintain a viable effort in hydrogen-fueled supersonic combustion ramjet propulsion since the 1960s. Ground tests of subscale engines conducted in the Scramjet Test Complex have demonstrated levels of net thrust sufficient to accelerate at Mach 4 and to cruise an airplane at speeds up to Mach 7 and beyond. These results are entirely consistent with the projection of attractive performance up to much higher speeds, even approaching orbital velocity.

SMALL SCALE COMBUSTOR TESTS

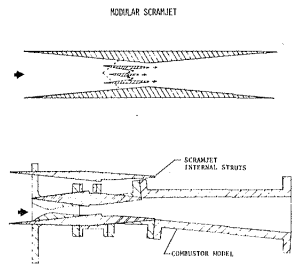

COMBUSTOR MODELING

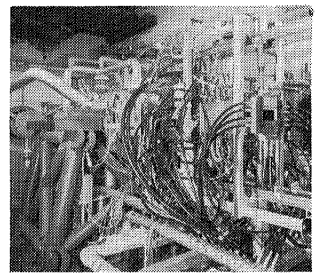

TEST CELL #2

ENGINE MODEL TESTS

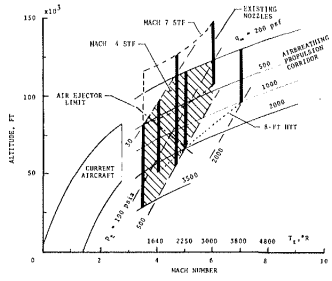

POTENTIAL TEST CAPABILITY

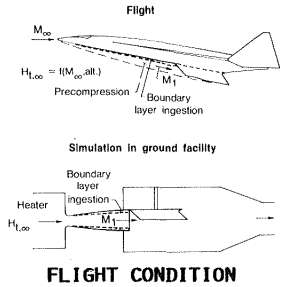

FLIGHT CONDITION SIMULATION

SMALL SCALE INLET TESTS

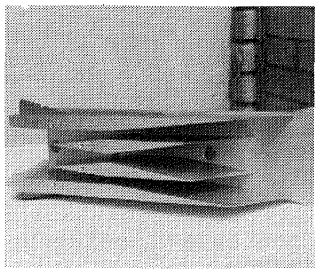

INLET MODEL

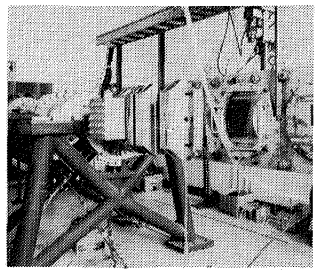

MACH 4 BLOWDOWN TUNNEL

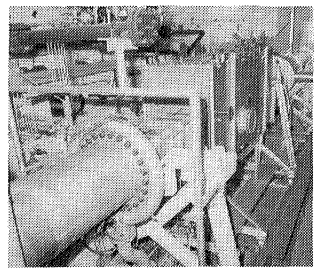

MACH 4 STF TEST CELL #1

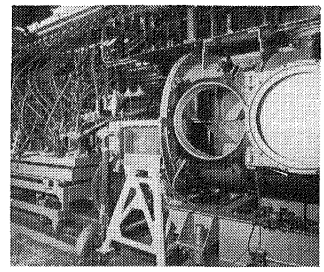

MACH 7 STF

A research program to develop technology for a hydrogen-burning airframe-integrated supersonic combustion ramjet (scramjet) propulsion system has been under way for several years at Langley. The experimental portion of this research consists of tests of engine components (inlets, combustors, and nozzles) and complete, component integration engine models.

Small-scale inlet tests for "screening" potential inlet designs are performed in a 9- by 9-in. Mach 4 blowdown tunnel. Larger-scale inlet tests are performed in various other Langley aerodynamic wind tunnels. Small-scale direct-connect combustor tests that simulate a portion of the engine combustor are conducted in Test Cell #2 to provide basic research data on supersonic mixing, ignition, and combustion processes. The hot test gas is supplied to the combustor models by a hydrogen-air-oxygen combustion heater, which maintains 21-percent free oxygen by volume to simulate air with enthalpy levels ranging up to Mach 7 flight speeds. Various facility nozzles produce the desired combustor entrance flow conditions.

Designs from the individual component tests are assembled to form component integration engines so that tests can be conducted to understand any interactions between the various engine components and to determine the overall engine performance. These component integration tests are conducted in engine test facilities. The feature that separates these propulsion facilities from aerodynamic wind tunnels is their capability to produce true-velocity, true-temperature, and true-pressure flow for flight simulation.

The Mach 4 Scramjet Test Facility (Test Cell #1) uses a hydrogen-air-oxygen combustion heater to duplicate Mach 4 flight enthalpy. The test gas is exhausted to the atmosphere with the aid of an air ejector. A Mach 3.5 contoured nozzle with a 13-in.-square exit is presently attached to the heater to yield a free-jet tunnel flow (simulating Mach 4 flight conditions) for subscale engine tests. The Mach 7 Scramjet Test Facility uses an electric-arc heater to produce enthalpy levels corresponding to flight speeds up to Mach 7. The tunnel exhausts into a 100-ft-diameter vacuum sphere. Eleven-in.-square exit nozzles (Mach 4.7 and 6) are used to deliver a free-jet tunnel flow for scramjet engine tests. The same size models (frontal view about 6 by 8 in.) are tested in both these facilities.

By 1989, an oxygen replenishment system and new facility nozzles will be added to the Langley 8-Foot High Temperature Tunnel, which is presently part of the Aerothermal Loads Complex. This tunnel will then be capable of testing large-scale engines (about 20 by 28 in.), multiple engines, or engines that have full nozzle expansion surfaces at Mach numbers of 4, 5, and 7. In addition, the operational capability of the Mach 4 Scramjet Test Facility is being enhanced by a new test gas heater, a new Mach 4.7 nozzle, and a new vacuum sphere/steam ejector system. Upon completion of these modifications, the 8-ft HTT, together with the smaller scale facilities described above, will comprise a Scramjet Test Complex at Langley unequaled in the western world. The potential operational envelope of this complex would extend over a flight Mach number range from 3.5 up to 7.

Scramjet Performance

Airbreathing hypersonic propulsion research at Langley has been focused on development of the technology for a fixed-geometry airframe-integrated scramjet engine that will operate in a flight Mach number range from 4 to 10. To date, design variations of this engine concept have been tested at Mach 4 and 7. More than 1000 engine firings have been achieved with gaseous hydrogen as the fuel. Testing has been aimed at overcoming problems related to fuel-air mixing, flameholding, and combustor-inlet interaction. In addition, significant improvements have been made in inlet design to increase the amount of airflow captured.

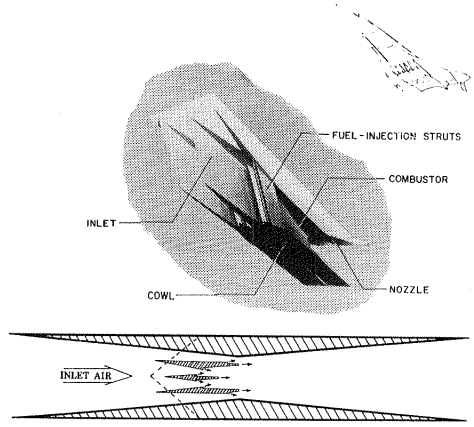

Airframe-integrated supersonic combustion ramjet.

The test results obtained in hypersonic propulsion wind tunnels (the Langley Mach 4 and Mach 7 scramjet test facilities and a NASA Mach 7 facility at General Applied Science Laboratories) at both Mach 4 and Mach 7 showed that the measured thrust levels agreed well with theoretically predicted thrust levels for this class of two-dimensional fixed-geometry airframe-integrated scramjet engines. More importantly, the projection of the ground facility thrust data to a flight situation indicated that thrust significantly greater than vehicle drag can be achieved at both Mach 4 and Mach 7.
(R. Wayne Guy, 3772)

Ignition/Flameholding Characteristics of Wedge Injectors

A parametric scramjet engine model has been tested extensively in the Langley Mach 4 Scramjet Test Facility. The most basic configuration for this engine had smooth internal walls with no protruding surfaces. Hydrogen fuel, injected from the combustor sidewalls perpendicular to the air flow, was ignited by injection of a pyrophoric fuel mixture (20 percent monosilane/80 percent hydrogen by volume). However, ignition of the pyrophoric fuel mixture was not achieved at Mach 4 flight total-temperature conditions (i.e., T_t = 1640° R), and the test gas total temperature had to be increased to about Mach 4.7 conditions before ignition occurred. To overcome the ignition problem, wedges were added at the primary fuel injector location to provide a base region to increase fuel/air residence time. These wedges effectively lowered the auto-ignition temperature to below Mach 4 conditions. With the initial lateral spacing of the wedges in the Mach 4 engine tests, a small, continuous flow of hydrogen upstream of the wedges was required for flameholding after the pyrophoric silane/hydrogen ignitor gas flow was terminated. Subsequent engine tests investigated the effect on engine performance of wedge height, number of wedges per wall (thus lateral spacing change), and longitudinal location of the wedges in the engine. These factors had little effect on the engine overall performance. However, when the wedge lateral spacing was decreased by half and new wall fuel injectors were located between the wedges, flameholding could be maintained without the upstream flow of hydrogen.

Because of the lack of visibility within the engine, Mach 2 tests of a single wedge injector mounted on a flat plate were conducted in Test Cell #2 to investigate the wedge ignition phenomenon. The figures show combustion of the silane/hydrogen mixture (injected upstream of the wedge) and the wedge primary hydrogen fuel at a free-stream total temperature of 1700° R at both low and high flow rates of fuel injection. Ignition at a low fuel flow rate occurred only in the recirculation region downstream of the wedge, and in subsequent tests this occurred at total temperatures below Mach 4 conditions. At higher fuel flow rates, interactive burning occurred from the upstream silane/hydrogen injectors and encompassed the entire wedge. These modes of flameholding and burning are believed to be representative of the mode of combustion with the wedges in the scramjet engine.
(Earl H. Andrews, 3772)

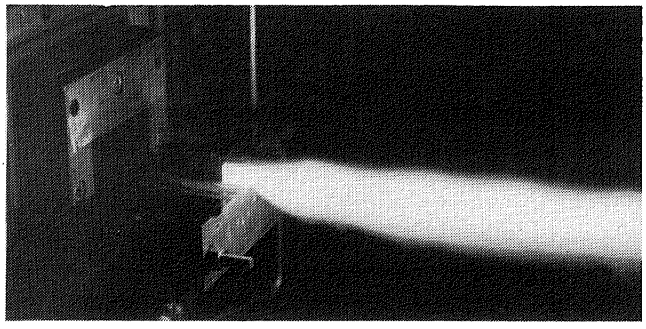

L-85-9212

Ignition and burning in wedge base region with low fuel flow rates at T_t = *1700° R.*

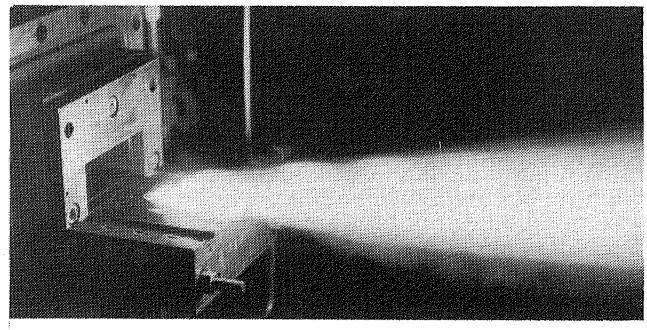

L-85-9213

Ignition and burning in region of upstream boundary layer separation with high fuel flow rates at T_t = *1700° R.*

Evaluation of Storable Fluorine-Based Pilot for Scramjets

An ignitor and pilot for supersonic combustion ramjet engines were devised and tested in Test Cell #2 with gaseous hydrocarbon fuels in a Mach 2 flow. This pilot was designed to use storable, nontoxic propellants in an effort to avoid the safety hazard associated with pyrophorics and other highly reactive compounds. The pilot consisted of a mixture of ethylene, oxygen, and sulfur hexafluoride. This mixture, when burned in a preburner, was calculated to yield 20.9 percent fluorine atoms by volume at adiabatic conditions. Fluorine atoms react rapidly with hydrogen and hydrocarbons, which results in an increase in the overall rate of their reactions with oxygen.

This pilot was tested with ethylene, ethane, and methane fuels under simulated scramjet combustor conditions, and was shown to reduce the minimum temperature at which each of these fuels would ignite. In a free-jet configuration, the minimum total temperatures at which the fuels would burn were 1450° R for ethylene, 2070° R for ethane, and 3240° R for methane. For ducted tests that simulated scramjet combustor flow, combustion efficiencies were calculated. The current pilot was compared with an identical pilot that used nitrogen in place of the sulfur hexafluoride (i.e., a hot nitrogen/C-H-O radical generator). This nitrogen substitution allowed the effect of the fluorine to be isolated from the pilot's thermal, C-H-O radical, and stream disturbance effects. The pilot was also compared with an equivalent-energy silane-hydrogen pilot, which provided a comparison with a known effective pilot.

Results showed that although the current pilot was competitive with the silane, it was not superior to the nitrogen-based pilot. This chemically unexpected result was shown to be due in part to pilot preburner heat loss. Equilibrium calculations demonstrated that the preburner heat loss, which was measured to be 13 percent, would result in a product gas with less than 50 percent of the adiabatic fluorine atom content by mass. More important than the heat loss, however, was probably the lack of fuel-pilot mixing, which is essential for the success of this pilot. Better fuel-pilot mixing (to promote fluorine-fuel reaction) and a pilot that produces a greater amount of fluorine atoms should improve the performance of this pilot concept.

(Glenn S. Diskin, 2803)

Dual-Camera OH Visualization System

A special dual-view UV-sensitive imaging instrument system has been developed to study fuel ignition and flameholding techniques in the hypersonic propulsion Test Cell #2 facility research program. This unique television system provides real-time test visualization and simultaneous recording of flame location, as indicated by hydroxyl molecule (OH) emission, for post-test analysis. The two cameras utilize UV-sensitive vidicons and optical filters specific to OH emission in the 310-nm spectral range. This UV sensitivity allows direct viewing of the normally invisible OH emission combustion byproduct. The instrument control panel is located remotely from the propulsion test cell and provides remote operator control of shutter, interference filters (two each) and attenuation. The recorded data are automatically marked with time, test number, and view information for after-test data correlation.

An important early application of this instrument involved the exploration of a continuous-operation plasma torch as an ignitor and flame holder for a scramjet combustor in Test Cell #2. The figure shows the complete system and a typical single-channel view of recorded data in an early experiment. The OH visualization system utilizes a naturally occurring feature of the combustion process to provide the experimenter with a full-view picture. Data obtained from the OH visualization system allow the

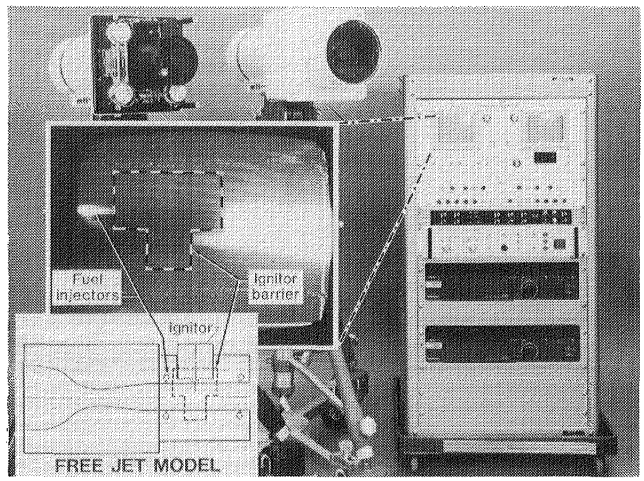

L-85-10,167

UV-sensitive imaging system.

experimenter to determine ignition occurrence and flameholding location within the ramjet engine test apparatus. The results have verified the effectiveness of mixtures at injection rates required for a hot fluorine gas chemical ignitor. This system will be used to test other possible ignition and piloting methods in the supersonic combustion ramjet engine development program.
(Ray W. Gregory, 2791)

Aerothermal Loads Complex

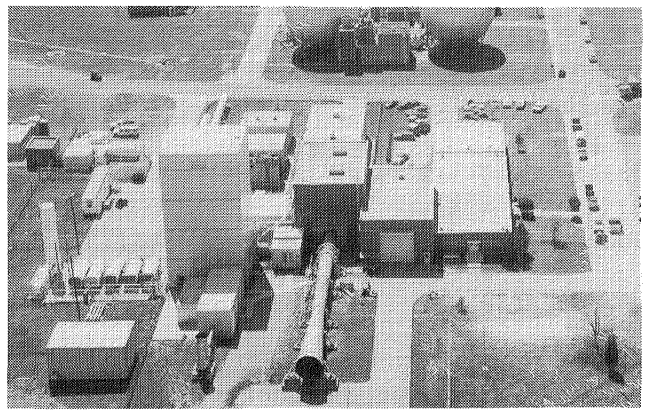

The Aerothermal Loads Complex consists of six facilities that are used to carry out research in aerothermal loads and high-temperature structures and thermal protection systems. The 8-Foot High Temperature Tunnel is a Mach 7 blowdown type facility in which methane is burned in air under pressure and the resulting combustion products are used as the test medium with a maximum stagnation temperature near 3800° R in order to reach the required energy level for flight simulation. The nozzle is an axisymmetrical conical contoured design with an exit diameter of 8 ft. Model mounting is semispan or sting with insertion after the tunnel is started. A single-stage air ejector is used as a downstream pump to permit low-pressure (high-altitude) simulation. The Reynolds number ranges from 0.3 to 2.2 × 10^6 per foot with a nominal Mach number of 7, and the run time ranges from 20 to 180 sec. The tunnel is used for studying detailed thermal-loads flow phenomena as well as for evaluating the performance of high-speed and entry vehicle structural components. A major effort is under way to provide alternate Mach number capability as well as O_2 enrichment for the test medium. This is being done primarily to allow models that have hypersonic airbreathing propulsion applications to be tested.

The 7-Inch High-Temperature Tunnel is a 1/12-scale version of the 8-ft HTT with basically the same capabilities as the larger tunnel. It is used primarily as an aid in the design of larger models for the 8-ft HTT and for aerothermal loads tests on subscale models. The 7-in. HTT is currently being used to evaluate various new systems for the planned modifications of the 8-ft HTT.

The 20-MW, 5-MW, and 1-MW Aerothermal Arc Tunnels are used to test models in an environment that simulates the flight reentry envelope for high-speed vehicles such as the Space Shuttle. The amount of energy available to the test medium in these facilities is 9 MW, 2 MW, and ½ MW, respectively. The 5-MW is a three-phase AC arc heater and the 20-MW and 1-MW are DC arc heaters. Test conditions such as temperature, flow rate, and enthalpy vary greatly since a variety of nozzles and throats are available and model sizes can range from 3 in. in diameter to 1- by 2-ft panels.

8-FOOT HIGH-TEMPERATURE TUNNEL
M = 7 R_n = 0.3 - 2.2 x 10^6

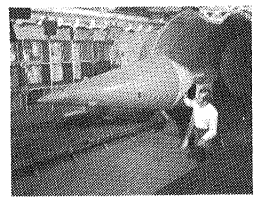

7-INCH HIGH-TEMPERATURE TUNNEL
M = 7 R_n = 0.3 - 2.2 x 10^6

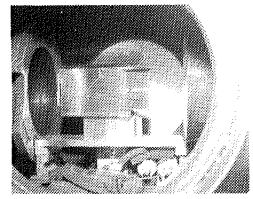

1 x 3 HIGH ENTHALPY AEROTHERMAL TUNNEL
M = 3.5 - 4.7 R_n = 0.3 - 1.4 x 10^6

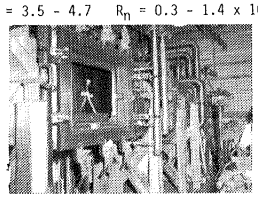

AEROTHERMAL ARC TUNNEL

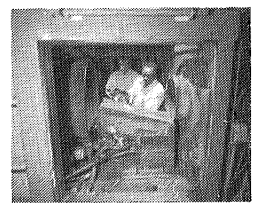

Quilted Tile Array Simulating Thermally Bowed Metallic TPS

Metallic TPS panels on high-speed vehicles are subject to thermal distortions when they experience large through-the-thickness temperature gradients. The panel, anchored at the corners, bows up into the

flow field and alters a smooth vehicle moldline to a quilted-surface configuration. Although the bowed height of the panels is expected to be less than the local boundary layer thickness, the complex interaction of the high-speed flow field and the bowed surface will affect the local and global aerothermal loads to the vehicle. An experimental aerothermal study has been completed which complements analytical studies of this problem.

A quilted array of ceramic tiles was designed and fabricated to fit the 8-ft HTT panel holder, which provides two-dimensional laminar and turbulent boundary layer flow. The tiles were 10 in. square with protuberance heights of 0.1, 0.2, and 0.4 in. The same tiles were designed to be tested in both aligned and staggered-array configurations. The array included two types of instrumented metallic tiles to be inserted into the ceramic tile array for surface pressure and thin-wall heat transfer measurements. Aerothermal tests were performed at a free-stream Mach number of 6.5, a unit Reynolds number of 0.4×10^6 per foot, and a total temperature of 3500° R. The quilted dome array that simulated thermally bowed metallic TPS was tested in the 8-ft HTT and the preliminary data analysis has been completed.

Preliminary results include pressure and cold-wall heating rate distributions, boundary layer profiles, and temperature contours obtained from infrared thermographic measurements. In general, the laminar flow results agree qualitatively with previously obtained three-dimensional Navier-Stokes solutions for the quilted dome configuration. Regions of high temperature, or "hot spots", were identified, and these correlated well. In addition, temperature contours showed that the heating rates in the upstream tiles were higher than those in the downstream tiles.

(Christopher E. Glass, 3423)

Curved Metallic TPS

Although much of the surface of a typical Space Transportation System (STS) is flat or nearly flat, some areas are necessarily curved. Wind tunnel test data for flat superalloy honeycomb (SA/HC) prepackaged thermal protection systems (TPS) have indicated that heating in the gaps between panels can occur and that surface pressure gradients may increase the severity of gap heating. Also, analysis indicates that thermal stresses are much higher for curved TPS than for flat TPS. The objective is to evaluate gap heating between curved SA/HC panels under pressure gradient conditions and to assess the severity of thermal stresses in curved panels.

An array of curved SA/HC panels was fabricated for testing on the curved surface test apparatus (CSTA). The radii of the panels varied from 9 to 12 in. A section of the CSTA was cut out so the curved array could be inserted flush with the CSTA skin.

After the windward panels were preheated to a surface temperature of 2000° F, the array was exposed for 34 seconds to the most severe conditions

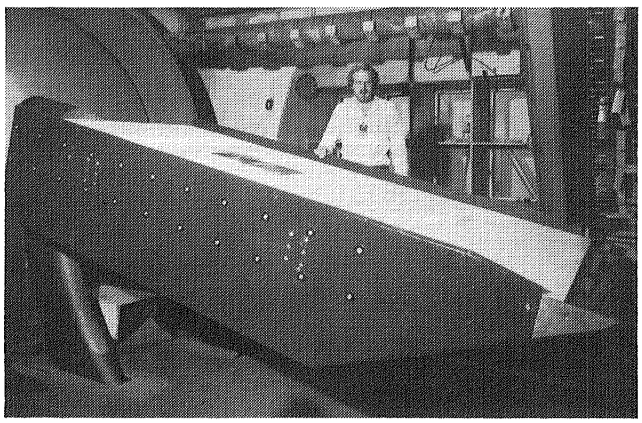

L-85-2648

Simulated thermally bowed metallic TPS installed in 8-ft HTT panel holder.

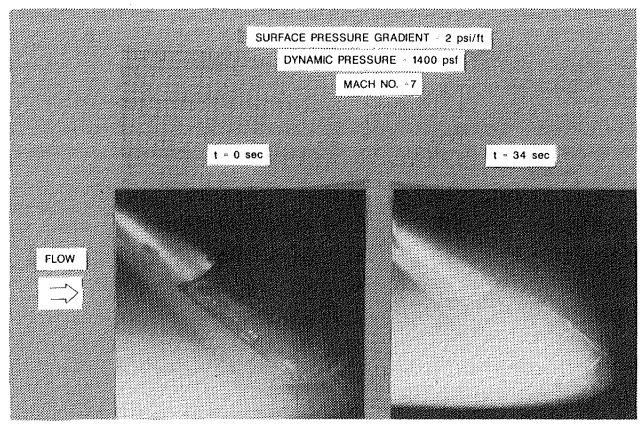

L-85-12,016

Aerothermal test of curved superalloy honeycomb prepackaged TPS.

within the normal operating range of the 8-ft HTT. The figure shows the model in the stream at 0 seconds and 34 seconds. Unacceptably high temperatures were again measured in the gaps between panels. Examination of the model revealed that the aft seal of the cavity into which the panels were installed had failed. Failure of this seal would allow the hot gas on the surface of the panels to flow through the gaps between panels and through the cavity seal to the base of the model. This condition (pressure difference of about 4 psi) is even more severe than the severe 2 psi/ft surface pressure gradient purposely imposed on the model. Preliminary results indicated that the cause of the high gap temperatures could not be distinguished between the imposed surface pressure gradient and leakage through the cavity seal.

Before additional aerothermal tests, which are scheduled for CY 1986, are made, the model and cavity seal will be repaired and modification of the concept to further inhibit gap heating will be considered.

(John L. Shideler, 2425)

Aircraft Noise Reduction Laboratory

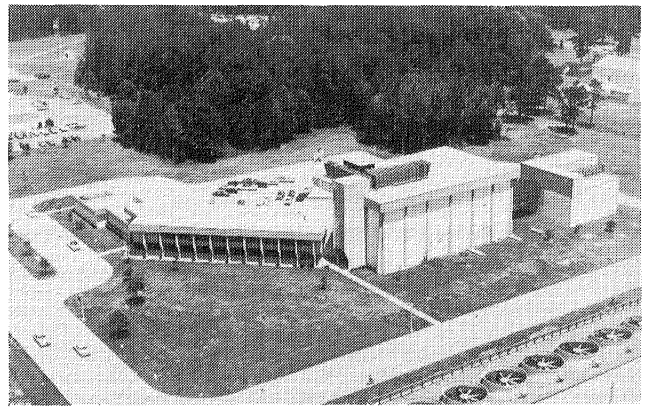

The Langley Aircraft Noise Reduction Laboratory (ANRL) provides the principal focus for acoustics research at Langley. The ANRL consists of the quiet flow facility, the reverberation chamber, the transmission loss apparatus, and the human response to noise laboratories. The quiet flow facility has a test chamber treated with sound-absorbing wedges and is equipped with a low-turbulence, low-noise test flow to allow aeroacoustic studies of aircraft components and models. The test flow, which is provided by either horizontal high-pressure or vertical low-pressure air systems, varies in Mach number up to 0.5. The reverberation chamber is used to diffuse the sound generated by a noise source and provides a means of measuring the total acoustic power spectrum of the source. The transmission loss apparatus has a source room and a receiving room, which are joined by a connecting wall. A test specimen such as an aircraft fuselage panel is mounted in the connecting wall for sound transmission loss studies. The human response laboratories consist of the exterior effects rooms and the anechoic listening room.

Two laboratory companions of the ANRL are the Anechoic Noise Facility and the Jet Noise Laboratory. The Anechoic Noise Facility is equipped with a very high pressure air supply, which is used solely for simulation of nozzle exhaust flow. The Jet Noise Laboratory has two coannular supersonic jets for the study of turbulence evolution in the two interacting shear flows that are typical of high-speed aircraft engines.

Effect of Sound Source Angle on Cabin Noise

With the renewed interest in propeller-driven aircraft has come the need to study the effect on cabin noise of propeller (noise source) location and the angle at which the sound strikes the sidewall. Most of the recent experimental work on the transmission of sound through aircraft sidewalls has been performed on flat panels in the laboratory. This does not take into account the interior acoustic space nor the vibrational modes of the aircraft as a whole. The acquisition of data from in-flight tests is expensive and time consuming. In addition, the repeatability of the exterior sound field is questionable, and variation of propeller position is not possible. For these reasons, a study of the effect of sound source angle on interior noise was performed on an actual aircraft fuselage in the laboratory.

A small airplane fuselage surrounded by fiberglass baffles was placed in a large chamber in the Aircraft Noise Reduction Laboratory. The interior sidewalls were covered with 3 in. of fiberglass. Broadband white noise was emitted from an exponential horn attached to a pneumatic air driver. The horn was positioned at angles of +45°, 0°, and –45° with respect to the normal to the fuselage sidewall. Interior sound pressure levels were measured at the approximate head positions of the six possible passengers.

Results for the one-third octave band sound pressure level at the pilot's (front left) position are shown. Above 400 Hz the sound pressure level is greater for the –45° source angle than for either the 0° or +45° source angles. In addition, the effect of source angle on sound pressure level increases with increasing frequency. These results agree qualitatively with a

previous analytical study which showed that the directivity of reradiated sound from a flat panel in a baffle is greater at higher frequencies than at lower frequencies, with the major lobe of the reradiated sound at the same angle as that of the incident sound. Thus the sound pressure level should be largest for the source angle that directs the sound at the microphone of interest, in this case the –45° source angle. Examination of the data for the other interior microphones results in similar conclusions. However, the effect of source angle on space-averaged interior sound pressure levels is much less than the variation shown for a particular location in the cabin.
(Karen Heitman, 3561)

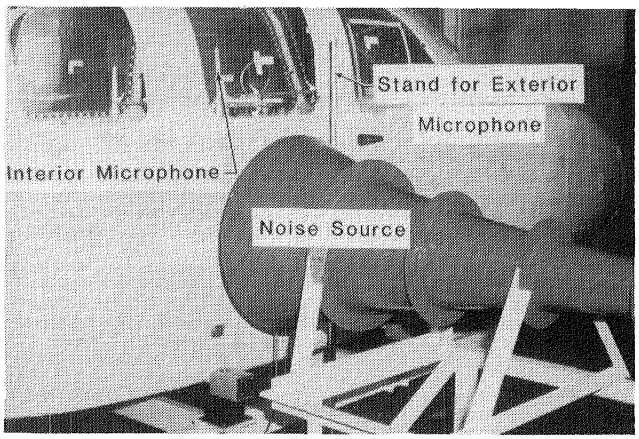

Experimental setup.

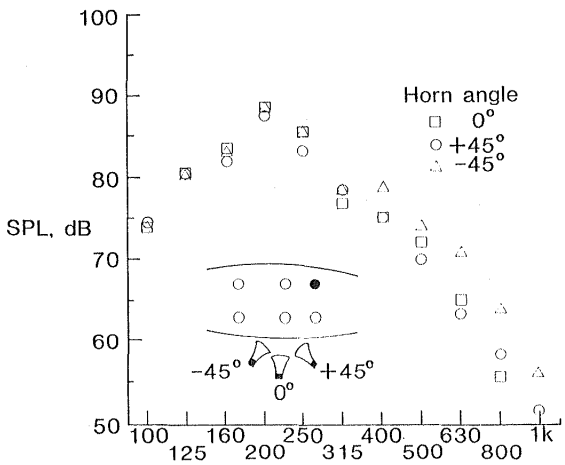

Sound pressure level for various source angles.

Reduction of Twin Supersonic Plume Resonance

Closely spaced supersonic engines are commonly utilized by the aircraft designer to improve performance. However, aircraft that utilize this engine configuration, such as the F-15, F-18, and B1-A, have experienced fatigue failures in the internozzle region. The subsequent loss of the affected components has degraded performance due to an increase in boattail drag. In the present study it was conjectured that the observed fatigue failures were caused by strong coupling between natural jet instabilities of each plume, which led to significantly higher near-field dynamic pressure levels.

To illustrate this concept, a 1/40 scale model empennage of the F-15 aircraft was constructed for testing in the Jet Noise Laboratory. Both fluctuating dynamic pressures and optical phase-averaged schlieren videotape records were recorded. The optical records clearly showed that each supersonic plume was dominated by helical instabilities, that they were coupled together as they evolved downstream, and that a strong pressure field propagated upstream. The intense acoustic wavefronts contained four times the energy expected for a single plume. The energy levels obtained were sufficient to cause sonic fatigue. Optical records were also obtained to show that suppression of the twin plume resonance phenomenon can be achieved easily by uncoupling the flow development between each plume. Future studies of this phenomenon will involve full-scale static and flight tests.
(John M. Seiner, 3094)

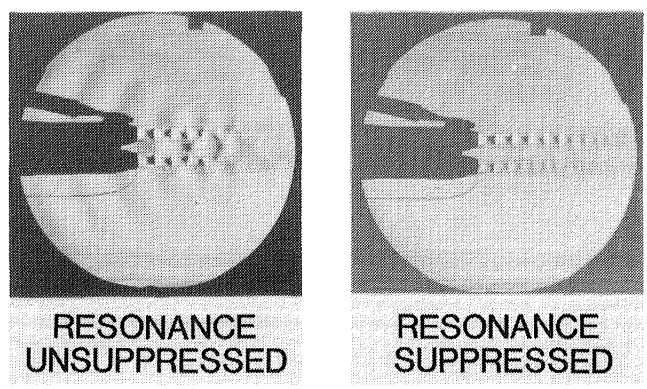

Visualization of preferred plume structure.

Scale Model Experiment To Study Long-Range Sound Propagation Over Ground Terrain

The objective of this research was to use a scale model experiment to assess the effects of ground terrain on long-range sound propagation at near-grazing incidence. Because of the challenge involved in including realistic effects such as wind, hilly terrain, thermal gradients, and irregular terrain absorption, there is a need for small-scale parametric experiments to develop appropriate propagation models in a systematic procedure. Preliminary results are presented from an experimental setup designed to conduct such studies in the Anechoic Noise Facility.

The figure shows the relative distribution of sound pressure levels at 12.5 kHz along a radial microphone array for both hard and soft surfaces. Multiple runs at an incidence angle of about 3° indicate the variability of the data. The hard plywood surface was covered with a 1/8-in.-thick layer of felt to produce the soft surface condition.

The data for the hard surface exhibit good repeatability and approximately 6 dB drop per distance doubling. The corresponding drop with distance for the felt-covered surface is much greater, as is the data variability at the more distant microphones. Some of this scatter is attributable to the signal strength approaching the noise floor of the instrumentation. Continuing data analysis for off-the-surface measurements suggests that other as yet unknown factors may be responsible. It should also be noted that the 1/8-in. felt-covered surface represents the most absorptive surface of interest in scale model propagation experiments of this type.

(T.L. Parrott, 4312)

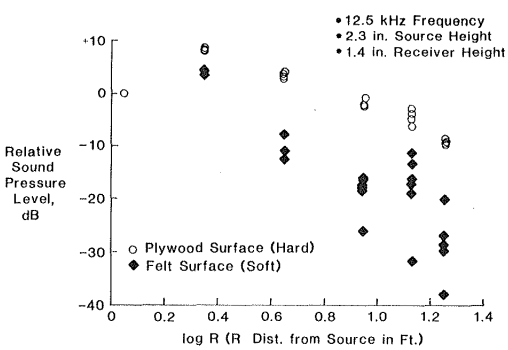

Comparison of hard and soft surface attenuation.

Characterization of Two-Dimensional Blade-Vortex Interaction

Blade-vortex interaction (BVI) is the source mechanism of an intense, impulsive helicopter noise dominant during powered descent and landing. Two-dimensional BVI was examined with the use of flow visualization techniques to understand the fundamental nature of this unsteady aerodynamic interaction.

In order to produce two-dimensional BVI, a vortex generator was placed upstream of a rotor blade section model in the quiet flow facility. The vortex generator, an oscillating airfoil, created a wake of alternating transverse vortices which impinged the blade model parallel to the blade span. The vortex structure, which was rendered visible by smoke, was recorded optically. Vortex trajectories and details of vortex changes during the interaction process were extracted from the data.

Data analysis resulted in a qualitative characterization of a close encounter region depicted schematically in the figure. Representative data illustrating BVI in each encounter zone are included in the figure. A region within a half blade chord length ($c/2$) above and below the blade defines a close encounter region. Outside this region, the blade has little or no apparent effect on the trajectory or structure of the vortex core. Inside this region is a deflection zone, in which the blade deflects the vortex trajectory but causes no change in the vortex core (diameter d_c). A distortion

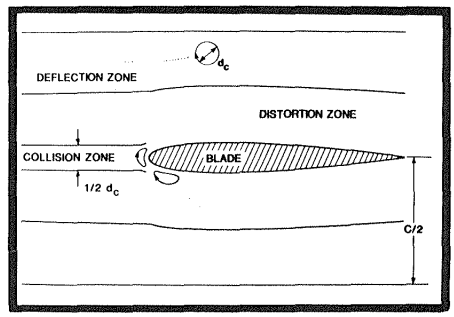

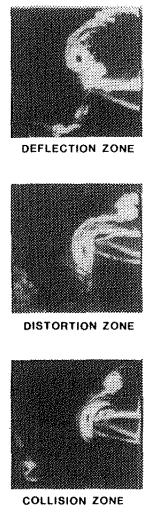

Two-dimensional BVI encounter zones.

zone, in which distortion of the vortex core is dominant, lies inside the deflection zone. Finally, in a collision zone surrounding the blade stagnation streamline, the vortex core is severed by the blade, the so-called direct encounter. Therefore, severe BVI features vortex core disruption.

Future work will include measurement of unsteady blade leading edge pressure during encounter with incident vortices in all encounter zones and measurement of the velocity field of the transverse vortex structures.

(E.R. Booth, Jr., 2645)

Annoyance of Advanced Turboprop Aircraft Community Noise

Advanced turboprop (ATP) noise is unique in that the pure-tone harmonic content occurs at frequencies higher than those generated by conventional propeller aircraft, but lower than those of conventional jet aircraft noise. The ATP aircraft will come into general usage only if its noise meets standards of community acceptability currently applied to conventional aircraft. An experiment was conducted in the Anechoic Listening Room to compare the annoyance of ATP aircraft flyover noise with the annoyance of conventional turboprop and jet aircraft flyover noise.

The Aircraft Noise Synthesis System was used to generate 18 realistic, time-varying simulations of ATP aircraft flyover noise in which the harmonic content was systematically varied to represent the factoral combinations of six fundamental frequencies and three tone-to-broadband noise ratios. The simulations were based on takeoff conditions and assumed a single-rotating-propeller tractor configuration with a thin, highly swept, twisted blade. Thirty-two subjects judged the annoyance of the 18 synthesized ATP takeoffs along with recordings of five conventional turboprop takeoffs and five conventional jet takeoffs. Each of the 28 noises was presented at three levels in a small anechoic chamber.

Analyses of the subjects' annoyance judgements indicated small but significant differences in annoyance response between the advanced turboprops and the conventional turboprops and jets. As shown in the figure, the advanced turboprops were slightly less annoying. Other results of the study indicated that the interaction of fundamental frequency with tone-to-broadband noise ratio had a significant effect on annoyance. Also, the addition of duration corrections and corrections for tones above 500 Hz to the noise measurement procedures improved prediction ability.

(David A. McCurdy, 3561)

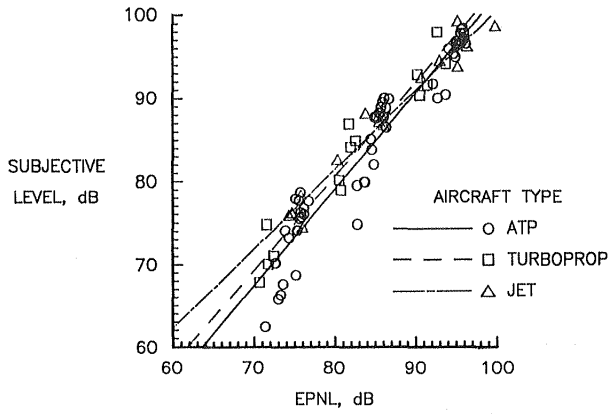

Annoyance responses.

Noise Study of Propeller in a Wake

Introducing a wake into an operating propeller has been shown to increase the noise generated by the propeller. Experimental studies have shown that these noise increases are directional. A thorough mapping of the radiated noise is thus required for a complete description. To obtain a better understanding of wake-induced propeller noise, an experiment was conducted in the anechoic environment of the quiet flow facility.

Data were acquired with a vertically traversing circular microphone array, as shown in the photograph. This array provided data from 30° to 140° to the propeller axis. Circumferentially, the propeller noise was mapped from 10° to 350° in 20° increments. A pylon attached to a dummy nacelle upstream of the propeller produced the wake. A vertical jet provided airflow over the model to simulate forward flight.

The data for the propeller without an incoming wake showed that the noise was concentrated in a relatively uniform band in the plane of rotation of the propeller. When the wake was introduced upstream of the propeller via the pylon, a nonuniformity was observed in this plane. In particular, a sharp decrease (about 10 dB) in the noise was observed normal to the pylon. On either side of this dip, a noise increase of about 8 dB was observed which extended upstream. The test yielded data necessary for the evaluation of current prediction technology and also provided a data base from which to infer noise trends for given propeller operating conditions.
(P.J.W. Block, 4910)

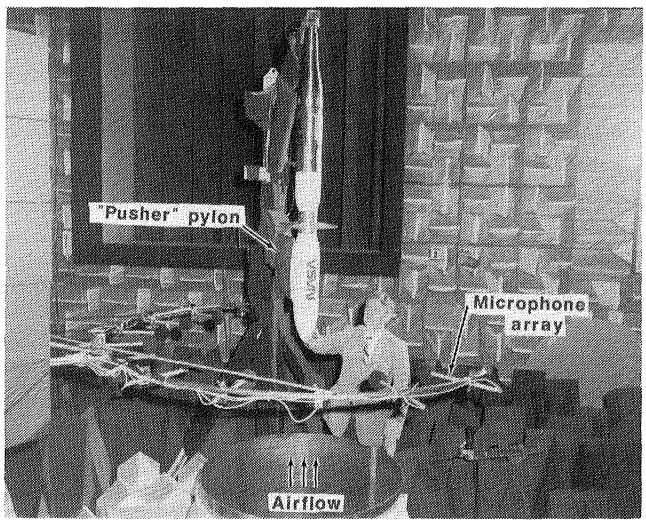

L-85-3337

Test setup for pusher propeller noise study.

Avionics Integration Research Laboratory - AIRLAB

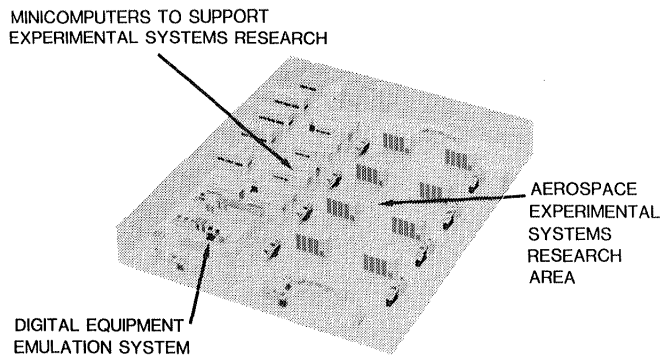

The United States leads the world in the development, design, and production of commercial and military aerospace vehicles. To maintain this leadership role throughout the 1990s and beyond will require the incorporation of the latest advances in digital systems theory and electronics technology into fully integrated aerospace electronic systems. Such efforts will entail the discovery, design, and assessment of systems that can dramatically improve performance, lower production and maintenance costs, and at the same time provide a high, measurable level of safety for passengers and flight crews.

AIRLAB has been established at Langley Research Center to address these issues and to serve as a focal point for U.S. government, industry, and university research personnel to identify and develop methods for systematically validating and evaluating highly reliable, fully integrated digital control and guidance systems for aerospace vehicles. The increasing complexity of electronic systems entails multiple processors and dynamic configurations. These developments allow greater operational flexibility in both normal and faulty conditions, thus impacting and compounding the validation process. Whereas a typical reliability requirement for current electronics systems is a probability of failure of less than 10^{-6} at 60 minutes, the requirement for current electronics systems is a probability of failure of less than 10^{-6} at 60 minutes, the requirement for flight-critical electronic controls is for a probability of failure of less than 10^{-9} at 10 hours. Obviously, a new validation process is essential if this significant increase in reliability (four orders of magnitude) is to be achieved and believed.

Validation research in AIRLAB encompasses analytical methods, simulations, and emulations. Analytical studies are conducted to improve the utility and accuracy of advanced reliability models and to evaluate new modeling concepts. Simulation and emulation methods are used to determine latent fault contributions to electronic system reliability and hence aircraft safety. Experimental testing of physical systems is conducted to uncover the latent interface problems for new technologies and to verify analytical methods.

AIRLAB is a 7600-ft^2 environmentally controlled structure located in the high-bay area of Building 1220. There are three rooms within the laboratory. The largest room is the experimental systems research area, which is configured into eight research stations and a central control and/or software development station. Each research station is supported by a VAX 11/750 minicomputer system that can be used, for example to control experiments (fault insertions, performance monitoring, etc.) and retrieve, reduce, and display engineering data. A VAX 11/780 minicomputer system supports the central control and/or software development station. The second largest room contains the VAX minicomputers, disk drives, and tape drives that support the research work stations. The third room contains the Digital Diagnostic Emulator, which is a special minicomputer (Nanodata QM-1A) interconnected to a VAX 11/750. The QM-1A is a nanocodable host computer with a unique emulation algorithm that allows gate logic level emulation of a target computer at a very fast rate. The diagnostic emulator provides the capability to experimentally address design issues of new fault-tolerant computer concepts and reliability issues in the fault behavior of fault-tolerant computers. Also included in AIRLAB are two advanced fault-tolerant computers, SIFT (software-implemented fault tolerance) and FTMP (fault-tolerant multiprocessor), which are designed to explore fault-tolerant techniques for future flight-critical aerospace applications. These computers, which have been under development by Langley Research Center for years, serve as research test beds for validation studies in AIRLAB.

AIRLAB provides research resources needed by the aerospace electronics research community to address design and validation issues of flight-critical fault-tolerant flight control systems. In this role, AIRLAB functions as a "community center" in which AIRLAB researchers with diverse backgrounds can conduct research with common goals.

Modeling the Effect of System Design Parameters on System Reliability

Central to the issue of validation methodology is whether the system under scrutiny contains errors in the design. The correctness of a system can be obtained only to the degree that the specifications provide. If there is an error in the specification, the validation methodology will fail to uncover it. An extension to the clock synchronization validation methodology developed previously in AIRLAB allows the probability of such a design failure to be added to the system reliability model. With such a model, the effect of system design parameters and assumptions on system reliability can be determined. In this latest effort the clock synchronization subsystem of the SIFT (software-implemented fault-tolerant) computer was subjected to validation.

The first step in the validation process is to formally state the algorithms the system will compute. The algorithms are then proven correct. The effect of the proof is two-fold. First, a precise statement of the system specifications is produced which serves as a fundamental description of system behavior. Second, the algorithm's performance is stated explicitly in terms of underlying hardware and software characteristics. For example, in the synchronization theorem, the maximum skew the processors' clocks will obtain is stated in terms of clock read error and clock drift rate. These relationships are explicitly stated in the algorithm's proof.

Other relationships are produced when the algorithm is implemented in a system. For example, in order to design the communications subsystem, the designer must assume values for clock read error and clock drift rate to calculate an expected maximum skew. The correct operation of the communications subsystem is now dependent on the clock subsystem meeting the requirements on read error and drift rate. When the system is built, real values for the system's clock read error and drift rate will exist. These values can be measured, but they are statistical quantities with a finite probability of exceeding the values assumed by the designer. Since an ultrareliable system can have a requirement that the probability of failure be very small (e.g., 10^{-9} at 10 hours), the slightest probability that the initial design assumptions are violated can contribute to system failure.

In the figure, the probability of system failure is plotted as a function of the amount of delay in microseconds (PSI) built into the communications subsystem. The SIFT system has a delay of 202.6 microseconds which puts the probability of failure safely below the 10^{-9} mark.

(D.L. Palumbo, 3681)

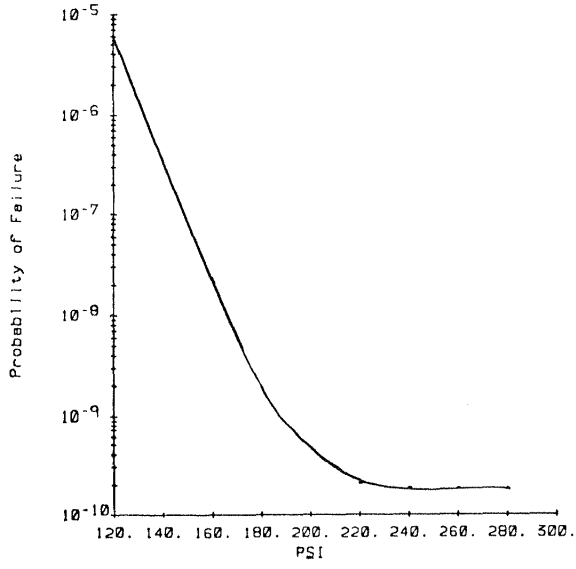

SIFT probability of failure as a function of communications delay.

New SURE Capabilities

An investigation of methods for analyzing the reliability of fault-tolerant system architectures has occupied nearly a decade of NASA-sponsored research. One reason for this is that traditional methods of analysis for redundant system configurations do not handle the type of features that characterize

reconfigurable, fault-tolerant avionics systems. For example, the traditional fault-free analysis method cannot be used to calculate the probability that a reconfigurable system fails due to coincident faults (i.e., the arrival of a second fault before the system can remove the first fault). In response to this problem, one line of investigation followed at AIRLAB was the development of generalized theory and a computer-aided method of determining upper and lower bounds on system reliability.

One major advantage of the generalized theory is that the effect on reliability of any number of competing recovery times can be studied when the form of their distributions is unspecified. The recovery processes can be described in terms of simple quantities-conditional means and percentiles or conditional means and variances. This theory also applies when data are available in a time-censored form. This is significant because fault-injection experiments lead to such data and often are the only available source of information for such recovery processes.

SURE (semi-Markov unreliability range estimator), the computer-aided method for implementing this theory, was developed in AIRLAB in late 1983. Using AIRLAB, SURE has recently been enhanced by the utilization of a new recursive graph traversal algorithm that enables the analysis of models with renewal (i.e., nonpure death processes), such as those incorporating transient faults. This new traversal algorithm also permits the addition of a simple, user-controllable model truncation strategy that is useful for the analysis of extremely large-state space problems. The SURE program's ability to perform automatic analysis of the effect of varying a parameter on system reliability has also been enhanced.

The new features of the SURE program include the following capabilities. Models with multiple competing recoveries can be analyzed; censored experimental data describing the recovery processes can be accommodated; models with renewal can be analyzed; user-controllable model truncation strategies are supported; and the capability for parameter sensitivity studies can be increased.
(R.C. Butler, 3681)

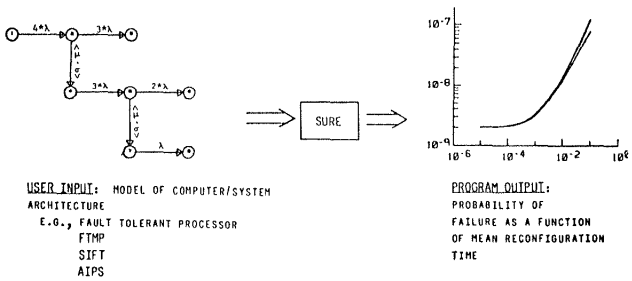

SURE reliability analysis program.

Software Error Studies

Credible predictions of digital system reliability cannot be made without considering the contribution of software embedded in systems. Today, there is effectively only one model for software module "reliability" analysis, the simple constant error rate model. Although many "reliability" growth models have been proposed for estimating that rate, none has yet been shown to be adequate for prediction purposes in the context of highly reliable digital systems. The goal of these studies is, of course, the development of credible statistical methods for estimating the (un)reliability of software modules embedded within (flight) control systems. One aspect of the problem of credible evaluation of the "reliability" of software is the collection of software error data — of laboratory controlled quality.

As part of a software error data collection activity, experiments have been conducted with the computational facilities of the AIRLAB. For the experiments in AIRLAB, four versions of each of several types of software for a radar tracking application were generated. Three versions from each set of four formed the core of the study. (The fourth versions of each set was used as a special comparator.) Data on the frequency of software errors and the nature of the software faults causing the errors were collected in a laboratory controlled manner. The technique of *N*-version programming was used as an error detector. The specific goal of the experiment was to see whether the software error rates (corresponding to distinct software faults) were on the average significantly different, as had been observed in a previous study, or essentially equal, as is assumed in published software reliability growth models. The three independently coded versions of the radar tracking software were tested with millions of input cases. Results of the testing corroborate the previous study; that is, distinct faults have error rates of different magnitudes. In fact, a discernible log-linear relationship appears to be present.

The collected data also revealed the possibility that "reliability" decay may occur when faults are removed (without introducing additional faults) from the software. That is, the error rate associated with a distinct fault in the software would be affected (in a currently unpredictable manner) by the presence or absence of other faults in the software. This phenomenon may provide an explanation for the poor quality of predictions given by the software reliability growth models in the literature. Secondary experiments have been started to determine whether this fault interaction phenomenon warrants further major investigation.
(G.E. Migneault, 3681)

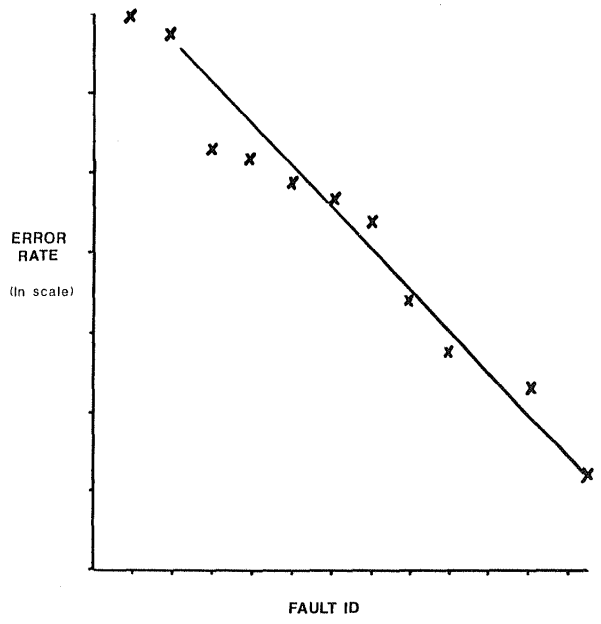

Probabilistic software error rate.

Transport Systems Research Vehicle (TSRV) and TSRV Simulator

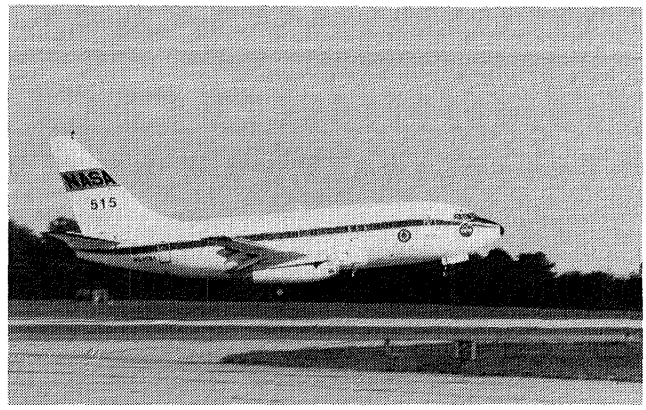

The TSRV and the TSRV simulator are primary research tools used by the Advanced Transport Operating Systems (ATOPS) Program. The goal of the ATOPS Program is the improvement of operational efficiency and safety in the evolving National Airspace System (NAS). Specific program objectives are to develop aircraft systems concepts and companion procedures that will permit the use of more airborne capabilities within the evolving NAS to achieve more efficient operations, and to improve aircraft capability to cope with external factors such as adverse weather and airspace restrictions. In addition, the TSRV affords NASA the capability to respond to unique flight test opportunities in a timely manner. A joint NASA/FAA runway friction and braking flight test program used the TSRV to evaluate braking performance and assess performance predictions made with various runway friction ground measurement techniques. Tests were conducted over the full speed range under a wide variety of test conditions, including surface textures, grooving, wetness, snow, ice, and slush.

The TSRV is a specially equipped Boeing 737 airplane used to conduct research flight tests. The airplane has a special research flight deck located about 20 ft aft of the standard flight deck. Two research pilots fly the airplane from the aft cockpit during test periods. In order to extend the viability of the TSRV as a research tool for the next decade, an experimental system upgrade has been undertaken. The first phase provides increased computational power and speed, higher order programming language, single global bus (DATAC) in lieu of a multiple-bus architecture, display of real-time engineering data on strip charts and TV terminals, and provisions for reducing engineering units data on 540 channels in 1 day instead of 10 days. The second phase of the upgrade, targeted for completion in mid-1986, will encompass provisions for an "all glass" flight deck in the aircraft with eight large color hybrid displays.

The TSRV simulator provides the means for ground-based simulation in support of the ATOPS research program. The simulator is also being modified to duplicate the upgraded aft flight deck located in the TSRV. It allows thorough evaluation of proposed concepts in such areas as guidance and control algorithms, new display techniques, operational procedures, and man/machine interfaces. Promising simulation research results become the subjects of actual flight test research.

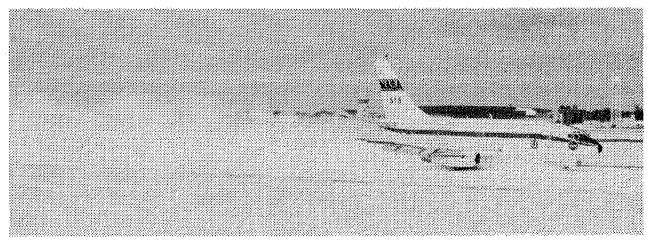

Maximum braking distance in 7 in. powder snow at Brunswick Naval Air Station, Maine.

Idle Engine Performance Model for Optimal Trajectory Calculations

Optimal descent trajectory calculations for jet transport aircraft require accurate knowledge of engine thrust and fuel flow at idle power. A research

effort was undertaken using the NASA TSRV airplane to develop a compact, smooth, and efficient method for mathematical definition of idle-engine performance of jet transport aircraft for use in advanced airborne energy management systems. Identification of potential error levels associated with idle-engine performance was a secondary objective.

Since thrust and fuel flow for turbofan engines are unique functions of power setting, aircraft speed, and atmospheric conditions, a mathematical representation of power setting at idle would provide the desired thrust and fuel flow values without requiring separate idle functions. Tabulated values of thrust and fuel flow for the TSRV 737 were converted to required engine pressure ratio power settings (EPR) using engine handbook data. A series of flight conditions consisting of idle descents and level flight decelerations were then flown on the NASA TSRV aircraft to map the actual idle EPR values throughout the operational envelope of the aircraft.

Analysis of engine handbook data provided a mathematical relationship that was valid for all flight conditions with engine surge bleeds open. Additional data not shown in the figure revealed highly inconsistent operation of the engine surge bleeds, which resulted in EPR increments on the order of 0.06 to be measured when the surge bleeds remained closed. Modeling of surge bleed operation would not be practical without additional internal engine pressure sensors.

(David H. Williams, 3621)

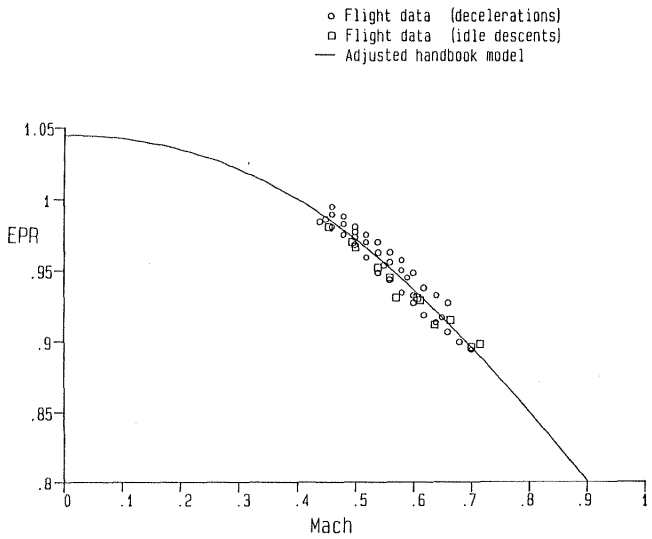

Idle engine performance model for TSRV 737.

Global Data Bus Technology Development

A joint program of development and application of the Digital Autonomous Terminal Access Communication (DATAC) system to the TSRV aircraft has been completed. The DATAC bus represents one of the most advanced forms of system networking under development today. It has the features deemed necessary for future systems, such as autonomous operation of each terminal, a high-speed low-impedance bus medium, and direct memory-to-memory transfer of data. Two systems have been developed, one for the Experimental Avionics Integration Laboratory at Langley and one for the TSRV. Each system consists of a display bus for talking to the all-glass cockpit and a systems bus for all sensor effector and data communication between subsystems.

The DATAC system, which presently networks six major functions of the TSRV flight management/control/display system, has been tested extensively and used in several different research programs conducted under the ATOPS program. The versatility, reliability, and simplification possible through the networking data bus approach have been amply demonstrated. In a short period of time, the TSRV has been reconfigured into three different major operational configurations from which successful experimental programs have been conducted. The DATAC advanced data networking system has been brought from a concept to a proven system that has materially advanced the application of data busing to future commercial transport aircraft.

(David C.E. Holmes, 4757)

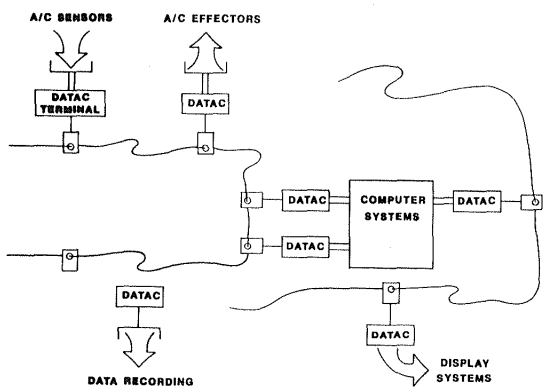

DATAC application in TSRV.

Basic Display and Guidance Requirements for Flying Near-Optimal Trajectories

The advent of the flight management computer in airplanes has provided the potential to compute cost-optimal flight profiles and has fostered the development of several profile optimization algorithms. Assuming these algorithms can be implemented into flight management computers, the question arises as to what the basic guidance requirements to fly these optimized trajectories are. The trajectories that are generated by these algorithms characteristically differ from conventional handbook profiles in that they are constantly varying in both flight path angle and airspeed, resulting in approximately a 2-percent improvement in cost efficiency. Considering the dynamic nature of the pilot's control task, various guidance concepts require testing to assure pilot acceptability with low workload levels. In an effort to address this issue, simulation tests were conducted to investigate the basic display and guidance requirements for flying the near-optimal trajectories.

Three display configurations and four control modes were tested in the experiment to investigate their relative merits in flying the climb and descent trajectories. The path tracking accuracy and the pilot's control activity were the quantitative measures used to evaluate the various display and guidance options. A subjective evaluation of the associated workload and situation guidance was provided through a pilot questionnaire. Although the study was preliminary in nature, the trends in the data and the pilot comments yielded interesting results. The study indicates that the current state-of-the-art flight director type display and guidance, as well as the two more advanced display and guidance configurations tested, were acceptable for flying these profiles.

(Dan D. Vicroy, 3621)

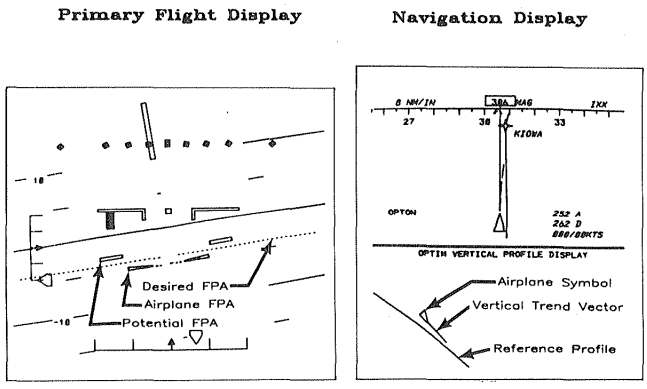

Advanced display/guidance configuration for flying cost-optimized profiles.

Investigated Methods for Integrating Altitude and Airspeed Information Into Primary Flight Display

Computer-based display generation and electronic media technologies offer the potential for improved cockpit display formats through consolidation of information currently presented on several displays. Industry has expressed an interest in eliminating the electromechanical displays of airspeed and altitude and integrating that information into the electronic primary flight display. There are issues, however, regarding how such information should be represented, as well as concern about the resultant impact on crew performance.

This study focused on moving-tape formats for the representation of airspeed and altitude information within electronic primary flight displays. Key questions related to the presentation of information in such formats were examined, including tape centering, tape orientation, and supplementary information. These representations provided eight display configurations for the test. A typical display configuration is shown in the figure. A ninth display configuration was employed as a baseline and used the conventional electromechanical airspeed and altitude instruments. Six subjects participated in this simulation study, which was conducted in the TSRV simulator.

The subjective results indicated that the presentation of information using the moving-tape formats was preferred to that of the conventional instruments, although a slightly lower workload was perceived when the conventional instruments were used. Results regarding tape orientation indicated that workload was lower when the airspeed tape had the high numbers, rather than the low numbers, at the top of the scale. Formats not containing acceleration information produced better performance on the secondary task. Overall, no significant difference was noted in performance among the display configurations. An extension of the study is now being con-

ducted using an increased-difficulty task and a less-intrusive workload measurement technique in a further attempt to differentiate among the various presentation approaches.
(Terence Abbott, 3917)

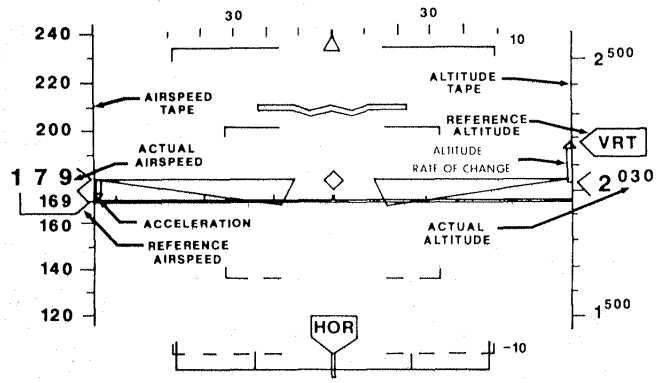

TSRV simulator experimental primary flight display showing one example of altitude/airspeed integration.

mode panel mounted on the glare shield of the cockpit. The system also includes automatic safety modes such as stall protection, overspeed protection, acceleration limiting, and engine throttle limiting. The integrated design of TECS results in a generalized algorithm structure that is largely airplane independent. This offers significant cost reductions in development, testing, and verification of the flight software for new aircraft applications.
(James R. Kelly, 2541)

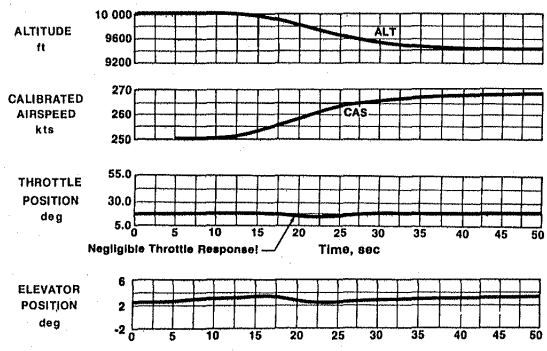

Altitude-airspeed energy exchange for TSRV 737 with TECS.

Total Energy Control System

The Total Energy Control System (TECS), an advanced control concept, has completed flight evaluation in Langley's TSRV. This integrated control concept, originated by Langley and developed by the Boeing Commercial Airplane Company, is unique in that it uses a full-time autothrottle to control the total energy of the aircraft and the elevator to distribute the energy between speed and flight path angle. The major operational benefit of the system is that it eliminates or reduces throttle activity due to flight path perturbations and turbulence. This benefit was readily apparent during flight testing, when the throttle activity during coupled approaches with TECS was compared with that of the baseline TSRV autothrottle, which is a conventional (nonintegrated) design. The reduced throttle activity with TECS has direct payoffs in reduced engine wear, improved passenger comfort, and improved handling qualities.

TECS is a relatively mature control design that includes numerous flight path and speed control modes that can be selected by the pilot using a control

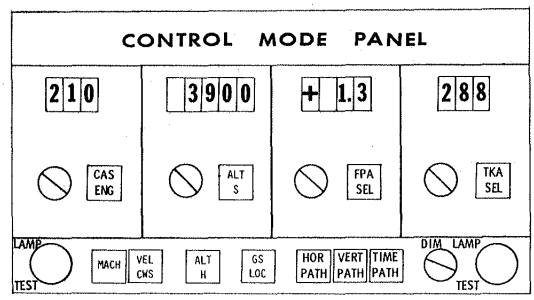

ATOPS/TECS panel.

Satellite Antenna Interference Evaluation

Langley conducted an intensive analytical and experimental program at the request of the Air Force Space Command to evaluate interference effects of

aircraft penetrating the highly directional antenna beams of satellite-to-ground communication links. The project was conducted on an extremely compressed 4-month schedule to meet an Air Force requirement. The program encompassed detailed analysis of aircraft blockage effects, electromagnetic code development, compact antenna range scale model testing, development of experimental instrumentation to detect and record signal perturbations induced by aircraft overflights of the antenna, and development of two aircraft guidance systems and control laws to provide extremely precise tracking accuracy for the TSRV Boeing 737 and a C-5A. Delivery accuracy of 3 ft and 1 sec was achieved over a wide range of test conditions in the 70-hour flight test program. The photograph shows the 737 as it penetrates the satellite antenna beam at low level.

Experimental techniques were developed and validated at Wallops Flight Center for transfer to the test site at Denver, and results have been submitted to the Air Force.

(Jim Hall, 2435)

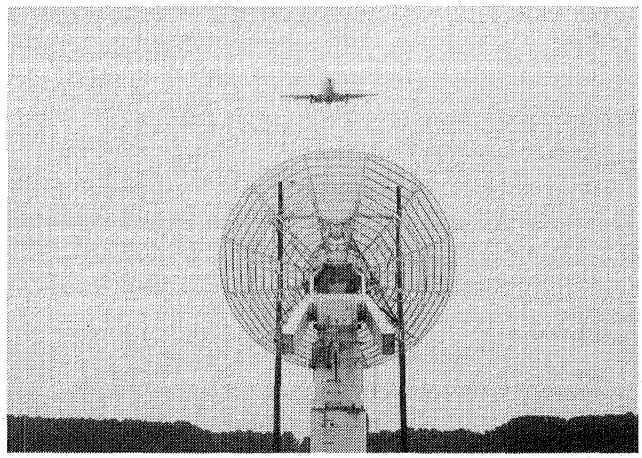

TSRV 737 penetrating satellite antenna beam at low level.

Crew Station Systems Research Laboratory (CSSRL)

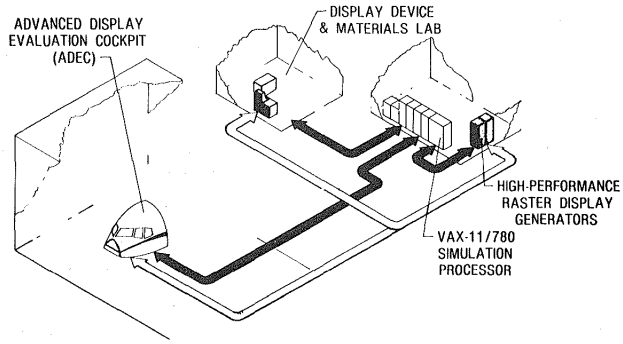

The trend in modern civil cockpits has been to replace electromechanical instruments with electronic control and display devices. The NASA Crew Station Electronics Technology research program is at the forefront of this trend with research and development activities in the areas of advanced display media, display generation techniques, integrated control panels and keyboards, and cockpit systems integration. The experimental devices being developed have unique drive, interface, and systems integration requirements (as opposed to noncockpit electronics) as well as unique testing facility requirements. The Crew Station Systems Research Laboratory (CSSRL) is being implemented in order to provide for candidate device research in a near-real operational electronic and lighting environment in a timely and effective manner. This laboratory provides a unique civil capability to conduct display materials, device, and photometric characteristics research; establish combined display and graphics generation systems performance; determine synergistic features of integrated systems; and establish a data base on cockpit display systems that utilize emissive and reflective devices which are markedly different from their electromechanical counterparts and may be "washed out" by high ambient light or have poor viewability in darkness.

Major elements of the CSSRL are the Advanced Display Evaluation Cockpit (ADEC), which is a reconfigurable research cab, a simulation host processor, high-performance raster display generators to drive cockpit displays, and a Display Device and Materials Lab. During FY 85-86 a variable lighting system is being added for the ADEC to provide the capability of lighting intensities from darkness up to 10,000 footcandles with diffuse through direct-sunlight conditions.

Simulation Investigation of Sunlight Legibility of Flight Displays as a Function of Display Size and Intensity

Modern aircraft cockpits are in a transitional period between reliance on mechanical instrumentation for representations of traditional flight variables and reliance on electronic displays to provide the same information in more reliable and more easily assimilated ways, as well as to provide additional information of increasing sophistication. This transition has occurred because of improved sensor technology and the advent of digital avionics. As more cockpit space is devoted to electronic displays and new display media become available for use, considerations of ambient lighting and direct sunlight effects on the legibility of displays are of increasing concern.

The CSSRL is adding a variable lighting system for the Advanced Display Evaluation Cockpit (ADEC) to allow investigation of lighting effects on various display media in a simulated flight environment. In the interim, a simulation experiment conducted in the ADEC utilized two metal halide lamp sources to provide both ambient and direct illumination of a primary flight display shown on a color CRT. The experiment investigated the legibility of various sizes of displays with several levels of display intensity. The direct illumination of the display surface and the amount of ambient light were also controlled as experimental factors. The situation awareness of the pilot was used as an indicator of the legibility of the display. The subject pilots were presented with a static display of various flight conditions and asked to make the proper control input to return the aircraft to the desired state as indicated by the flight display commands.

The data collected in this experiment are currently undergoing statistical analysis to determine the effects of display size and intensity under the various levels of ambient and direct lighting. Preliminary results indicate that the concept of using situation awareness as a measure of display legibility is indeed a viable technique for laboratory evaluations.
(Russell V. Parrish, 4681)

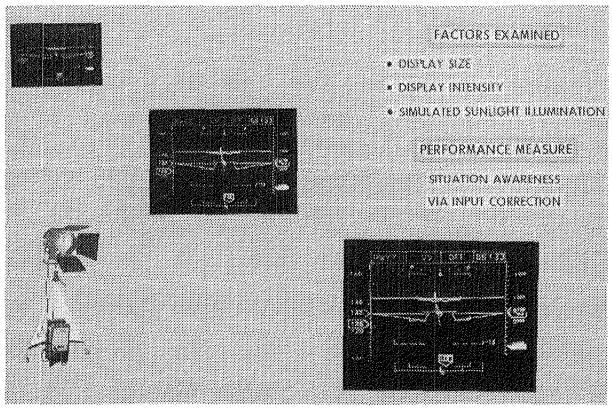

Representation of CSSRL simulator experiment showing primary flight display format used, factors examined, and performance measure.

Human Engineering Methods Laboratory

SIMULATOR WITH BIOINSTRUMENTATION DATA ACQUISITION & ANALYSIS

The Human Engineering Methods (HEM) Laboratory has been established to develop measurement technology to assess the effects of advanced crew station concepts on the crew's ability to function without mental overload, excessive stress, or fatigue. The laboratory provides the capability for measurement of behavioral and psychophysiological response of the flight deck crew.

The facility comprises state-of-the-art bioinstrumentation as well as computer-based physiological data acquisition, analysis and display, and experiment control capability. Software has been developed which enables the demonstration of workload effects on the steady-state evoked brain response and transient evoked response signals as well as the monitoring of electrocardiographic (EKG), electromyographic (EMG), skin temperature, respiration, and electrodermal activity.

The Langley-developed oculometer capability has been integrated with the other physiological measurement techniques. Subjective rating and secondary task methods for assessing mental workload have also been implemented. A computer-based criterion task battery is available for preliminary testing (with human subjects) of workload techniques that are being validated prior to evaluation and application in the simulators. Satellite physiological signal conditioning and behavioral response capture stations are located at the simulator sites to provide human response measurement support for flight management and operations research.

Brainwave Measure Applied to Display Evaluation

Because the nature of crew workload is significantly altered by emerging flight management concepts afforded by advanced crew station technologies, advanced human measurement techniques are required for their evaluation. An important evaluation consideration is the determination of differences in demand for crew mental resources imposed by these crew interface concepts.

One approach employed in this work involves examining the electrical activity of the brain for features that reflect mental resource expenditure. The transient cortical evoked response method—a technique for extracting information from the spontaneous brain activity—has previously been shown to exhibit features that reflect mental activity level.

An evoked response procedure originally developed at the University of Illinois has been implemented in the HEM Laboratory at Langley. A series of auditory tones was presented to the subject, and the electrical brain response to each tone was recorded. The subject counted the low-pitched tones within a series of both high- and low-pitched tones. When counting was the pilot's only task, the brain activity waveform peaked at about 300 milliseconds in response to the counted, low-pitched tones, and not to the uncounted, high-pitched tones (top part of figure). When the pilot was engaged in the flight task, the waveform did not exhibit the peak at 300 milliseconds in response to the counted tones (lower part of figure). Thus, the technique reliably discriminated between task and no-task conditions; however, its value lies in its potential ability to discriminate gradations between these two extremes. Therefore, the evoked response is

currently being assessed for its capacity to distinguish the different mental resource demands imposed by flight tasks performed with different display integration concepts.
(Alan Pope, 3917)

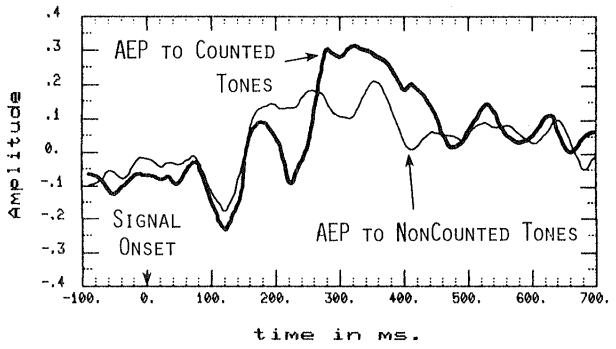

AEP WHEN NO FLIGHT TASK IS BEING PERFORMED

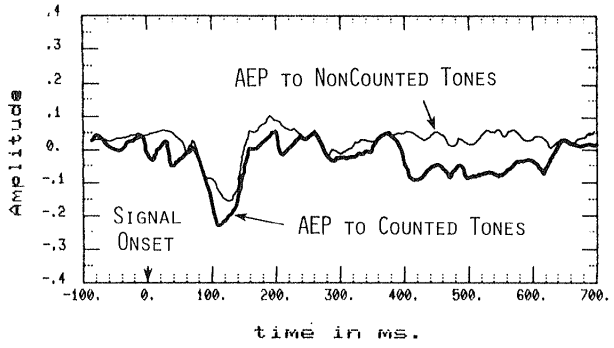

AEP WHEN FLIGHT TASK IS BEING PERFORMED

Mental demands effect on auditory evoked potential (AEP).

Heart Rate Measurements Contribute to Verification of Simulator Realism

The heart rate measurement capability of the HEM Laboratory is being applied in flight management simulation research. These heart rate measures are being investigated, along with other psychophysiological measures, as an indicator of stress level, and have revealed differences in pilots' psychophysiological responses to a simulation.

Electrocardiographic recordings were made from pilots executing a landing approach in the Visual Motion Simulator. An experienced simulator pilot exhibited attenuated heart rate responses to the final landing approach phase of the simulation scenario, whereas a line pilot exhibited a rise in heart rate nearing touchdown, similar to that observed in actual flight. Similarly, heart rate increases were observed in response to unexpected or anomalous conditions that would jeopardize safety if encountered in actual flight. The magnitude of the psychophysiological arousal response to conditions expected to induce stress provides an index of the degree to which the pilot is psychologically engaged by the simulation. This measure of pilot acceptance of a simulation provides a basis for confidence that the results obtained in simulation research are transferable to actual flight.
(Randall S. Harris, Sr., 3917)

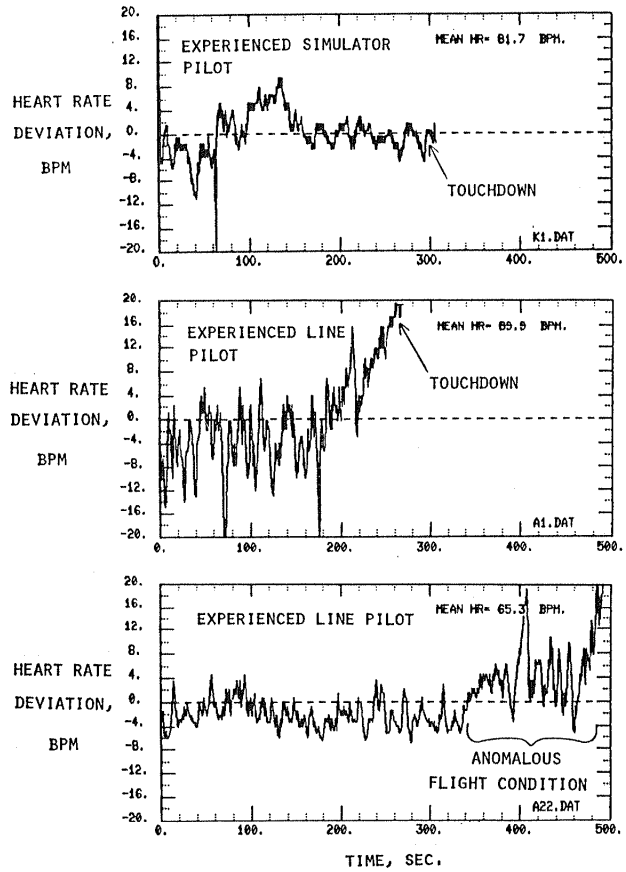

Heart rate deviation plots of experienced simulator pilot and experienced line pilot for landing approach (top and middle), including response of experienced line pilot to anomalous flight condition (bottom).

General Aviation Simulator

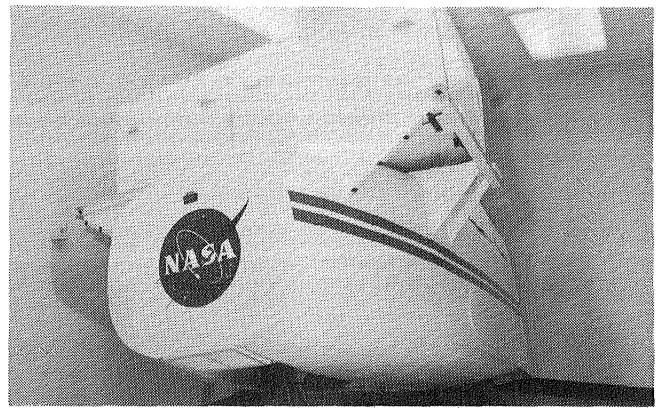

The General Aviation Simulator (GAS) consists of a general aviation aircraft cockpit mounted on a three-degree-of-freedom motion platform. The cockpit is a reproduction of a twin-engine propeller-driven general aviation aircraft with a full complement of instruments, controls, and switches, including radio navigation equipment. Programmable control force feel is provided by a "through-the-panel" two-axis controller that can be removed and replaced with a two-axis side-stick controller that can be mounted in the pilot's left-hand, center, or right-hand position. A variable force feel system is also provided for the rudder pedals. The pilot's instrument panel can be configured with various combinations of cathode ray tube (CRT) displays and conventional instruments to represent aircraft such as the Cessna 172, Cherokee 180, and Cessna 402B. A collimated-image visual system provides a 60° field-of-view out-the-window color display. The visual system can accept inputs from a terrain model board system and a computer-generated graphics system. The simulator is flown in real time with a CDC Cyber 175 computer to simulate aircraft dynamics.

Research conducted in the GAS on the single-pilot instrument flight rules (SPIFR) program has identified the pilot interface with cockpit controls and displays as a critical factor in reducing pilot workload and blunders. The air traffic control (ATC) mode-S transponder, planned for operational use in the next decade, will add the capability of a digital ground-air-ground data link to the general aviation (GA) SPIFR cockpit. A research program is under way to evaluate the impact of various levels of data link capability on GA SPIFR operations. The levels tested will vary from uplink only of short ATC messages to uplink and downlink of complex messages. Messages to be considered will include weather data, initial IFR clearances, and ATC tactical instructions. Initial tests will utilize current ATC procedures and conventional aircraft avionics suites. Follow-on tests will consider advanced ATC procedures and the interface of the airborne data link device with flight management system computers for execution of ATC clearances. Another research application using the GAS is the investigation of flight control problems encountered in recovering a twin-engine GA aircraft to normal flight after one engine fails.

Light Twin Automatic Engine-Out Trim System

An automatic trim system to reduce the control forces on a light twin airplane after an engine failure has been studied on the General Aviation Simulator. Previous work has concentrated on the fundamental characteristics of the proposed system and their effect on the handling qualities. The system was found to be highly beneficial for the evaluated maneuver, including the most critical maneuver, which involved an engine failure immediately after takeoff from the simulated runway.

The study has moved into more operational aspects of the proposed system. That is, the effects of failures in the automatic trim system itself are now being evaluated. Although the tests are not complete, system failures are not catastrophic even in the worst case in which the trim tabs are driven to their mechanical stops and remain there until a landing can be made. For the more optimistic and probably more realistic case in which the trim tabs can be returned to their normal position after the system failure, the system failure causes very minor difficulty.

Another aspect of the automatic trim system has also been investigated. The original system utilized dynamic pressure sensors in the propeller slipstreams to detect engine failures and drive the trim tabs to the necessary positions. Although this is the most direct method to accomplish the retrimming task, it requires sensors external to the skin of the airplane, where they are subject to undesirable environmental conditions. Therefore, an alternate sensor arrangement that uses fuel flow rate sensors is being investigated. The effect of the engine mixture setting and the nonlinear relationship of thrust with fuel flow rate is now being studied. However, in most cases the research pilots who have flown system with both types of sensors could not tell the difference between the two.
(Eric C. Stewart, 2184)

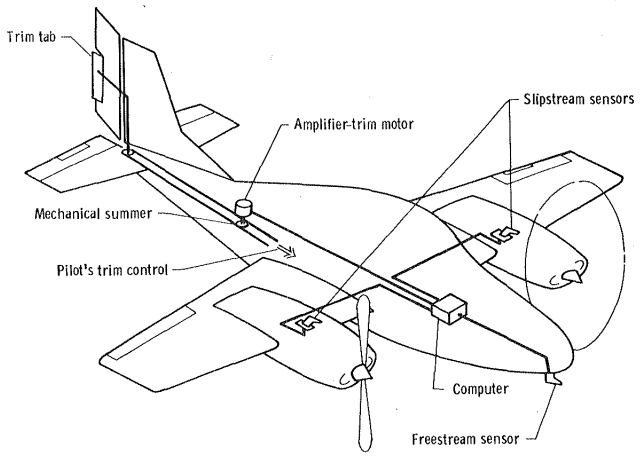

Engine-out trim system concept.

Mission Oriented Terminal Area Simulation (MOTAS)

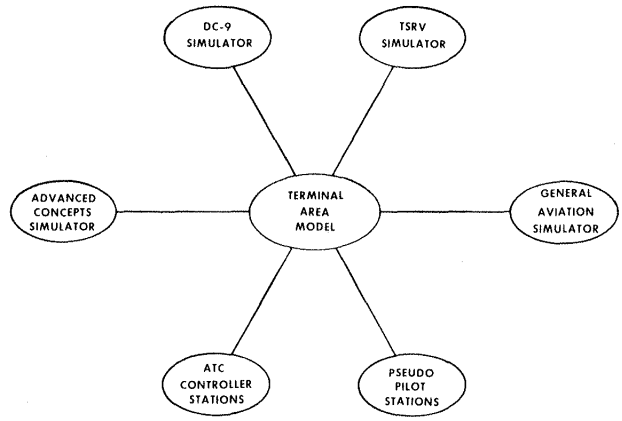

The Mission Oriented Terminal Area Simulation (MOTAS) Facility is an advanced simulation capability that provides an environment in which flight management and flight operations research studies can be conducted with a high degree of realism. This facility provides a flexible and comprehensive simulation of the airborne, ground-based, and communications aspects of the airport terminal area environment. The major elements of the MOTAS facility are an airport terminal area environment model, several aircraft models and simulator cockpits, four pseudo pilot stations, four air traffic controller stations, and a realistic air-ground communications network. The airport terminal area environment model represents today's Denver Stapleton International Airport and surrounding area with either a computer-generated automated metering and spacing system of control or a present-day vectoring system of control with air traffic controllers. In addition, the model simulates various radar systems, navigation aids, wind conditions, and so forth.

The MOTAS facility combines the use of several cockpit simulators and pseudo pilot stations to fly aircraft in the airport terminal area. The MOTAS facility is presently fully operational with the Transport Systems Research Vehicle (TSRV) Simulator and the General Aviation Simulator. The DC-9 Full-Workload Simulator has been interfaced to the facility in a simplified mode and will be converted to full operational capability when called for by research requirements. The Advanced Concepts Simulator will be interfaced to the facility once it becomes operational as a stand-alone simulator. These cockpit simulators will allow full crews to fly realistic missions in the airport terminal area. The remaining aircraft flying in the airport area are flown through the use of the pseudo pilot stations. The operators of these stations can control five to eight aircaft at a time by inputting commands to change airspeed, altitude, direction, and so forth. The final major components of the facility are the air traffic controller stations, which are presently configured to display and control the two arrival sectors, the final approach sector, and the tower and/or departure sectors.

Because of its flexibility in reconfiguring according to research requirements, the MOTAS facility can support a variety of flight vehicle and/or air traffic control system research studies that would not be possible in the real world due to safety, economy, and repeatability considerations. One such study being initiated addressed operational issues in the integration of data link transfer of ATC information and advisories in the advanced National Airspace System (NAS) being developed by the Federal Aviation Administration. The NAS Plan currently includes a mode-S data link capability to become operational in 1988. Other air-ground data transfer facilities such as communication satellites are being considered for

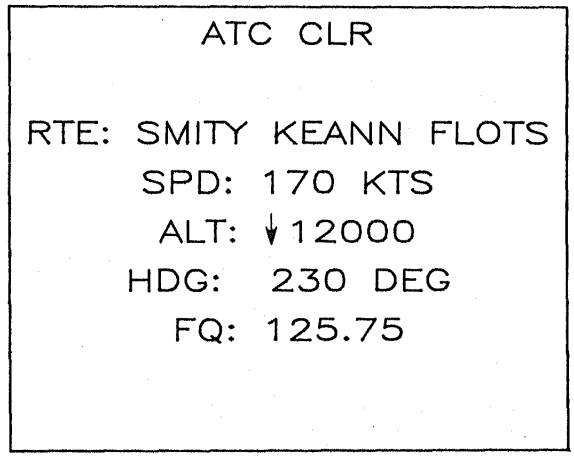

Experimental page: CDU displayed data-linked ATC clearances.

later applications. The MOTAS facility, in conjunction with the TSRV simulator, is being used in development tests to evolve a transport cockpit interface for air-ground exchange of ATC messages.

The first phase of this study will determine the acceptability of the Control-Display Unit (CDU) of the flight navigation and control computer as a data link interface. The CDU includes a keyboard input and a 4-in. CRT for display. Research pilot opinion and the expertise of researchers in the areas of flight systems, human factors, and the ATC system are being used to guide the research and development. This study will address such questions as how to appropriately alert the crew of incoming messages and their urgency, which data exchanges are appropriate for data link and which should continue to be transmitted via voice radio, and what software and hardware assistance should be provided in the cockpit to enable efficient message exchange. Tests on the MOTAS/TSRV facility will determine the effects of data link information transfer with well-designed interfaces on operator workload, gains in system capacity, fuel saving, and safety through more efficient air-ground information transfer.

Environmental Impact of Proposed Denver Stapleton Airport Expansion

The MOTAS facility was recently used in support of the Airport '85 Project, which is a study conducted by Langley and its research support contractors for the Air Force Space Command to predict satellite downlink signal amplitude and phase variations due to aircraft transit of the ground receiving antenna beam. In particular, the capabilities of MOTAS were used to assist in the evaluation of the environmental impact of the proposed Denver Stapleton airport expansion project on the satellite signal communications environment at the Buckley Air National Guard site located outside Denver. Three potential airport runway configurations were evaluated in the MOTAS facility. For each configuration, the proposed runway environment was coded into the Manual Vectoring (MAVEC) terminal area model, which was developed for MOTAS by the Research Triangle Institute. Approximately 100 aircraft tracks, arrivals, and departures which would be typical for the runway configuration were generated in real time. The expertise of a former air traffic controller was utilized to issue the appropriate commands to the aircraft in the simulation to create the desired aircraft tracks.

The data recorded from these aircraft tracks were subsequently analyzed for possible interference of civil aircraft with the Buckley satellite receiving stations. The ultimate objective of the MOTAS runway configuration analysis is to provide valuable data for the Stapleton Airport Planning Commission, the Air Force, and the Federal Aviation Administration to consider in making the selection of the most appropriate site for the new runway system at Denver. **(Jacob A. Houck, 2981)**

Differential Maneuvering Simulator

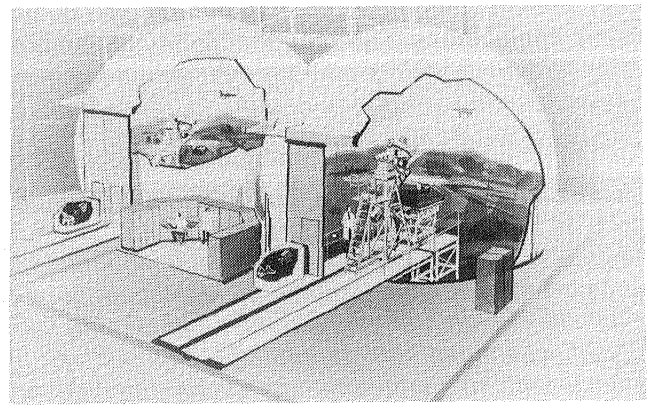

The Langley Differential Maneuvering Simulator (DMS) provides a means of simulating two piloted aircraft operating in a differential mode with a realistic cockpit environment and a wide-angle external visual scene for each of the two pilots. The system consists of two identical fixed-base cockpits and projection systems, each based in a 12.2-m-diameter (40 ft) projection sphere. Each projection system consists of a sky-Earth projector to provide a horizon reference and a system for target image generation and projection. The internal sky-Earth scene provides reference in all three rotational degrees of freedom in a manner that allows unrestricted aircraft motions. The present sky-Earth scene has no translational motion. The internal visual scene also provides continuous rotational and bounded (300 to 45,000 ft) translational reference to a second (target) vehicle in six degrees of freedom. The target image presented to each pilot represents the aircraft being flown by the other pilot in this dual simulator. Each cockpit provides three color displays with a 6.5-in.-square viewing area and wide-angle head-up display. Kinesthetic cues in the form of a *g*-suit pressurization system, helmet loader system, *g*-seat system, cockpit buffet, and programmable control forces are provided to each pilot consistent with his aircraft's motions. Other controls include a side arm controller, dual throttles, and a rotorcraft collective. Research applications include studies of high-angle-of-attack flight control laws, evaluation of evasive maneuvers for various aircraft and rotorcraft, and evaluations of the effect of parameter changes on the performance of several baseline aircraft.

Thrust Vectoring Controls for Supermaneuverability

Results of air combat studies have emphasized the importance of providing future fighter aircraft with extreme levels of agility and maneuverability throughout their flight envelope ("supermaneuverability"). As part of an effort to develop technologies to enable realization of this capability, studies are under way to investigate the concept of vectoring the entire thrust for control at low-speed high-angle-of-attack conditions. The high levels of control power provided by thrust vectoring offer the potential of dramatic improvements in maneuverability in this flight regime. To investigate this concept, a study was conducted on the DMS with a mathematical model of an advanced fighter configuration which incorporated thrust vectoring for pitch and yaw control. The objectives were to determine the levels of thrust and vectoring angles required, to investigate the improvements in maneuverability provided by the vectoring controls, to investigate the improvements in maneuverability provided by the vectoring controls, to study the flight dynamics problems associated with this enhanced capability, and to assess control law requirements and pilot and weapon interface considerations.

The results of the study showed that the increased control from thrust vectoring allowed significant enhancement of low-speed high-angle-of-attack controllability and maneuverability. As a result, the airplane with thrust vectoring was found to be considerably more effective in simulated one-on-one air combat situations than the baseline airplane. The study also identified design requirements that must be met to maximize the benefits obtained from this concept.

(Marilyn E. Ogburn, 2184)

Visual/Motion Simulator

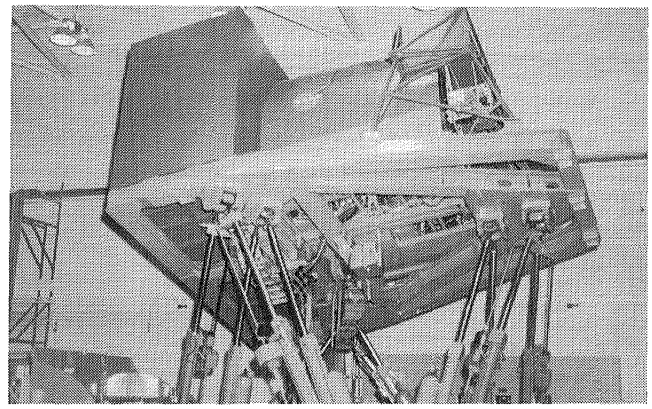

The Visual/Motion Simulator (VMS) is a general-purpose simulator consisting of a two-man cockpit mounted on a six-degree-of-freedom synergistic motion base. A collimated visual display provides a 60° out-the-window color display for both left and right seats. The visual display can accept inputs from several sources of image generation. A programmable hydraulic-control loading system is provided for column, wheel, and rudder in the left seat. A second programmable hydraulic-control loading system for the right seat provides roll and pitch controls for either a fighter-type control stick or a helicopter cyclic controller. Right-side rudder control is an extension of the left-side rudder control system. A friction-type collective control is provided for both the left and the right seat. An observer's seat will be installed in 1986 to allow a third person to be in the cockpit during motion operation.

A realistic center control stand was installed in 1983 which, in addition to providing transport type control features, provides autothrottle capability for both the forward and reverse thrust modes. Motion cues are provided in the simulator by the relative extension or retraction of the six hydraulic actuators of the motion base. Washout techniques are used to return the motion base to the neutral point once the onset motion cues have been commanded. In addition, a *g*-seat is provided which can be interchanged between the left and right seats to augment the motion cues from the base.

Research applications have included studies for transport, fighter, and helicopter aircraft. The studies addressed problems associated with wake vortices, high-speed turnoffs, microwave landing systems, energy management, multibody transports, and maneuvering stability flight characteristics. Numerous simulation technology studies have also been conducted to evaluate the generation and usefulness of motion cues.

F-106B Vortex Flap Flying Qualities

Wind tunnel tests and theoretical studies have shown that the vortex flap concept can provide significant maneuvering performance improvements for aircraft configurations with highly swept wings. A flight demonstration program is planned to test the vortex flap concept on an F-106B airplane.

Although wind tunnel experiments on the F-106B configuration have shown the expected performance improvements, the results indicate that the vortex flaps can affect stability characteristics as well. To assess the resulting impact on the flying qualities of the airplane, a piloted simulation investigation was initiated on the VMS. Data from several Langley wind tunnel facilities were used to develop mathematical models to represent both the basic F-106B and the F-106B with vortex flaps. Although the simulation allows study of the flying qualities of the airplanes throughout their operational flight envelopes, the initial phase of the investigation focused on the approach-to-landing segment of flight.

Results to date showed that the reduction in longitudinal stability caused by the vortex flaps resulted in degraded handling qualities at approach flight conditions. Satisfactory handling qualities can be maintained by limitations on the operational center-of-gravity range of the airplane. The simulation results also indicate minor effects of the vortex flaps on lateral-directional flying characteristics.

Further tests are under way to evaluate higher speed and maneuvering conitions. The effects of flap deflection angle will also be investigated.

(Jay M. Brandon, 2184)

60-Foot Space Simulator

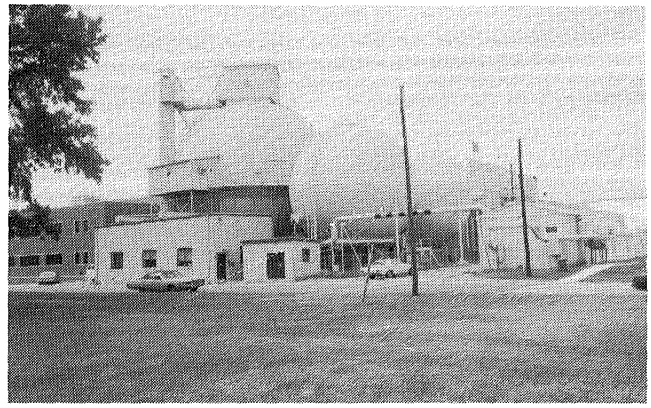

This 60-foot-diameter sphere facility can simulate an altitude of 320,000 ft (2×10^4 mm Hg). This vacuum level is attainable in 7 hours with a three-stage pumping system. The carbon steel sphere is accessible through a personnel door, a 12-ft-diameter specimen door, and a 4-ft maintenance door at the top. A 2-ton hoist located at the top enhances specimen handling inside the sphere. Sight ports are located both at the top and at the equator. Two closed-circuit television cameras, a video cassette recorder, and an oscillograph are available. Firing circuitry and a programmer are available for the use of pyrotechnics, and a system of flood lights is installed in the sphere to facilitate high-speed photography. The sphere is used primarily for dynamic testing of aerospace components and models at near-space environment.

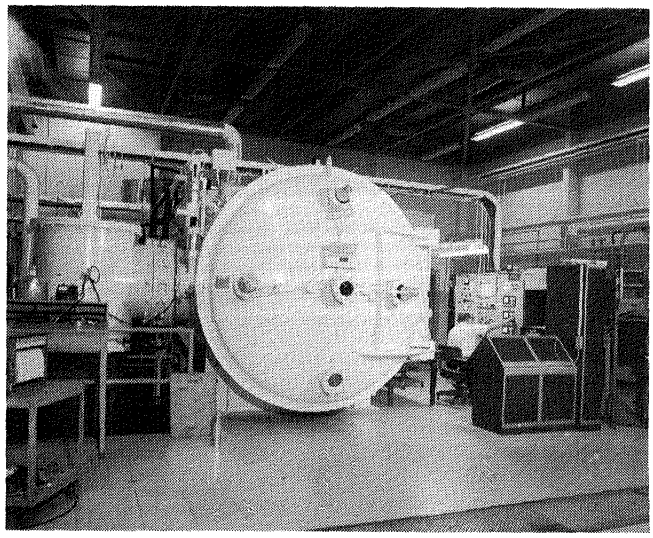

L-80-5739

8 by 15 thermal vacuum chamber.

Thermal vacuum testing has long been a prerequisite to the active deployment of space experiments. A series of experiments that optically sense characteristics of the Earth's atmosphere from outer space necessitated the creation of an ultra-high-cleanliness thermal facility. The optical components of these experiments would be severely degraded by contamination by oils or other vaporous materials commonly found in thermal chambers and vacuum pumping systems. Langley created the 8×15 Thermal Vacuum Chamber Facility by repeated vacuum bake-out and solvent wipedown of a previously used chamber. Two 35-in. cryogenic pumps were installed and cold traps were inserted in the roughing pump lines to eliminate back contamination from the pumps. The chamber is capable of -300° F to +1000° F temperatures and has glass ports for solar illumination simulation. A one unit flux solar simulator is installed with the chamber.

Chemical Canister Gas Spring Ejection Tests

Tests were conducted in collaboration with the Goddard Space Flight Center to qualify the gas spring powered ejection system for a chemical canister. The canister was to be launched into space from Wallops Flight Test Facility as a part of a continuing upper-atmosphere test series. The ejection is accomplished by the parallel action of three pneumatic cylinders within the canister. The tests of the system were accomplished while the canister was in freefall from the top of the sphere, with the canister spinning at four revolutions per second. Facility instrumenta-

tion, high-speed photography, pyrotechnics, and the facility video system were used to complete the successful tests.
(Roger Messier, 2156)

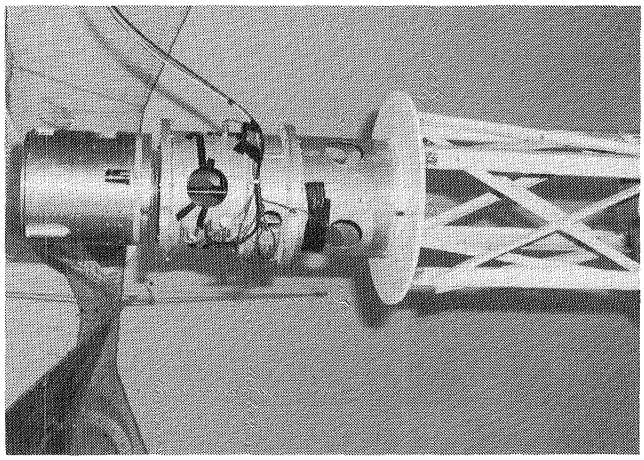

L-85-4642

Canister test setup suspended in 60-ft sphere.

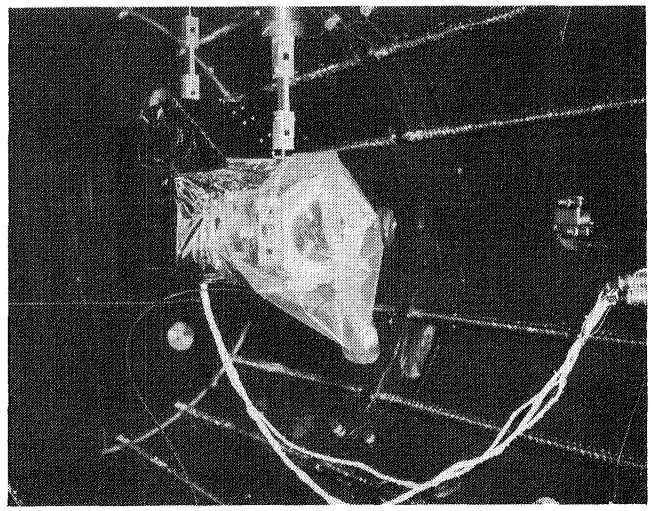

L-84-839

HALOE engineering test in ultra-high-cleanliness thermal vacuum chamber.

Halogen Occultation Experiment Thermal Vacuum Test

The Halogen Occultation Experiment (HALOE) is designed to make measurements of the vertical distribution of a number of key upper-atmospheric trace gases from space. Accurate interpretation of the satellite measurements requires precise knowledge of the spectral characteristics of the dominant optical elements, the spectral filters, and calibrated gas cells located in the optical path. To accomplish the thermal vacuum qualification tests for this experiment, a chamber was needed which would have little chance of introducing contaminants to the optical components. The 8 × 15 Ultra-High-Cleanliness chamber was selected. The photograph shows the HALOE experiment installed in the chamber for a preliminary engineering evaluation test of the thermal expansion characteristics of the telescope and Sun sensors. Results indicated a satisfactory thermal design had been achieved with respect to thermal expansion, and also showed that no optical contamination occurred.
(Jim Raper, 2668)

Structural Dynamics Research Laboratory

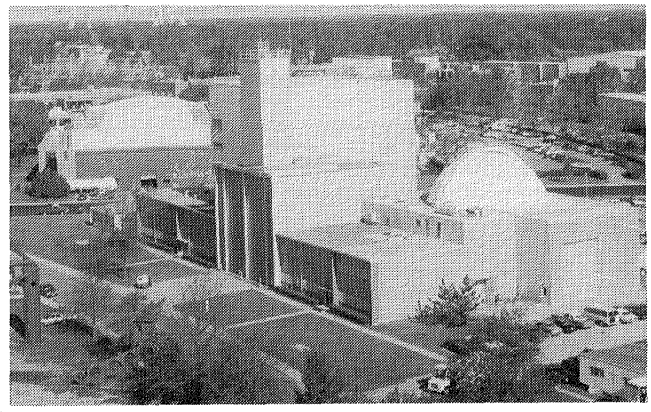

The Structural Dynamics Research Laboratory is designed for the conduct of research on the dynamic behavior of spacecraft and aircraft structures, equipment and materials. It offers a variety of environmental simulation capabilities, including acceleration, vacuum, and thermal radiation.

A main feature of the laboratory is a 55-ft-diameter thermal-vacuum chamber with a removable 5-ton crane, flat floor, 64-ft dome peak, and large centrifuge or rotating platform. Access is by an airlock door and an 18-ft high, 20-ft-wide test specimen door. There are 10 randomly spaced 10-in.-diameter view ports, and closed-circuit televison visually monitors tests. A vacuum level of 10 torr can be achieved in 120 minutes and, with diffusion pumps, 10^{-4} torr in 160 minutes. A centrifuge attached to the floor of the chamber is rated at 100 *g*, with a 50,000-lbf capacity and a maximum allowable specimen weight of 2000 lb. Six-ft test specimen mounting faces are available at 16.5-ft or 20.5-ft radius. A temperature range of 100° F is obtained from 250 ft^2 of portable radiant heaters and liquid-nitrogen-cooled plates.

The other predominant feature of the laboratory is a 38-ft-high backstop of I-beam construction. Test areas available around this facility are 15 by 35 by 38 ft high and 12 by 12 by 95 ft high. Available excitation equipment includes several types of small shakers. The largest is a hydraulic shaker with a capacity of 1200 lbf, a 3-in. stroke, and a range of 0 to 170 Hz.

Closed-circuit television cameras monitor all tests areas. Both the vacuum chamber and the backstop test areas are hard-wire connected to a central data acquisition and processing room. This room contains signal conditioning equipment and analog and digital data recording capability for up to 220 channels of data. A Hewlett-Packard 5451C Fourier Analyzer System is available along with a VAX 11-780/EAI 2000 hybrid computer system for simulation and on-line test control. A variety of auxiliary data logging and signal processing equipment is also available.

Slewing Control Successfully Demonstrated for Flexible Solar Panel

This experiment is designed to verify theoretical analyses concerning the application of modern control methods to the control of flexible structures. A 13-ft-long flexible solar panel model with a cross section of 2.1 ft by 0.13 in. is used for experimental validation. The test model is cantilevered in a vertical plane and rotated in the horizontal plane by an electric gearmotor. Instrumentation consists of three full-bridge strain gauges to measure bending moments and two angular potentiometers to measure the angle of rotation at the root. Signals from all four sensors are amplified and then monitored by an analog data acquisition system. An analog computer closes the control loop, generating a voltage signal for the gearmotor based on a linear optimal control algorithm with terminal constraints in finite time.

The controller successfully performed large-angle maneuvers and damped out flexible modes by the end of the maneuver. The figure shows an example of results for a 30° slew in 3.5 seconds. When no control is used, residual motion is significant, whereas the controller produces the same maneuver with virtually no residual motion. Satisfactory agreement was achieved between experimental measurements and theoretical predictions. In vacuo values of frequency and damping correlated with less than 10 percent

error. Nonlinear effects due to large bending deflections during the maneuver did not cause significant changes in performance of the control laws, which were designed using linear control theory.
(Jer-Nan Juang, 2881)

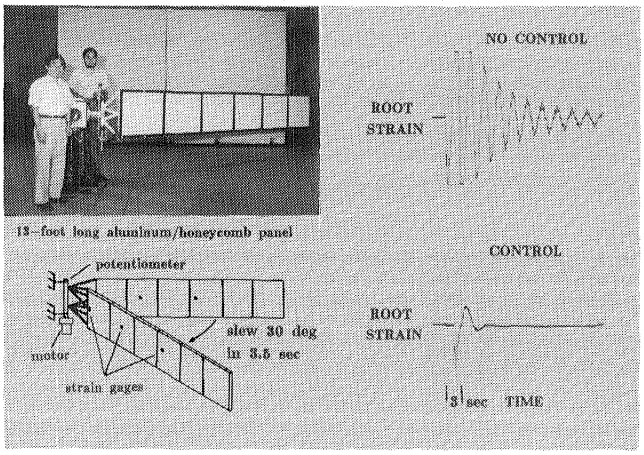

L-85-11, 996

Test setup.

Hoop/Column Antenna Dynamic Tests

Large space antennas require accurate dynamic analysis to determine their in-space performance when subjected to control forces or to structural vibrations. Large, lightweight antenna concepts are being developed which use complex structures to maintain close surface tolerances. New, advanced analysis methods are needed to analyze the structures, and these methods must be verified by test data. A 15-m hoop/column antenna, an advanced tension-stiffened concept, is being tested in the Langley 16-m Vacuum Facility to verify analysis methods for use in predicting the dynamic behavior of this type of antenna. An additional objective to the test program is the development of ground vibration test methods for large flexible space structures.

Modal vibration tests are the principal means being used to extract dynamic data for comparison with analytical predictions. These tests are performed by the application of vibratory forces to the structure and measuring the response. The response is quite sensitive to the method used to hold the structure and to ambient air. The 15-m antenna is being tested in two ways: mounted on a tripod support system, as shown in the figure, and suspended in pendulum fashion. Test results from differing support systems allow a cross check in verifying analysis methods and provide a basis for extrapolating the analysis to the unsupported conditions in space. Ambient air effects are being studied by testing the antenna in both air and near vacuum conditions. These tests provide frequency and damping data to evaluate the necessity of using vacuum during ground vibration tests of future space antennas. Preliminary results showed that the measured frequencies are approximately 15 percent lower than analysis predicted. In an attempt to increase the prediction accuracy, measured stiffness data are being acquired for use in updating the analytical finite element model. High measured damping values (much higher than typical truss type space structures) are attributed to the joints in the telescoping center column.
(W. Keith Belvin, 2446)

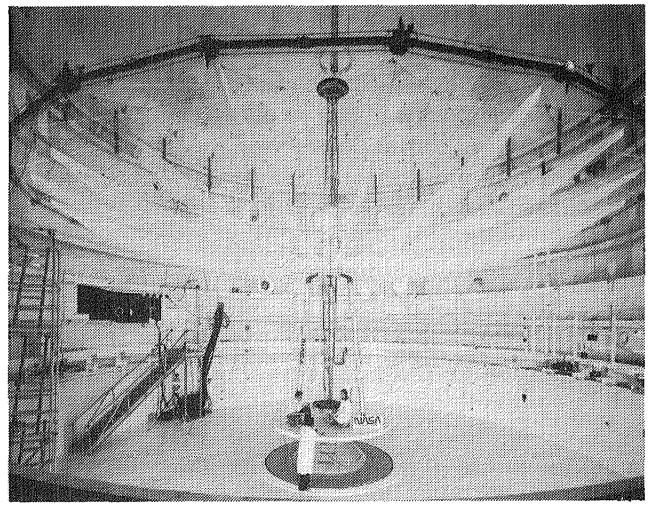

L-85-13,262

Test of hoop/column antenna.

NDE Research Laboratory

The reliability and safety of materials and structures is of paramount importance to NASA. The assurance of reliability must be based on a quantitative measurement science capability that is nondestructive. The Langley NDE Research Laboratory has as its prime focus the development of new measurement technologies that can be directly applied to ensuring material integrity. Furthermore, the laboratory activity is strongly directed towards developing relationships between measurable physical properties and the necessary engineering properties required for structural performance.

The Langley NDE Research Laboratory is a combination of research facilities providing advanced nondestructive evaluation (NDE) capabilities for NASA and is an important resource for government and industry technology transfer. The laboratory is the Agency's focal point for NDE and combines basic research with technology development and transfer. The activity concentrates on NDE materials measurement science for composites, metal fatigue, applied and residual stress, and structural NDE.

The facility is a state-of-the-science measurement lab linking 16 separate operations to a central computer consisting of a VAX-750 with 10 megabytes of internal memory and over 500 megabytes of fast storage. The system interfaces with a real-time video input-output so that NDE images can be obtained, processed, and analyzed on line. The major laboratory operations include a 100-KIP load system for stress/fatigue NDE research, a magnetics laboratory for residual stress, three computer controlled ultrasonic scanners for imaging material properties, a technology transfer laboratory, an electromagnet impedance characterization laboratory for composite fiber integrity, a composite cure monitoring laboratory for process control sensor development, a nonlinear acoustics laboratory for advanced NDE research, a laser modulation applications laboratory for remote strain sensing, a pressure and temperature derivative laboratory for higher order elastic constant measurements, a thermal NDE laboratory, and a signal processing laboratory for improved image resolution and information transfer.

Correction for Energy Shadowing of Defects in Ultrasonic Scan Data

Conventional ultrasonic investigation of defects in the bulk of complex materials is a common industrial technique. A usual procedure is to scan the specimen in a water bath, where the ultrasonic transducer transmits waves into the investigated material. When the propagating waves reach acoustical discontinuities such as defects, partial reflection occurs. The reflected waves are detected by the transducer, and a graphical representation of the integrity of the specimen is displayed. Some advanced systems even correct for simple attenuation.

However, this method has a major drawback. As the waves continue to propagate through the material, any major reflection causes reduction in the transmitted wave. This effect, which may be even more dominant than the simple attenuation, causes any further reflections to appear weaker than they actually are. This effect thus misrepresents the defects that are "shadowed" by previous defects.

A numerical algorithm developed in the NDE signal processing laboratory enables the correction of such shadowing by digital signal processing. This algorithm is fast and simple enough to be adopted for

real-time applications in industry. The figure shows an example of such a correction. Deep reflections, which look very small in the raw data (represented by weak amplitudes, late in time, in the top figure), show up much stronger in the corrected case (bottom figure). Images of material defects with the shadowing corrections permit more quantitative interpretation of the material state.
(Joe Heyman, 3036)

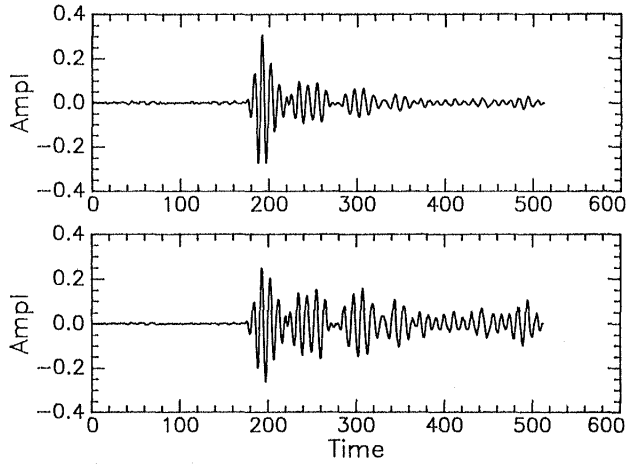

Ultrasonic reflections before (top) and after (bottom) digital signal processing.

Time Gain Compensation Circuit for General Use in NDE and Ultrasonics

A high-frequency time gain compensation circuit was designed and built in the NDE signal processing laboratory for a wide variety of applications in nondestructive evaluation and ultrasonics measurements. The circuit features a wide signal bandwidth (in excess of 50 MHz) and a large dynamic range (greater than 50 dB). The control bandwidth of 5 MHz assures accuracy to the control signal. The signal-to-noise ratio is 100 dB.

The circuit is presently being used in a number of applications. In one case, its use permits retrieval of more information from ultrasonic signals sent through composite materials, which are highly attenuating. Another application has been in the use of ultrasonics to measure the depth of skin burn in humans. The circuit affords the wide bandwidth necessary for adequate resolution of burn depth while compensating for the large high-frequency ultrasonic attenuation of human skin.

The figure shows a typical pulse echo pattern received after an ultrasonic tone burst has been sent through an aluminum sample. The tone burst patterns decay nearly exponentially. The middle trace is the control signal, which is designed to offset the exponential decay. The trace shows the effect of "removing" the exponential decay.
(W.T. Yost, 3036)

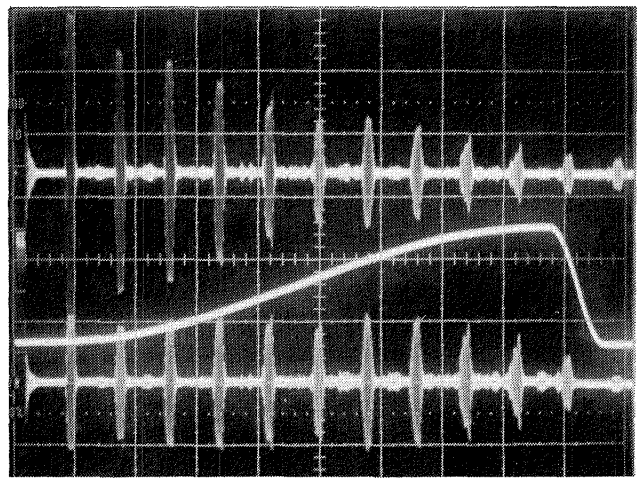

Typical pulse echo pattern.

Digital Pulse Shaping of Ultrasonic Data

Quantitative analysis of defects and flaws in complex material such as composite materials requires the ability to identify the distinct reflections in the ultrasonically investigated material. Composite materials in particular pose a problem when the waves have to be transmitted at relatively low frequencies due to the high attenuation at higher frequencies. Overlapping of echoes becomes significant then, and complex wave propagation patterns complicate positive identification of signals.

A digital time domain pulse shaping technique developed in the NDE signal processing laboratory

was applied to experimental results from graphite-epoxy materials. This method, which was developed by Doron Kishoni of the National Research Council during his research associateship at Langley, significantly enhanced the sharpness of the ultrasonic waveforms and improved the analytical resolution of the system, enabling clear detection of damaged regions that were difficult to identify otherwise.
(Joe Heyman, 3036)

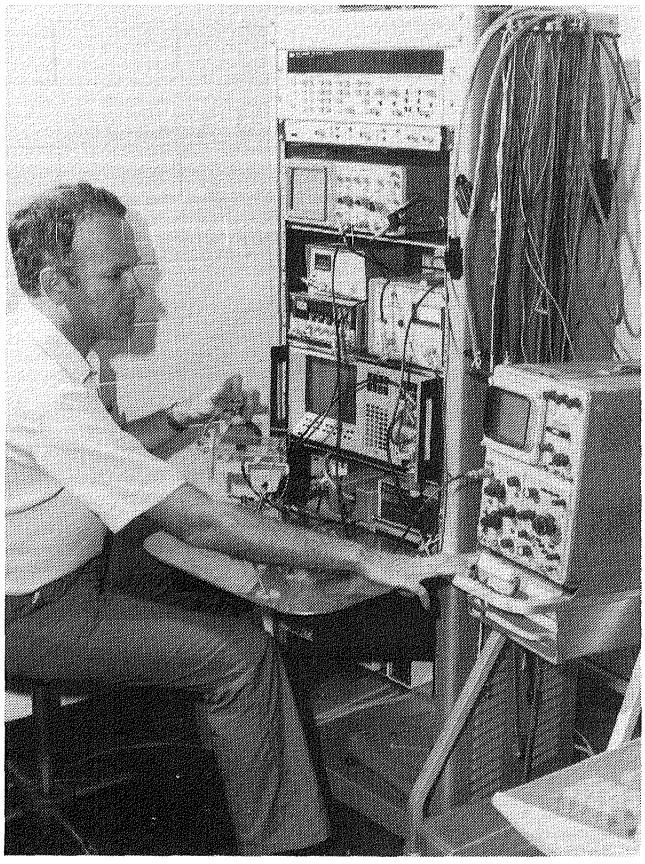

L-85-11,438

Ultrasonic tests demonstrate improved resolution.

Magnetic Ultrasonic Stress Technique

A new class of NDE instrumentation developed in the NDE magnetics laboratory can determine the sign of residual or applied stress without requiring any calibration. The technique, which was developed by Min Namkung of the College of William and Mary while working on a grant at Langley, depends on the interaction of ultrasonic waves in ferrous materials and on the state of stress. A high-resolution ultrasonic phase-locked loop, also designed at Langley, is used to measure small changes in the sonic velocity that accompany magnetization of the specimen. The resulting magnetic derivative determines the type of stress field present. With calibration as to material carbon content, the technique can also determine the amplitude of the internal stress.

The system is being tested on railroad wheels in a technology transfer program with the Federal Railroad Administration and the American Association of Railroads to help solve a $100 million problem that industry is having with wheel failures.
(Joe Heyman, 3036)

L-85-1884

Demonstration of final tests of residual stress sensor.

Development of Ultrasonic Ice Detection System

Icing conditions represent one of the most severe weather hazards encountered during aircraft flight and one of the hardest weather conditions to forecast

accurately. The potential for aircraft icing exists whenever an aircraft encounters liquid moisture at outside temperatures at or below the freezing point. Any exposed surface on an aircraft is subject to icing, with a subsequent change in lift characteristics due to drag forces. A practical ice detection warning system would be useful to warn pilots when icing conditions are encountered.

The feasibility of using a pulsed-echo ultrasonic system to detect ice on an airfoil has been investigated. Initital tests were conducted in a laboratory experiment that used refrigerated ice on an aluminum surface. Tests were conducted with both compressional and shear waves at a test frequency of 5 MHz. The figure shows how sound wave reflections are detected at the interface of aluminum and ice and at the interface of ice and air. In each figure, ΔT_1 represents the time required for a compressional wave and a shear wave to travel through 20-mm-thick type 7075 aluminum, and ΔT_2 represents the time required for a shear wave and a compressional wave to travel through ice 6.1 and 4 mm thick, respectively. From these and other measurements, it was determined that the speed of sound in refrigerated ice was approximately 1.93 mm/μsec for a shear wave and approximately 3.98 mm/μsec for a compressional wave.

Data obtained from these NDE technology transfer laboratory studies showed that ultrasonics can be used to detect icing on a surface. This technique could be used in the aircraft industry with the incorporation of electronic signal processing to determine the growth rate of ice on an airfoil.

(Alphonso C. Smith, 3036)

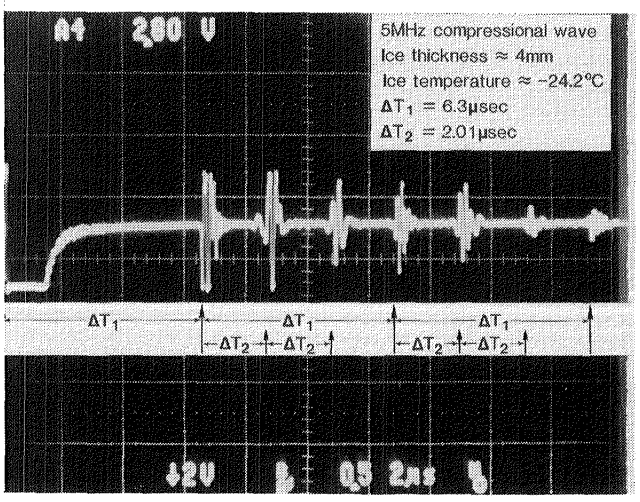

Laboratory test of pulsed-echo ultrasonic system.

Quantitative Thermal Diffusivity Tensor Measurements for NDE of Composites

A radiometric technique has been developed in the thermal NDE laboratory to measure the thermal diffusivity tensor components in the plane of a graphite-epoxy composite plate. The technique has been shown to have strong potential as an NDE nondestructive evaluation tool to image broken fiber damage in composites. At present, no satisfactory NDE technique is available for rapid imaging of large composite structures in field settings. This technique has the potential to satisfy these demands with a noncontacting one-sided quantitative measurement of a material property.

The technique utilizes a remote laser heat source and a scanning infrared radiometric detector. A sample is heated and the time evolution of the resulting temperature distribution is measured and recorded. The one-dimensional thermal diffusivity is then extracted from the temperature measurements. The orientation of the source can be changed to measure the prime diffusivity components in the plane of the sample. Since the diffusivity along the fibers is much greater than that perpendicular to the fibers, information about the condition of the fibers can be obtained. The technique has been shown to give quantitative diffusivity measurements that are accurate to within 2 percent for composite materials. Diffusivity measurements have been made which illus-

L-85-11,420

NDE thermal instrumentation.

trate a factor of 7 change between the components perpendicular and parallel to the fibers in a unidirectional composite. The functional dependence of diffusivity with angle to fiber direction has been shown to agree closely with cos(2*a*), where *a* is the angle to the fiber direction. In addition, diffusivity measurements have been made of a composite sample with cut fiber damage. A 13-percent decrease in diffusivity was observed between the cut fiber region and the intact region.
(D. Michele Heath, 3036)

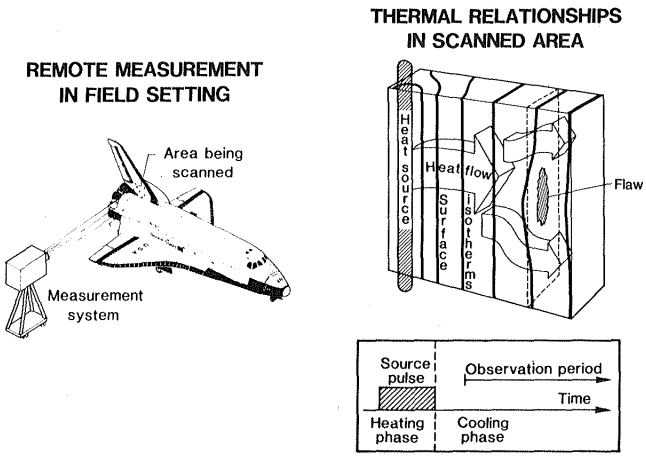

NDE by thermal diffusivity imaging.

Laboratory Technique for Detection of Composite Fiber Damage

A technique has been developed in the NDE electromagnetic impedance characterization laboratory for detection of fiber damage in graphite-epoxy composites. The technique couples electric current into the graphite fibers and maps the resulting magnetic fields. The technique differs from eddy-current techniques in that the current is coupled directly to the fibers and is not an induced current. Because of this, the "skin effect" does not limit the depth of inspection. The magnetic field is detected with an air gap toroid and a high-gain synchronous amplifier. Since broken fibers appear as disruptions in conductivity paths, detected field gradients are directly related to broken fibers.

This technique has been used to detect back-surface holes 0.25 mm deep and 1 mm in diameter in a 2-mm-thick composite sample. Subsurface defects of various sizes have also been detected. Work is being performed to make this laboratory technique into a practical method of material evaluation.
(Travis N. Blalock, 3036)

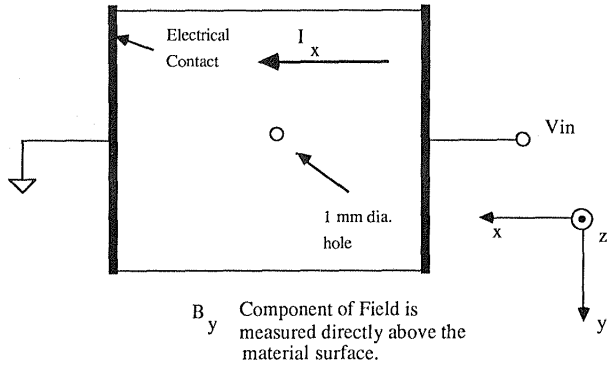

Schematic of magnetic field image.

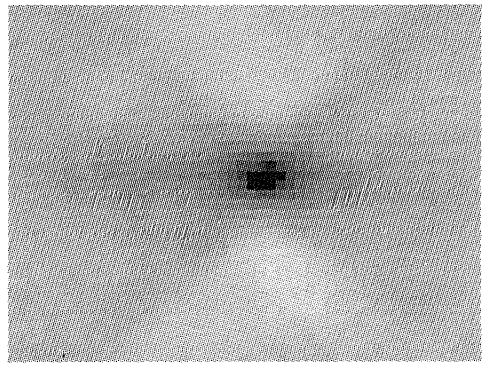

Magnetic field image of 1-mm-diameter hole.

Hyperthermia Temperature Monitoring Technique

It has been known historically that localized heating of a tumor (greater than 42° C) can be an effective treatment. The performance of chemotherapy is improved and the cancerous cells can be killed.

Close temperature monitoring and control of this process, which are essential to prevent damage to the surrounding normal tissue, are extremely difficult. Current methodology involves the insertion of catheters and thermocouples into the tumor and the surrounding area on a repeated basis. The risk of metastasis and infection, as well as the mechanical damage to the tissue of the patient, has limited the usefulness of this treatment. Ultrasonic techniques being developed at Langley offer the potential for a significant improvement in this form of therapy.

The NDE technology transfer laboratory at Langley, in concert with the Technology Utilization Office, is developing a technique wherein small beads of a waxy material (3 to 5 mm in diameter) would be implanted in the immediate vicinity of the tumor. The material used would have a custom-tailored melting point, which would give rise to an ultrasonically measurable alteration in its characteristics. A candidate material has been selected and is being formulated at various melting points in the region of interest. A tissue phantom capable of withstanding in excess of 70° C has been developed. Beads of the phase transformation material (PTM) have been implanted in samples of the tissue phantom and successfully scanned ultrasonically. The technique is being refined prior to clinical tests at Duke University Medical Center. The results of this project will provide the medical community with a considerably enhanced tool for the treatment of cancer.

(Joe Heyman, 3036)

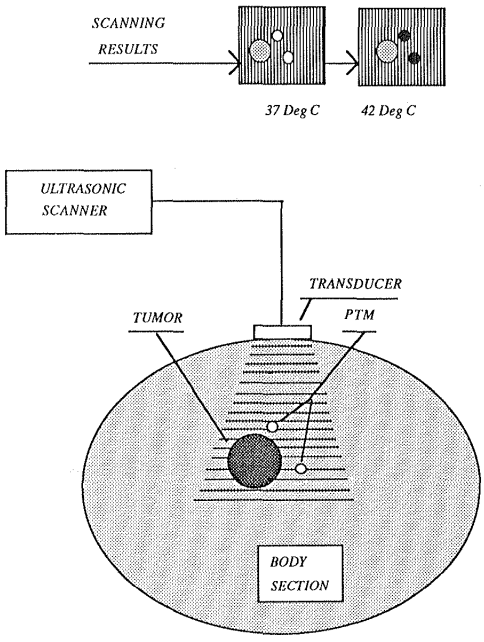

Phase tranformation material used to monitor temperature during heat treatment.

Vehicle Antenna Test Facility

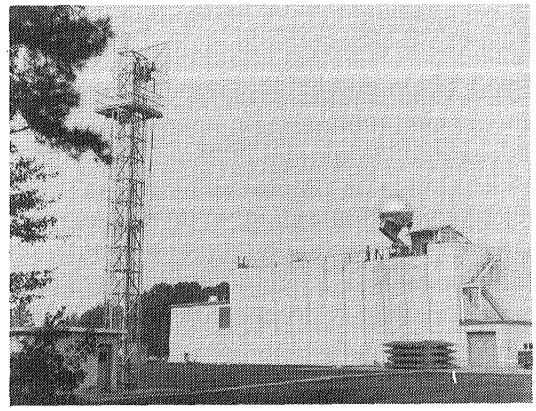

The Vehicle Antenna Test Facility (VATF) is a research facility used to obtain data for new antenna performance and electromagnetic scattering data in support of various research programs. The VATF consists of two indoor radio frequency anechoic test chambers and an outdoor antenna range system. The anechoic chambers provide simulated free-space conditions for measurements from 100 MHz to greater than 40 GHz. The anechoic chambers, which are shaped like pyramidal horns to reduce specular reflections of the walls, are over 100 ft long and have test area cross sections approximately 30 by 30 ft.

A spherical near-field (SNF) measurement capability was added to the low-frequency chamber. A precision antenna positioning system, antenna source tower, and optical alignment system designed for SNF emasurements were installed in the low-frequency chamber and the capability now exists for automatic performance of precision SNF measurements up to at least 18 GHz. Antennas with diameters up to 12 ft can be measured if their electrical size is no greater than 100 wavelengths (i.e., diameter/wavelength $\leq$ 100). This limitation is imposed by the SNF system software, which transforms the near-field data to obtain the desired far-field data. Measured data stored on disc can be processed to provide antenna directivity, polar or rectangular plots of the radiation patterns, and three-dimensional contour plots of the antenna radiation characteristics.

The high-frequency anechoic chamber was used to establish a Compact Range Facility. The compact range is an electromagnetic measurement system used to simulate a plane wave illuminating an antenna or scattering body. The plane wave is necessary to represent the actual use of the antenna or scattering from a target in a real-world situation. The compact range utilizes an offset-fed parabolic reflector to create the simulated plane wave test conditions. The standard commercially available compact range is limited to the measurement of antennas or models with maximum dimensions of 4 ft over the frequency range of 4 to 100 GHz.

The outdoor antenna range system is available for use when the antenna or test model size or frequency precludes the use of the anechoic chambers. The outdoor range consists of two remote transmitting towers that are spaced 150 and 350 ft from the test positioner mounted on the VATF roof. The VATF has several electronic laboratories with the extensive measurement capability needed to support the design of unique antennas prior to their evaluation in the antenna chambers or on the outdoor antenna range system.

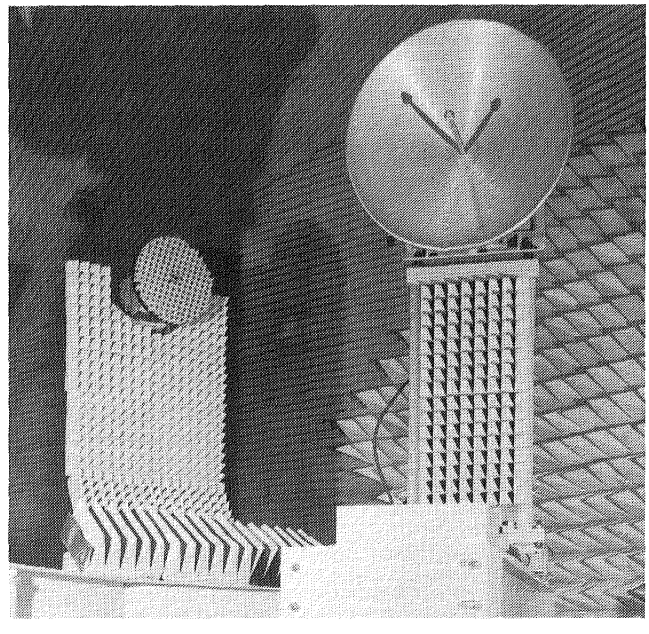

Spherical near-field equipment.

Development of 15-m Hoop/Column Large Space Antenna

During the past 6 years, a team composed of NASA, contractor, and university personnel has been using the VATF and other facilities to develop the technology of cable-stiffened deployable structures for large space antenna applications. This dedicated effort has now culminated in the development, assembly, and test of a 15-m hoop/column deployable antenna system with a cord-shaped mesh surface. This 15-m structure is about 60 percent larger than the previously largest deployable operational antenna, the Applications Technology Satellite (ATS-6), and is thereby suitable for scaling considerations to much larger applications. However, the 15-m structure is just small enough by design to allow testing in ground facilities.

Recent engineering tests of the 15-m antenna have included deployment kinematics, modal characteristics, reflector surface characterization during simulated zero-gravity conditions, and near-field electromagnetic testing. The electromagnetic performance was measured across a range of radio frequencies from 2 to 12 GHz at the Martin Marietta Near Field Test Facility, the only known facility capable of measuring a structure of this size. These measurements showed that high performance was achieved by this antenna.

The development of the 15-m engineering model paralleled the development, from measurements made in the VATF, of structural analysis and electromagnetic analysis computer codes for predicting the performance of mesh-deployable antennas. These analysis methods were used to predict the radio frequency performance of the 15-m antenna before the antenna was tested at Martin Marietta Corp. The significant agreement, as shown in the figure, verified the analysis methodology. The analysis method has the capability to include pillowed surface distortions that generate grating side lobes in the far-field pattern from the antenna.

The experimental results in the Near Field Facility and the comparison of those results with the analytical predictions represent a significant milestone in the technology development of large space antennas. These technological advances will provide new opportunities for the application of large space-based antennas in a variety of science and applications experiments in the areas of remote sensing, multiple-beam communications, and radio astronomy.

(Tom Campbell, 3631)

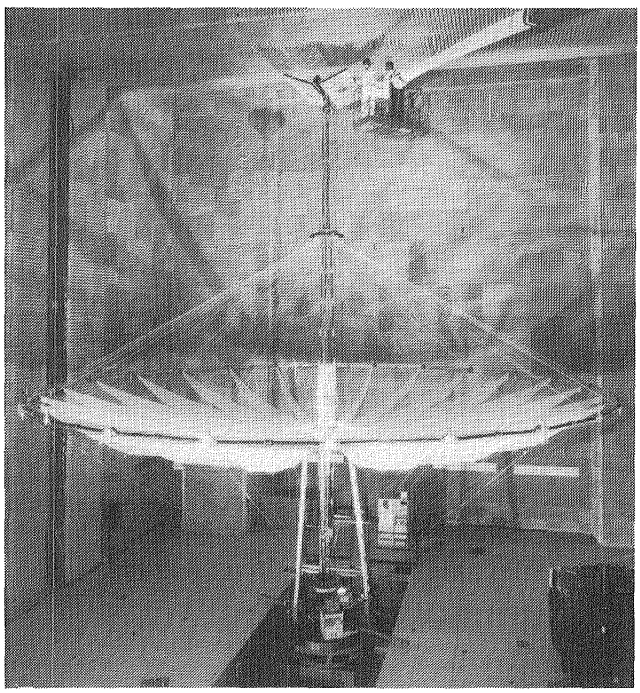

L-85-8488

Test of large space antenna.

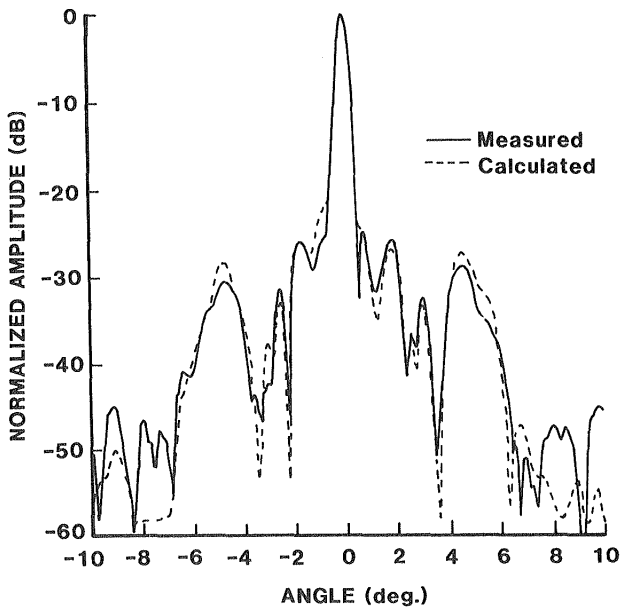

H-*plane radiation pattern at 7.73 GHz.*

Characterization of Antenna System Technology Mesh Materials

A gain degradation problem was observed on several flight-deployable antennas for the Tracking and Data Relay Satellite (TDRSS). This problem was eventually determined to be corrosive contacts on the mesh material. This TDRSS problem emphasized the need to develop a quantitative method for characterizing the electromagnetic properties of mesh materials. The gain degradation problem is severe for a communication mission, but emissivity values must be extremely low and nearly constant for radiometer missions. In that regard, a mesh characterization program has been initiated at Langley in the VATF.

Two experimental test configurations have been developed—an enclosed system that uses liquid nitrogen cold load and an open-bucket reflector system that reflects the sky brightness temperature into the mesh target and radiometer system. The transmissivity, reflectivity, and emissivity values are determined through interactive procedures that use mesh, absorber materials, and precision calibration splash plates and target conditions. Advanced proprietary mesh materials have been measured and found to be in the range of acceptability for radiometer missions that use large space antennas. The Naval Research Laboratory has requested that the mesh measurement laboratory be used to evaluate candidate materials for the Navy Remote Sensing System (NROSS) satellite. The mesh material for the 15-m antenna and samples from General Dynamics Convair have been tested.

(Richard F. Harrington, 3631)

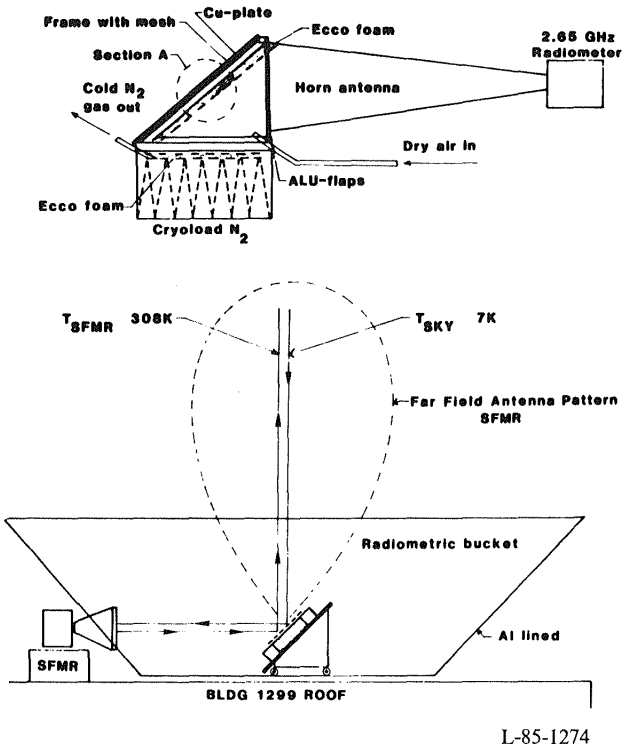

Radiometer system for electromagnetic measurements of surfaces.

Impact Dynamics Research Facility

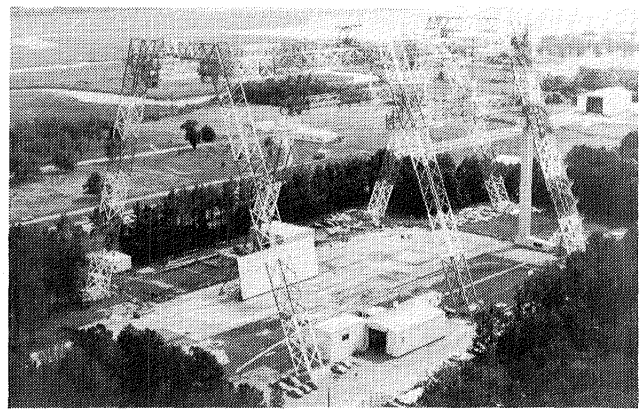

This facility, which was originally used by the astronauts during the Apollo Program for simulation of lunar landings, has been modified to simulate crashes of full-scale aircraft under controlled conditions. The aircraft are swung by cables, pendulum-style, into the concrete impact runway from an A-frame structure approximately 400 ft long and 230 ft high. The impact runway can be modified to simulate other ground crash environments, such as packed dirt with trees. In the past the impact runway has been modified with soil to meet a specific test requirement.

The aircraft is suspended by swing cables from two pivot points 217 ft off the ground. It is then pulled back along an arc to a predetermined height by a pullback cable from a movable bridge on top of the A-frame, released from the pullback cable, and allowed to swing, pendulum-style, into the ground. An instant before impact, the swing cables are separated from the aircraft by pyrotechnics. The length of the swing cables regulates the aircraft impact angle from 0° (level) to approximately 60°. Impact velocity can be varied up to approximately 65 mph (governed by the pullback height) and to 90 mph with rocket assist. Variations of aircraft pitch, roll, and yaw can be obtained by changes in the aircraft suspension harness attached to the swing cables. Onboard instrumentation data are obtained through an umbilical cable attached to the top of the A-frame. Data are transmitted by hard wire to the control room at the base of the A-frame. Photographic data are obtained by ground cameras and cameras mounted on top of the A-frame. Maximum allowable weight of the aircraft is 30,000 lb.

Full-Scale Impact Tests of Gliding Platform Delivery System

Three full-scale impact tests were conducted on an Army gliding parachute equipment delivery system in the Impact Dynamics Research Facility. The 3000 lbm platform test article was equipped with eight bellows-type air bag energy absorbers beneath the platform on which up to 1500 lbm of cargo such as trucks, jeeps, or other equipment was secured. The platform with parachute was deployed from a cargo aircraft to glide under radio control to a designated landing target. Test conditions of the platform were 42 ft/sec horizontal velocity and 30 ft/sec vertical velocity with a 30° yaw to the flight path. Deceleration loads on the platform at the simulated cargo center of gravity and pressure response in the bellows

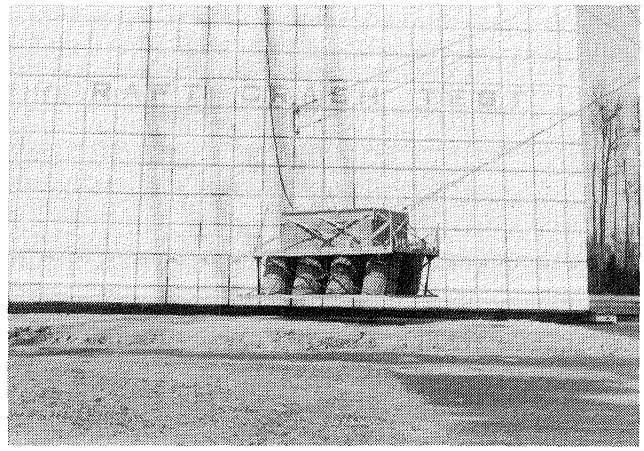

L-85-3993

Gliding platform at release point for impact test of energy absorber system.

energy absorbers were also measured. The bellows were designed to limit the bellows pressure to 3 psi or less and the center-of-gravity deceleration of the payload to 10 *g* or less.

Results from the drop tests uncovered some minor design weaknesses in the attachments of the air bag absorbers, but the delivery system requirements were met during the tests.
(Huey D. Carden, 3795)

Composite Fuselage Frame Impact Tests

As part of the research program addressing the global response and behavior of basic generic composite structural components subjected to typical crash loadings, three 6-ft-diameter Z-cross-section fuselage frames were drop tested. The frames, which had 3-in.-deep webs and 1.16-in. flanged frames, were fabricated from a 280 five-harness/3502 graphite epoxy composite fabric material. The components were 0.08 in. thick with a $(45/0/135/90)_S$ layup. The frames were fabricated from four 90° segments joined with splice plates on either side of the joints. The composite frames were drop tested at 25.5 ft/sec impact velocity in an apparatus with guide rails, backboard, and front plexiglass shield to maintain the frame inplane during the impact. Strain gauges and accelerometers were placed around the circumference to measure strain distribution and pertinent decelerations on the frames.

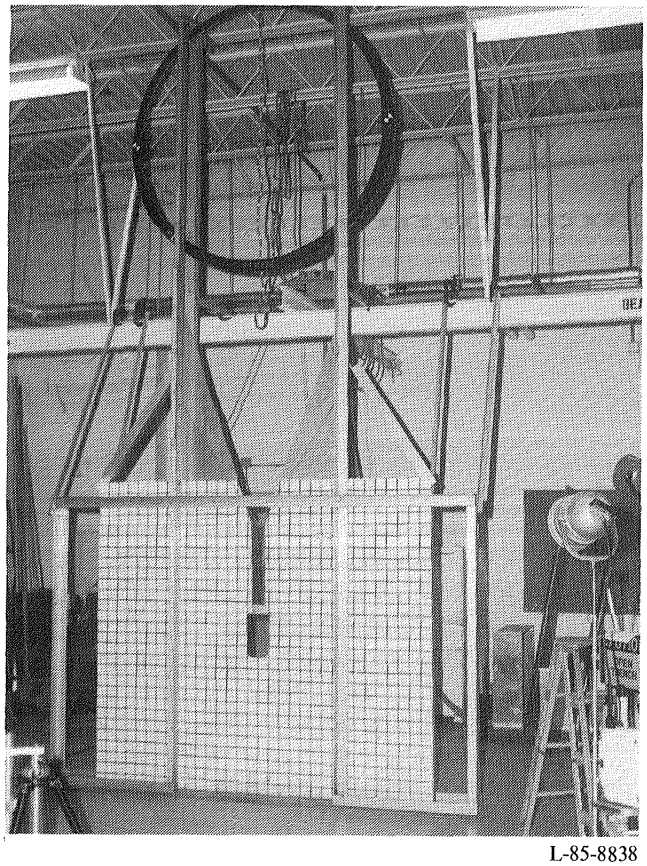

L-85-8838

Graphite-epoxy frame in drop tower before test.

Results of this test showed that high acceleration loads occurred at the point of impact and caused a shear failure at the bottom of the ring. Unlike a similar metallic noncomposite structure, the composite ring did not crush to absorb the impact energy. Additional tests are planned and data reduction is under way on the composite fuselage frames. Analysis of the response of such building blocks as the composite frames will provide insight into the global response and behavior of more complex structures, such as composite subfloor structures, which are part of the generic research of composite structural components.
(Richard Boitnoitt, 3795)

Full-Scale Helicopter Swing Tests for Wire Strike Protection System Evaluation

Three full-scale swing tests of a Huey Cobra helicopter equipped with a wire strike protection system were conducted at the Impact Dynamics Research Facility (IDRF). The wire strike protection system consists of passive cutters placed on the top and bottom of helicopters to cut communication cables and their steel carrier cables in the event of a wire/helicopter encounter. As part of the system evaluation and qualification, three tests were conducted in which the Huey Cobra helicopter was suspended under the IDRF gantry and swung into cables placed across the path of the helicopter. The test condition for the three tests of the upper cutter and cockpit guides was 30-mph wire strike velocity. In one test the

wire was placed at 90° to the path of the helicopter and struck the middle of the cockpit windshield. In two other tests the wire was at 30° to the flight path. One of these strikes was in the middle of the windshield and the other was at the bottom of the windshield.

Two successful wire cuts occurred, but the third uncovered a condition in which the cable snagged the bottom of the cockpit upper cutter guide and broke the cable rather than sliding into the cutter. The upper guide will be redesigned and additional tests will be needed.

(Huey D. Carden, 3795)

Helicopter with wire strike protection system severs communication cable.

Aircraft Landing Dynamics Facility

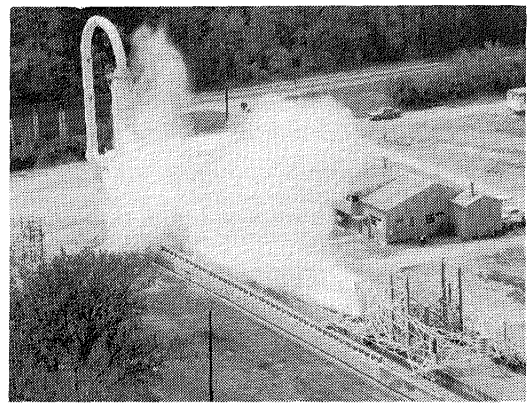

Langley Research Center has recently updated the landing loads track to the Aircraft Landing Dynamics Facility (ALDF) to improve the capability of low-cost testing of wheels, tires, and advanced landing systems. The main features of the updated facility are the propulsion system, the arresting gear system, the high-speed carriage, and the track extension.

The ALDF uses a high-pressure water jet system to propel the test carriage along the 2800-ft track. The propulsion system consists of an L-shaped vessel which holds 28,000 gallons of water pressurized to 3150 psi by an air supply system. A timed, quick-opening shutter valve is mounted on the end of the "L" vessel and releases a high-energy water jet, which cataputs the carriage to the desired speed. The propulsion system produces a thrust of 2 million lb at maximum pressure, which is capable of accelerating the 108,550-lb test carriage to 220 knots within 400 ft. This thrust creates a peak acceleration of approximately 20 *g*. The carriage coasts through an 1800-ft test section and decelerates to a velocity of 175 knots or less when it intercepts the five arresting cables that stretch across the track. The arresting system brings the test carriage to a stop in 600 ft or less. Essentially any landing gear can be mounted on the test carriage, including those exhibiting new concepts, and any runway surface and weather condition can be duplicated on the track. Research on slush drag, hydroplaning, tire braking, steering performance, and runway grooving has been conducted in the past.

Future research programs include the Space Shuttle orbiter main and nose gear tire spin-up wear characteristics and cornering force measurements at high speeds as well as frictional properties of radial and H-type aircraft tires for comparison with conventional bias ply tires. A surface traction program to study the effect of different runway surface textures and various runway grooving patterns on the stopping and steering characteristics of aircraft tires will be conducted. Finally, tests associated with the National Tire Modeling Program will also be conducted.

Space Shuttle Orbiter Main Gear Tire Tests

High speed tests to define the spin-up wear and cornering friction characteristics of the Space Shuttle main gear have been conducted on the newly updated Aircraft Landing Dynamics Facility. Simulated landings at speeds up to 226 knots and sink rates up to 4 ft/sec have been conducted on a concrete runway that accurately represents the surface characteristics of the Shuttle runway at Kennedy Space Center. The tests have established the tire wear characteristics on the KSC runway surface and have defined the effect

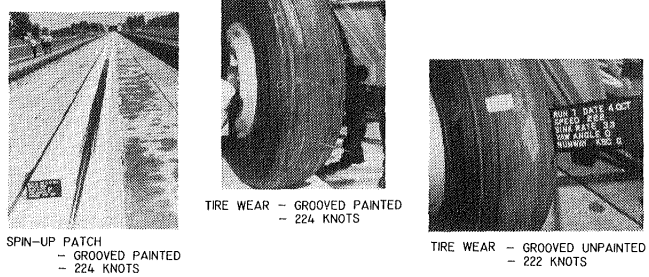

L-85-12,630

Shuttle main gear tire tests on simulated KSC runway.

of various runway surface treatments on tire wear and cornering friction characteristics.

The current runway surface at KSC has been shown to provide wet runway cornering friction forces nearly equal to the friction forces produced on the surface when dry. Painting the runway surface with runway marker paint reduced the severity of the tire spin-up wear, but at the expense of cornering coefficient when the runway surface was wet. When the surface was sandblasted to remove some of the surface texture in an effort to reduce tire wear, similar reductions in wet runway traction capability were observed. The data obtained from this investigation will be used to establish safe crosswind limits during landing for the orbiter fleet.

(Sandy M. Stubbs, 2796)

Vortex Research Facility

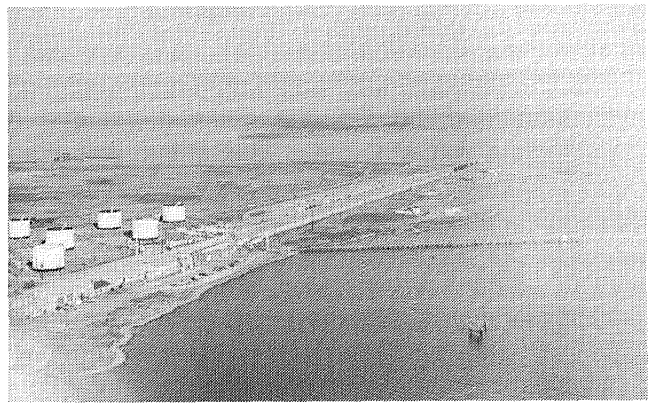

The Vortex Research Facility is a unique experimental facility in which the research model is towed the length of the facility instead of air being moved past the research model. With this method, aircraft wake flow fields may be studied for downstream distances of over 2 scale miles. The facility is a converted towing basin about 1800 ft in length with a test section length of 500 ft and a cross section 17 ft wide and 14 ft high. An instrumented automobile type research vehicle is used to accelerate the research test model to a constant test speed of approximately 100 ft/sec. The aerodynamic characteristics of the research model are measured while the vehicle traverses the entire length of the facility and are transmitted via an optical telemetry data link to a data acquisition system. A laser velocimeter system is located in the test area to acquire detailed wake velocity measurements. The laser velocimeter system incorporates a high-speed scanning system that provides 16 discrete measurements across the test section at rates up to 30 scans per second. Flow visualization, using a laser sheet of light, is simultaneously videotaped to provide an image of the wake and its descent profile.

The Vortex Research Facility has been involved in several research programs during the last 15 years, including the Aerial Applications program and the Wake Vortex Hazard/Alleviation program. The facility is currently being utilized primarily in the wake vortex program. The research objective for the facility is to provide a basic understanding of the physics of vortex flows. To achieve this objective, the facility has been upgraded and experimental data are being acquired to develop methods that reduce vortex wake intensity and to verify computational methods that predict vortex flow behavior. Preliminary investigations of aircraft dynamic ground effects on aerodynamics are also being conducted.

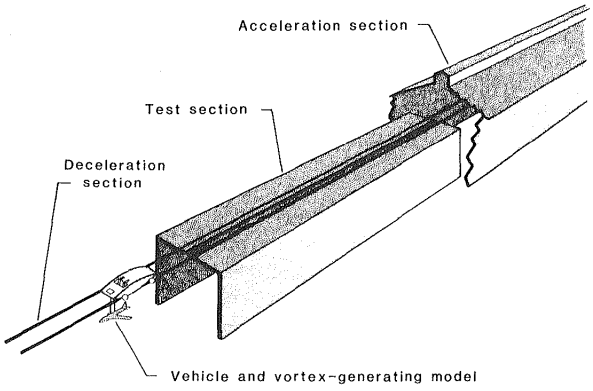

Diagram of Vortex Research Facility.

Density Stratification and Reynolds Number Effects on Vortex Flows

The state of the atmosphere plays a dominant role in determining the lifetime of an aircraft wake. Turbulence, wind shear, and cross winds are known to influence vortex decay. In addition, the variation of temperature with altitude (the lapse rate) can have a strong effect, both as a direct influence on wake lifetime and as a parameter characterizing the stability or turbulence characteristics of the atmosphere.

The Vortex Research Facility is currently being used to investigate the effects of density stratification in the test section in order to simulate the dynamics of wake development in the real atmosphere. Density stratification in the test section was produced by a

vertical temperature gradient and resulted in significant effects on the decay of the wake vortex system. The results showed that for cases with mild stratification, the dynamics of the wake vortex system were dominant over the buoyancy forces generated by the density stratification. Larger amounts of stratification produced larger effects on the wake vortex system and caused significant decreases in wake lifetime.

Wake trajectory data taken in the facility have been compared to data taken in full-scale flight. When wake data taken at different scales are compared, wake scaling principles call for comparing the data in nondimensional form. In principle, the trajectories should be nearly identical for the same atmospheric conditions (i.e., stratification, turbulence, and so forth). However, as indicated in the figure, experimental data taken in the Vortex Research Facility differ from the higher Reynolds number flight test data. Predictions made with a wake decay model, which includes the effect of Reynolds number on each trajectory, agree well with the data and indicate a significant Reynolds number effect that had not been anticipated prior to these tests.
(G. Thomas Holbrook, 2543)

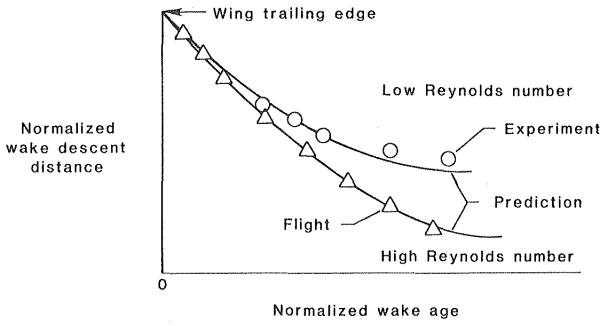

Effect of Reynolds number on vortex wakes.

Flight Research Facility

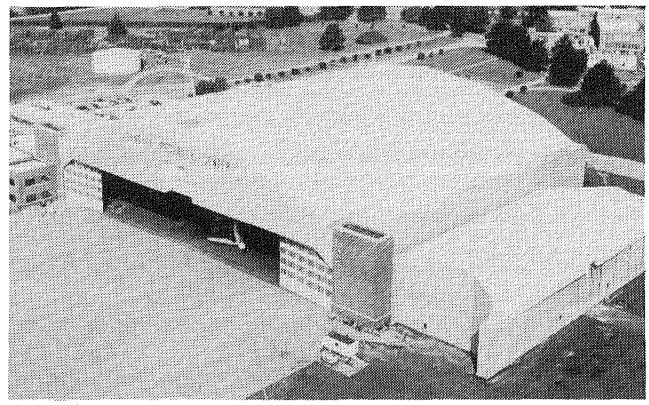

The truss-supported roof of the huge hangar of the Flight Research Facility provides a clear floor space with nearly 300 ft in each direction (over 87,000 ft^2).

Door dimensions will allow entry of a Boeing 747. Features such as floor air and electrical power services, radiant floor heating to eliminate corrosion-causing moisture, a modern deluge fire suppression system, energy-saving lighting, modern maintenance spaces, and entry doors and taxiways on either side of the building make this structure equal or superior to any hangar in the country. Extensive and modern maintenance equipment makes it possible to repair aircraft ranging in sophistication from modern metal and composite airliners, fighters, and helicopters to fabric-covered light airplanes. Surrounding the hangar are ramp areas with a load-bearing capacity sufficient to handle the largest wide-body jet now flying. The high-power turnup area can also handle a wide variety of aircraft.

The present array of research and research support aircraft includes an airliner, military fighters, trainers, experimental one-of-a-kind designs, helicopters, and single- and multi-engine light airplanes. This variety enables research to be carried out over a wide range of flight conditions, from hover to Mach 2 and from the surface to 60,000 ft. Research pilot currency in this wide spectrum of aircraft is important in conducting credible in-flight experiments as well as in flight simulator assessments. A variety of research can be conducted in such areas as terminal traffic flow, Microwave Landing System (MLS) approach optimization, airfoil properties, single-pilot IFR, engine noise, turbulence research, natural laminar flow, winglet studies, stall/spin, and severe storm hazards.

One of the support helicopters is used to drop unpowered remotely controlled models of high-performance airplanes to study high-angle-of-attack

NASA 501, modified American Aviation AA-1 Yankee

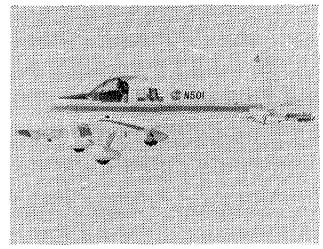

NASA 512, OV-1B Mohawk

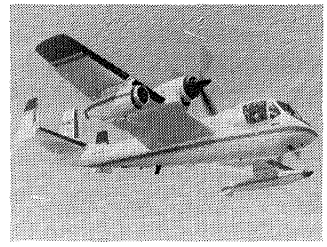

NASA 519, modified Piper PA-28RT-200 Arrow

NASA 266, Gates Learjet model 28/29

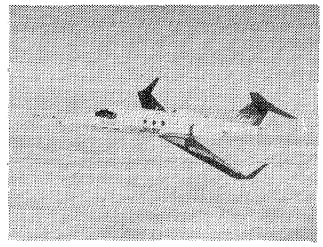

NASA 503, Cessna C-402

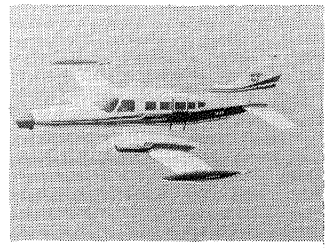

NASA 515, Boeing 737-100

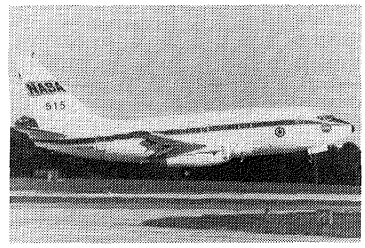

NASA 507, Cessna C-172

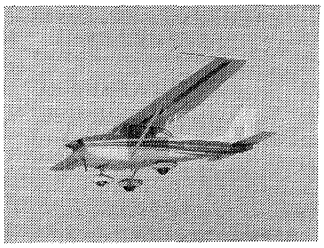

NASA 504, modified Beech C-23 Sundowner

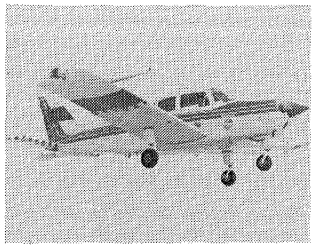

NASA 816, F-106B

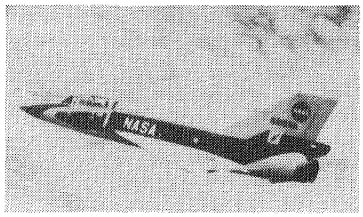

control characteristics. The drop model test site is located at Plum Tree Island, near Langley Research Center.

Transition behavior and measurement methods for natural laminar flow

A significant facet in the development of natural laminar flow (NLF) technology is the investigation of the boundary layer transition phenomenon for an airplane that has swept wings and is capable of flight profiles (Mach number, altitudes, and rates of climb) of the sort flown by transports and business jets. Current research is focused on the acquisition of a better understanding of conditions under which various transition mechanisms occur in flight, and on the development of improved instrumentation for determining these transition mechanisms.

Pressure belts for obtaining wing and fuselage pressure distributions and a multi-element hot-film gauge for electronic detection of transition are presently being tested on a Gates Learjet model 28/29. The pressures are simultaneously sensed electronically at 192 locations on the airplane. The multi-element transition gauge is a continuous strip with hot-film sensors and electrical leads embedded in its surface. This design overcomes a significant shortcoming of individual surface-mounted sensors used in the past. The individual sensors could not be installed in the streamwise alignment necessary to measure both stagnation location and downstream transition without the occurrence of mutual sensor interference.

A number of devices designed to detect modes of transition have been designed, tested in the wind tunnel and, in some cases, flight tested on the airplane. These include a cross-flow sensor to determine the existence and location of cross-flow vorticity disturbances, which can cause turbulence on laminar-flow surfaces; a laminar separation sensor to detect the presence of laminar separation bubbles; and microphones to measure free-stream acoustic disturbances. These devices are being flown concurrently with the multi-element gauge, pressure belts, and liquid-crystal applications.

Liquid crystals for high-altitude in-flight boundary layer flow visualization

The visualization of boundary layer transition from laminar to turbulent plays an important role in flight and wind tunnel research. When used along with other electronic and pneumatic transition detection methods, visualization can help provide a good understanding of boundary layer transition locations and modes. Without visualization, understanding why transition occurs where it does is difficult. In the past, transition visualization methods have relied heavily on sublimating chemicals. However, this method is impractical for use in subsonic applications much above altitudes of 20,000-ft because of the greatly reduced sublimation rates experienced at lower temperatures (less than –20° C). Thus, for many flight conditions, transition visualization has not been available.

One new method that has been developed uses liquid crystals for the visualization of laminar boundary layer transition in flight, and exploratory flight experiments have been conducted to evaluate the new technique. High-altitude flight experiments have focused on the wing and winglet of a Gates Learjet 28/29 as test surfaces. A thin coating of synthetic liquid crystal was brushed on the winglet surface prior to takeoff. In flight, the laminar transition locations at Mach 0.8 at 48,000 ft altitude could easily be observed by the vivid color changes on the winglet reflected by the liquid crystals as they were subjected to changing shear stresses in the boundary transition region.

Vortex flow visualization

The F-106 aircraft, which is used for the NASA Storm Hazards Program during summer seasons, was adapted during the winter of 1985 to develop a three-dimensional flow visualization technique. The technique, based on the vapor screen approach previously used in wind tunnels, incorporated a flow seeding system consisting of heated propylene glycol vapor, prepared and pumped from the missile bay pallet, and a probe placed under the wing leading edge. A high-intensity mercury vapor light screen was

projected from the light sheet box on the fuselage. The resultant sectional views of the upper wing vortex system were made available in the aft cockpit via video camera and were recorded for later aerodynamic analysis. Vortex system views from night maneuvering flights enabled analysis of the wing vortex behavior as a function of altitude, Mach number, attitude, and accelerations. The flow visualization technique was a great improvement over the use of natural atmospheric moisture condensation or surface-only tufting and oil flow approaches used previously.

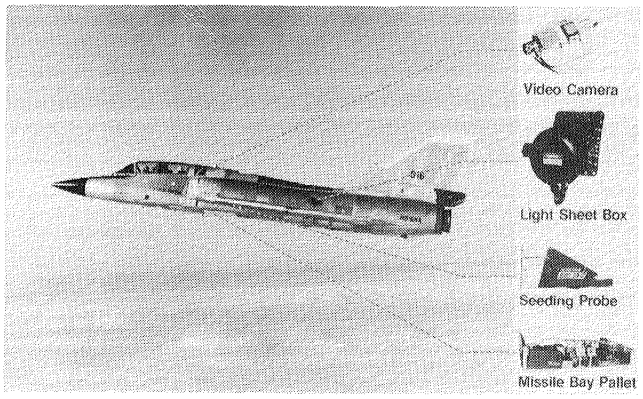

L-85-6276

F-106 flow visualization elements.

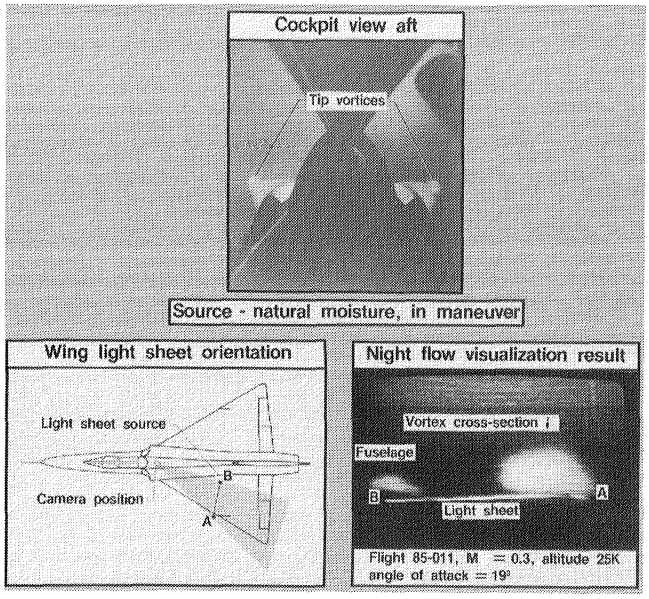

L-85-7723

Wing vortex flow visualization.

Storm Hazards Program—1985 Results

The NASA Storm Hazards Program continued operations in 1985 with the F-106B airplane receiving 53 additional direct lightning strikes. This brought the total to 690 hits in the 6 years of thunderstorm flying. The on-board instrumentation included 12 channels of electromagnetic data with 5- and 10-nanosecond time resolution and several video and film camera systems. In 1985, the film camera systems included a forward-facing pair of 70-mm Hasselblad cameras located in the cockpit to allow stereo photographs of lightning strikes to the nose boom to be taken.

Results obtained in 1985 confirmed the earlier experiences of higher strike rates at colder temperatures aloft. From 1980 to 1985, only 75 direct strikes were experienced at altitudes below 20,000 ft, where most strikes to commercial and military aircraft in routine operations have been reported. Ground-based data indicated that 10 strikes may have been cloud-to-ground strikes. Although the maximum current recorded to date is 54,000 amps, lightning erosion damage to the airplane exterior indicates that a strike with a peak current value of 100,000 amps may have been experienced. The stereo photograph shows a lightning channel attached to the nose

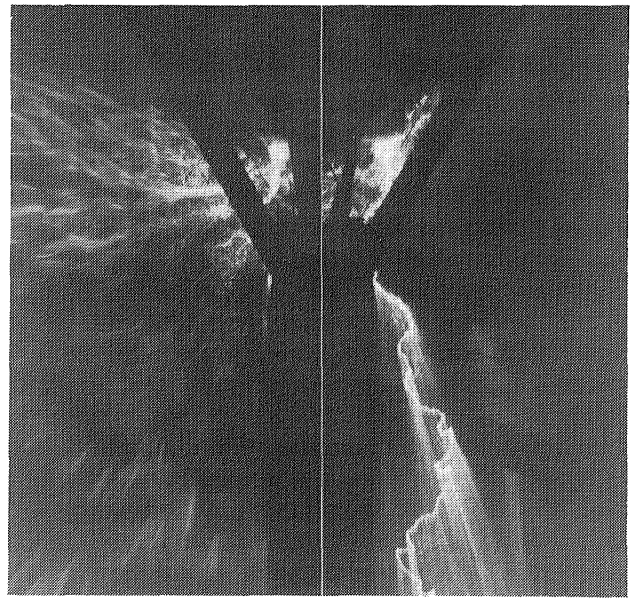

L-85-14,268

Lightning channel sweeping aft from F-106B nose boom.

boom with the channel sweeping aft along the right side of the fuselage. The on-board camera systems have shown that, contrary to established design guidelines, any exterior surface of this airplane may be susceptible to direct lightning attachment. Mathematical models that include thunderstorm electrification parameters are being developed to generalize the results from the all-metal F-106B airplane to composite aircraft with low-voltage digital systems.
(Bruce D. Fisher, 3274)

Research To Increase Stall/Spin Resistance for General Aviation Airplanes

Because a large number of fatal light-airplane accidents are attributed to inadvertent stalls and spins, research is being conducted to provide the technology needed to improve the stall departure and spin resistance of light general aviation airplanes. Flight tests of representative light airplanes are conducted to validate model test results and to research areas such as stall departure that cannot fully be studied in ground tests. Earlier tests of three low-wing configurations with NACA 6-series airfoils indicated the importance of wing leading-edge design and identified an outboard wing leading-edge droop that significantly improved spin resistance. Model tests are being conducted to study the applicability of this leading-edge concept to both conventional and advanced wing designs incorporating increased aspect ratio and other families of airfoils, including natural laminar flow.

Currently, a high-wing airplane with a NACA four-digit airfoil section is being flight tested. Included in the tests is a series of both vortex generators and outboard wing leading-edge droop configurations with different amounts of camber, to determine their effect on the overall airplane high-angle-of-attack characteristics. These flight tests are also being used to provide data to evaluate a proposed Federal Aviation Regulation that would enable certification of "spin-resistant" airplanes. Baseline tests with the unmodified wing and tests with the first (the least cambered) of the outboard wing modifications have been completed. The basic airplane was fairly spin resistant at forward center-of-gravity loadings. The wing modification generally improved spin resistance compared to the baseline, but did not provide sufficient improvement in spin resistance with flaps deflected. These tests agreed well with model test results. Alternate leading-edge droops with added camber have been designed through model tests to further improve the flaps-deflected configuration, and are to be flight tested in 1986.
(Daniel J. DiCarlo, 2064)

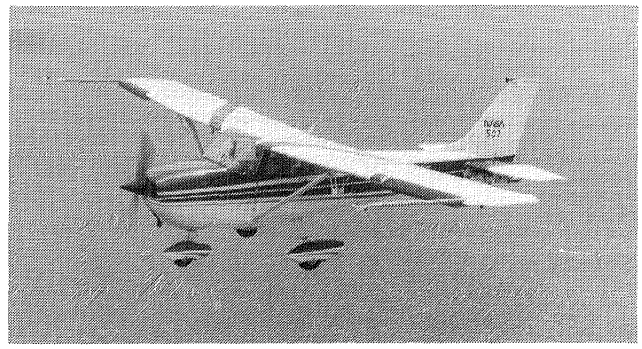

Cessna 172 airplane in flight.

Wing Tip Vortex Turbine Flight Test

The vorticity shed from an aircraft is a function of its weight and is responsible for approximately 35 to 40 percent of the drag of transport type aircraft. This vortex drag (induced drag) is a result of the additional downwash velocity behind the wing caused by the vortex flow and results in a reduction in the effective angle of attack of the wing. The largest effects stem from the regions of the wing tip where the change in the wing lift distribution is the greatest and the tip vortex is formed.

A small turbine device has been positioned in the center of the wing tip vortex in an attempt to recover a portion of this large energy loss. The turbine, driven by the vortex flow, will convert this vortical energy into usable rotational energy, and will thereby minimize the secondary power extracted from the engines of the aircraft. A flight test program of the vortex turbine was recently initiated. Tests were begun dur-

ing the latter part of September 1985. Data have been obtained for the first phase of the program, in which the vortex turbine mounted on each wing tip was operated at rotational speeds ranging from 0 to 600 rpm at the cruise velocity of the Piper PA-28 aircraft (140 mph). Preliminary on-line data indicate that each turbine is able to absorb over 2.0 horsepower from the vortex flow at each wing tip, for a total of approximately 4.5 horsepower, at a turbine rotational speed near 400 rpm. The device also affords a drag reduction equal to the drag increase caused by the installed turbines.

The second phase of this flight test will be conducted with a second set of turbine blades that will have a twist distribution designed to increase the vortex energy recovery and reduce the drag.

(J.C. Patterson, Jr., 2673)

L-85-13,211

Piper PA-28 with vortex turbines.

Natural Laminar Flow Nacelle Flight Experiments

Flight experiments have been conducted to explore the extent to which natural laminar flow (NLF) may be achieved on engine nacelles in flight. A major element in the test was to evaluate the effect of acoustic disturbances on the extent of NLF achieved. The tests used a fiberglass NLF glove attached to the exterior of a baseline nacelle installed on the right wing of the NASA OV-1. An external noise source was located in the pod outboard of the nacelle and glove. The right-hand propeller was feathered during the tests to minimize turbulent flow disturbances from the propeller.

Pressure distributions and boundary layer transition location data were measured on the glove at different airspeeds, engine thrust levels, and nacelle attitudes for several different acoustic levels and frequencies. Initial results indicated that extended regions of NLF could be obtained on the glove under some of the conditions tested. For example, the figure shows the transition front location photographed after a test at an airspeed of 180 knots with the jet engine operating and no external noise source. In this case, NLF was achieved over approximately 30 percent of the nacelle length.

When the tests with the NLF glove are completed, the jet engine and nacelle will be replaced with full-scale NLF flow-through nacelles contoured for NLF. Three instrumented NLF nacelles have been designed and built by the General Electric Company as part of a joint NASA/General Electric agreement. Each nacelle is designed for a different favorable pressure distribution over the forward portion of the nacelle, and flight tests are planned for mid-1986 to measure external pressure distributions, sound pressure levels, transition location, and internal flow characteristics.

(Earl C. Hastings, Jr. 3611)

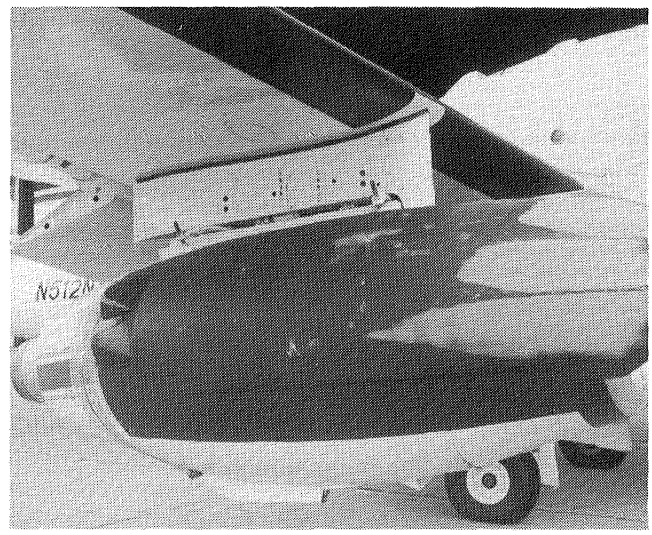

L-85-9406

Final fairing installed on Pratt & Whitney JT15D engine nacelle.

Flight Tests of Single-Pilot IFR Navigation Display Trade-Offs

Previous single-pilot instrument flight rules (IFR) simulator and flight studies have shown that the pilot interface with avionics systems can influence pilot workload, situational awareness, and blunder rate. A flight test study was conducted to examine these factors with various levels of navigation display capability. A Cessna 310 and a Cessna 402 were flown by NASA research pilots in the tests. The Cessna 310 was equipped with conventional electromechanical navigation displays, and the Cessna 402 was equipped with an experimental avionics system that provided the pilot with an electronic moving map display.

The pilots were given the task of flying IFR scenarios in simulated instrument conditions. Researcher observations of pilot activities, pilot comments, and workload ratings were recorded.

The results showed that navigation errors, such as radio mistuning or waypoint setup errors, were frequently detected by either cross-checks of navigation instruments or comparisons of instrument readings with expected values. Errors that did not cause changes in instrument readings tended to take longer to detect. Presenting the navigation data only on a moving map tended to remove the ability to cross-check instruments. Once programmed properly, the map was the best display for maintaining positional awareness. An interesting result was that the same types of setup errors that have occurred in previous high-workload studies also occurred in this study during periods of very low workload. This may indicate that the nature of the pilot/avionics interface contributes to certain types of errors.

(David A. Hinton, 3621)

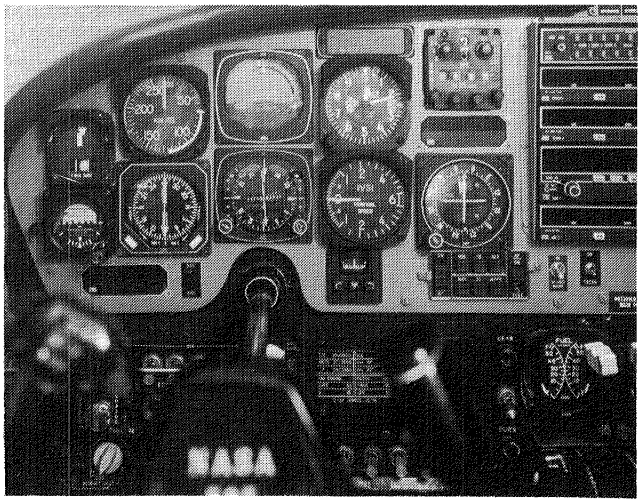

L-83-4987

Cessna 310 navigation system.

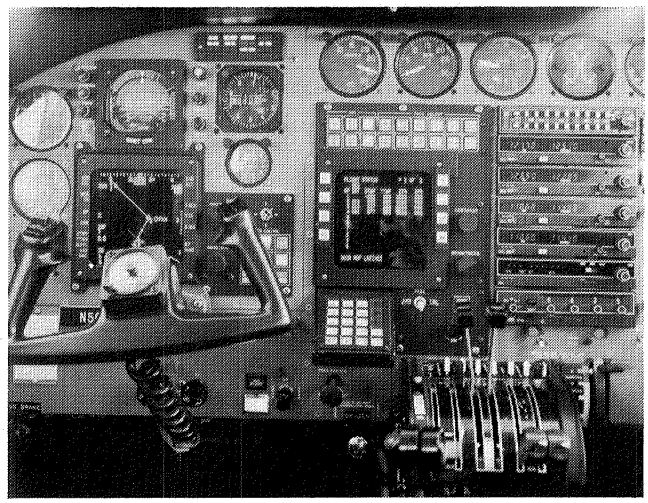

L-83-10,998

Cessna 402 avionics suite.

1. Report No.	2. Government Accession No.	3. Recipient's Catalog No.
NASA TM-87703		

4. Title and Subtitle	5. Report Date
LANGLEY AEROSPACE TEST HIGHLIGHTS—1985	May 1986
	6. Performing Organization Code
7. Author(s)	8. Performing Organization Report No.
	10. Work Unit No.
9. Performing Organization Name and Address NASA Langley Research Center Hampton, VA 23665	11. Contract or Grant No.
	13. Type of Report and Period Covered Technical Memorandum
12. Sponsoring Agency Name and Address National Aeronautics and Space Administration Washington, DC 20546	14. Sponsoring Agency Code

15. Supplementary Notes

16. Abstract

The role of the Langley Research Center is to perform basic and applied research necessary for the advancement of aeronautics and space flight, to generate new and advanced concepts for the accomplishment of related national goals, and to provide research advice, technological support, and assistance to other NASA installations, other government agencies, and industry. This report highlights some of the significant tests which were performed during calendar year 1985 in Langley test facilities, a number of which are unique in the world. The report illustrates both the broad range of the research and technology activities at the Langley Research Center and the contributions of this work toward maintaining United States leadership in aeronautics and space research. Other highlights of Langley research and technology for 1985 are described in *Research and Technology—1985 Annual Report of the Langley Research Center*. Further information about both reports is available from the Office of the Chief Scientist, Mail Stop 103, Langley Research Center, Hampton, Virginia 23665 (804-865-3316).

17. Key Words (Suggested by Author(s))	18. Distribution Statement
Research and technology Tests Facilities Wind tunnels Models	Unclassified - Unlimited Subject Category 99

19. Security Classif. (of this report)	20. Security Classif. (of this page)	21. No. of Pages	22. Price
Unclassified	Unclassified	98	A05

For sale by the National Technical Information Service, Springfield, Virginia 22161 NASA-Langley, 1986

End of Document